1. INTRODUCTION

Today there are approximately more than 1.500.000 patients under dialysis therapy and the anticipated number of dialysis patients by the year 2020 will reach to approximately 3.500.000 as foreseen in Figure 1.1 [1].

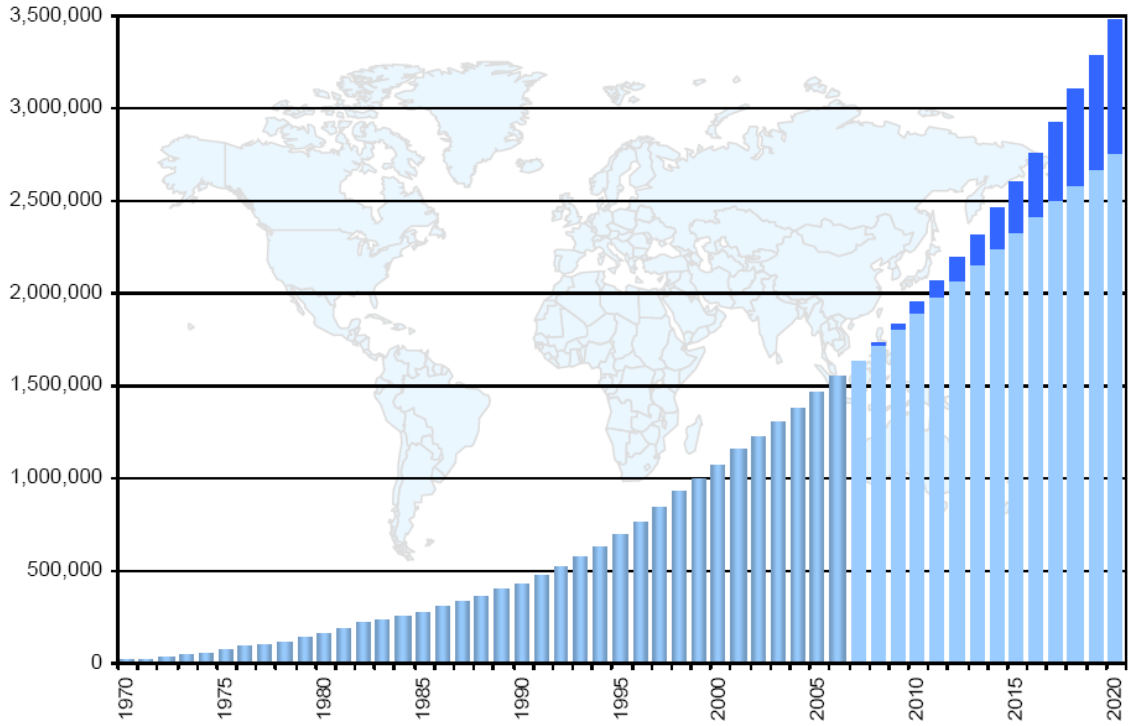

Figure 1.1 Number of dialysis patients in the world and estimated number of dialysis patients until the year 2010 [1].

The number of hemodialysis patients in Turkey between the years 1990 and 2006 is shown in Figure 1.2 [2].

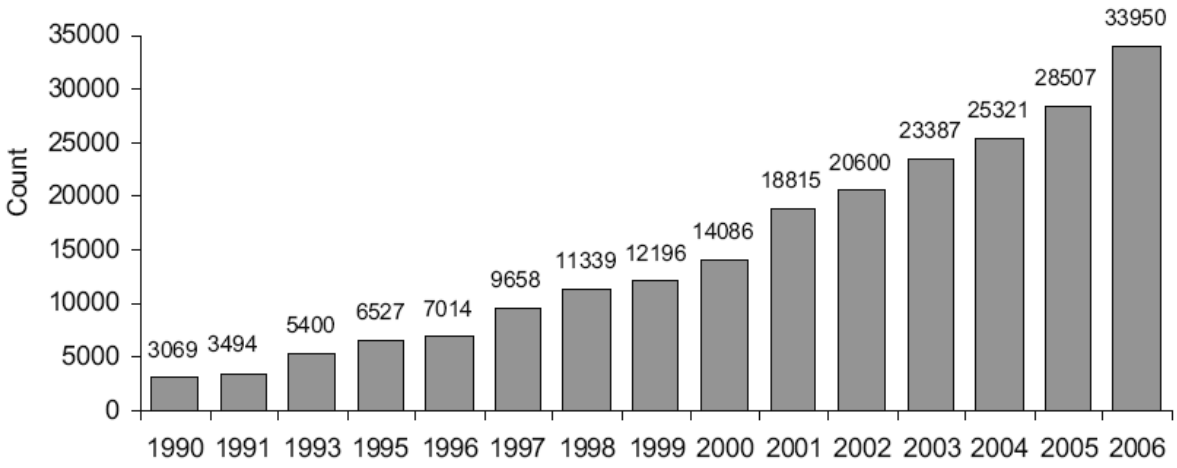

Figure 1.2 Number of hemodialysis patients between the years 1990-2006 [2].

According to the United States Renal Data System (USRDS) 2007 Annual Data Report the incidence of "end stage renal disease" (ESRD) in different countries is shown in Figure 1.3 [3].

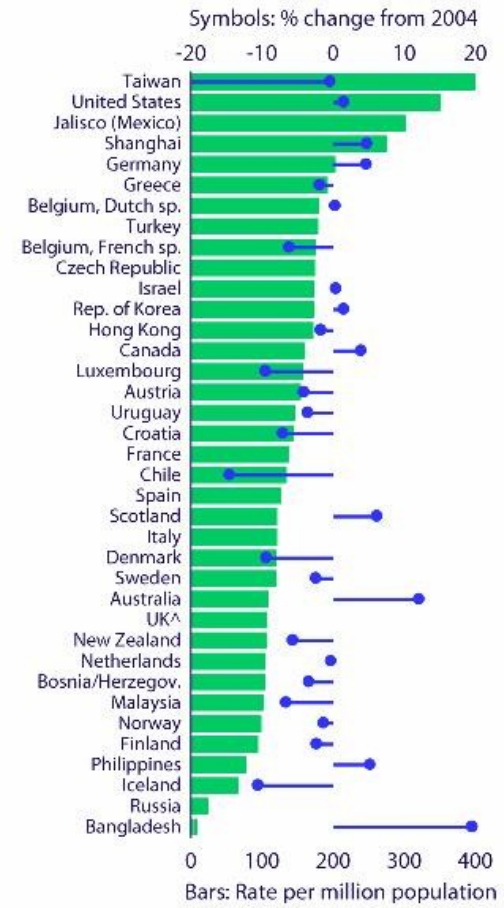

Figure 1.3 Incidence of end stage renal disease (ESRD) per million population in 2005 [3].

With the growing number of renal failure incidence among the population renal replacement therapies are becoming more important in medicine due to insufficient number of renal transplantations and high cost of the renal replacement therapy as seen in Figures 1 and 3. The annual cost of a patient under hemodialysis is approximately between 65.000 – 70.000 US$ in the United States of America [3]. Therefore an econometric analysis should be carried to investigate the problem of selection of medical centers for ESRD patients undertaking hemodialysis (HD), according to unobservable characteristics, related to various subjective and objective aspects [4, 5].

Due to health considerations, social requirements, economical values, certainly hemodialysis becomes an extremely important issue for all societies. Especially new techniques and innovations should be studied carefully in order to help to medical staff and to reveal scientific problems and to solve them.

In this study, it is intended to work extensively on new materials and as well as new considerations one of which is high flux hemodialysis in the course of this thesis.

1.1 The Human Kidney

The kidneys are critical in regulating the internal environment of the body. In particular, they regulate the total body water, as well as a number of substances which are essential to life.

1.1.1 Anatomy Of The Kidney

Kidneys are paired retroperitoneal organs situated in the posterior part of the abdomen on each side of the vertebral column. In the human, the upper pole of each kidney lies opposite to the 12th thoracic vertebra, and the lower pole lies opposite to the 3rd lumbar vertebra. The right kidney is usually slightly more caudal in position. The weight of each kidney ranges from 125 to 170 g in the adult man and from 115 to 155 g in the adult woman. In humans, the kidney is approximately 11 to 12 cm in length, 5.0 to 7.5 cm in width, and 2.5 to 3.0 cm in thickness. Located on the medial or concave surface of each kidney is a slit, called the hilus, through which the renal pelvis, the renal artery and vein, the lymphatics, and a nerve plexus pass into the sinus of the kidney. The organ is surrounded by a tough fibrous capsule, which is smooth and easily removable under normal conditions [6]. A sagittal section of a kidney is seen on Figure 1.4.

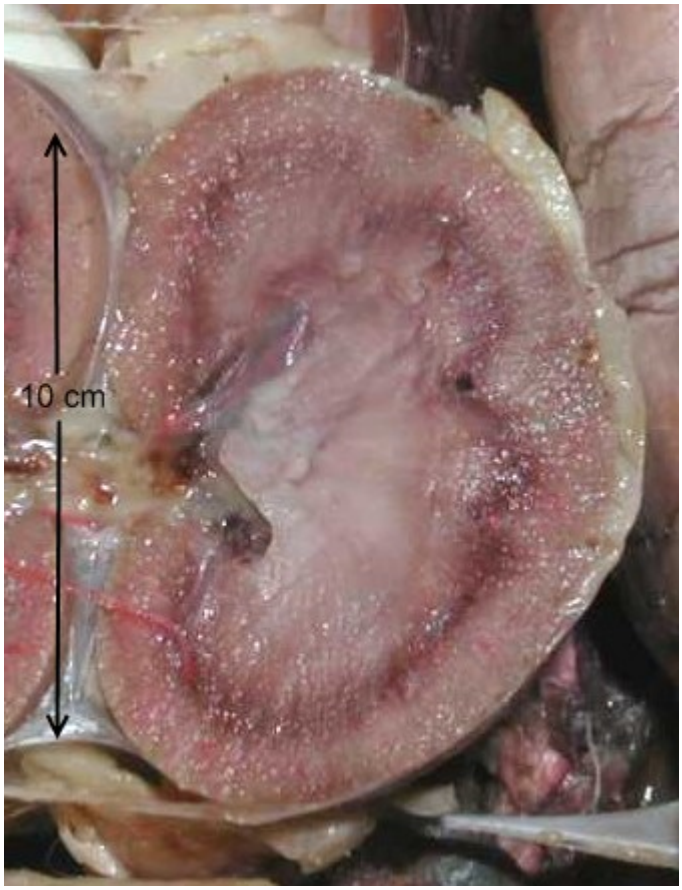

Figure 1.4 Sagittal section of a kidney [7].

Primary renal functions are excretion of metabolic waste products, regulation of extracellular volume, control of electrolyte and acid-base balance and synthesis of hormone-like substances that influence the function of other organs in the body and/or renal function. These additional functions are metabolizing the relatively inactive hormone 25-hydroxy-vitamin D_3 to the active form 1,25-dihydroxy-vitamin D_3, synthesis of the enzyme rennin, formation of vasoactive prostaglandins, kinins and erythropoietin, which is a potent stimulus for erythrocyte formation [7].

Chronic glomerulonephritis, hypertensive nephrosclerosis, diabetic nephropathy, chronic interstitial nephritis and polycystic kidney disease are the most common causes of chronic renal failure. Regardless of the primary cause, chronic kidney disease is categorized as one of five stages based on the glomerular filtration rate (GFR) and an action plan(Tab.1). The glomerular filtration rate (**GFR in ml/min/1.73m²**) is the main decisive factor for the planning of the therapy[7]. The action plan for the therapy of

chronic kidney disease is based on five categories, where the glomerular filtration rate (GFR) is taken as the decisive factor for determining these stages as seen on Table 1.1.

Table 1.1: Classification of chronic kidney disease [7].

STAGE	DESCRIPTION	GFR (mL/min/1.73m2)	ACTION
1	Injury, not acute, with preserved GFR	>90	Diagnose and treat, slow progression, check comorbid conditions, decrease cardiovascular risk
2	Mild kidney damage	60–89	Estimate rate of progression
3	Moderate	30–59	Treat complications, ESRD education
4	Severe	15–29	Prepare for ESRD treatment
5	Kidney failure	<15	Initiate ESRD treatment

Cardiovascular risk factors should be assessed as early as possible, and treatment should be instituted to prevent complications. Education should be provided sufficiently early so that permanent vascular access can be ready for use when the patient reaches ESRD. The patient can choose between a peritoneal dialysis or a hemodialysis program. This is particularly important if the patient chooses hemodialysis. A Cimino fistula offers a number of advantages, including lower rates of thrombosis and infection. However, the veins arising from the fistula often require a number of months to become sufficiently enlarged and thickened so that they can provide adequate blood flow [7]. There is also a chance that a fistula will not develop and that an entirely new alternative access plan will have to be developed. This can be a time-consuming process that, if not initiated early enough, may result in the patient reaching ESRD before the access site is mature. The undesirable consequence is the need for a percutaneous catheter, with its much higher risks of infection, thrombosis, and poor function, to bridge the interval between treatment initiation and the creation of a working, permanent access. Whenever possible, in patients with documented progression, a working, permanent hemodialysis access should be in place by the time the GFR falls below 20/mL/minute [7, 8].

Indications for initiating dialysis therapy in adults are oliguria (urine output <200 ml/12 h), anuria or extreme oliguria (urine output <50 ml/12 h), hyperkalemia ([K+] >6.5 mmol/l and rising), severe acidemia (pH <7.1), azotemia ([urea] >30 mmol/l or [creatinine] >300 mmol/l), pulmonary edema, uremic encephalopathy, uremic pericarditis, uremic neuropathy or myopathy, severe dysnatremia ([Na+] >160 or <115 mmol/l), hyperthermia, drug overdose with filterable toxin (Lithium, Vancomycin, Procainamide etc.), anasarca, diuretic-resistant cardiac failure and imminent/ongoing massive blood product administration [7, 8].

1.2 Historical Background Of Hemodialysis

Acute and chronic kidney failure, which can lead to death if untreated for several days or weeks, is an illness that is as old as humanity itself. In early ages, treatments for uremia included the use of hot baths, sweating therapies, blood letting and enemas. Current procedures for the treatment of kidney failure include physical processes such as osmosis and diffusion, which are widespread in nature and assist in the transport of water and dissolved substances.

Dialysis was first described by Thomas Graham in 1854 [9]. Graham worked as a chemist at Glasgow University, while physician Richard Bright was describing the clinical features and diagnosis of renal failure in Edinburgh. Graham prepared a bell-shaped vessel shown in Figure 1.5 [9].

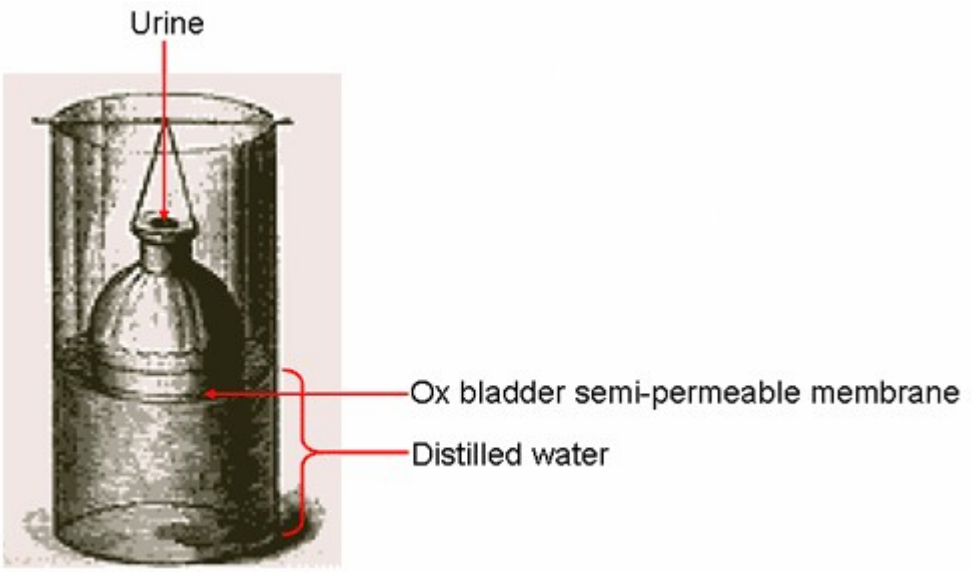

Figure 1.5 Experimental setup prepared by Graham Bell [9].

The wide open end of the bell was covered by a membrane created from an ox-bladder. He filled the bell-shaped vessel with urine and suspended it inside a larger container, filled with distilled water. After several hours, the bell-shaped vessel was removed. The larger container was heated so that the fluid inside boiled to dryness. Graham showed that the residue in the larger container consisted mainly of sodium chloride and urea, the principal components of urine. This proved that urea had passed

through the membrane. Graham termed this process “dialysis” and proposed, together with Richard Bright, that this would form the basis of a treatment for renal failure [9].

According to open literature Graham was the first scientist, who could describe the process of separating substances with a semi-permeable membrane. Graham was also the first scientist who could separate colloids and crystalloids using a parchment membrane [9]. Graham realized that, for successful treatment of renal failure, toxins, which accumulate in renal failure, would have to be removed. It would be necessary to understand the production rate of these toxins in the patient and the rate at which they can cross the membrane. So he made many measurements of the rates of transfer across the membrane for different solutes [9].

In 1855 the German physiologist Adolf Fick published a quantitative description of the diffusion process. Fick used cellulose trinitrate membranes to separate small molecular weight solutes (MW < 5000) from by using the process diffusion process [10]. Graham and Fick had discovered the underlying principle which led to the current forms of treatment for kidney failure [10]. Fick’s Laws are used extensively in engineering practices.

It is known that Abel et al. developed and tested the first efficient dialysis system at Johns Hopkins University School of Medicine. Their apparatus consisted of a filtering device made of cellulose trinitrate tubes and an attached burette containing hirudin solution obtained from leech heads used as anticoagulant. That same year, Hess and McGuigan recommended high blood flows to avoid clotting or need for anticoagulation [10].

According to open literature, the first human hemodialysis was performed in a uremic patient by Haas in 1924 at the University of Giessen in Germany [11]. In 1937, the first flat hemodialysis membrane made of cellophane was produced. Haas, like Abel, also used hirudin as the anticoagulant in his first dialysis [10]. Due to the side effects of hirudin Hass replaced hirudin with the substance called heparin which was first isolated in dog livers by an American named MacLean, in 1916. Heparin is the universal anticoagulant in mammals and has fewer complications compared to hirudin [10]. Heparin became the anticoagulant of choice and its fractioned forms are still being used for hemodialysis [10].

The Dutch scientist, Willem Kolff, introduced the rotating drum hemodialysis system as seen in Figure 1.6. By using cellophane membranes in an immersion bath the first recovery of an acute renal failure patient treated with hemodialysis was reported [10].

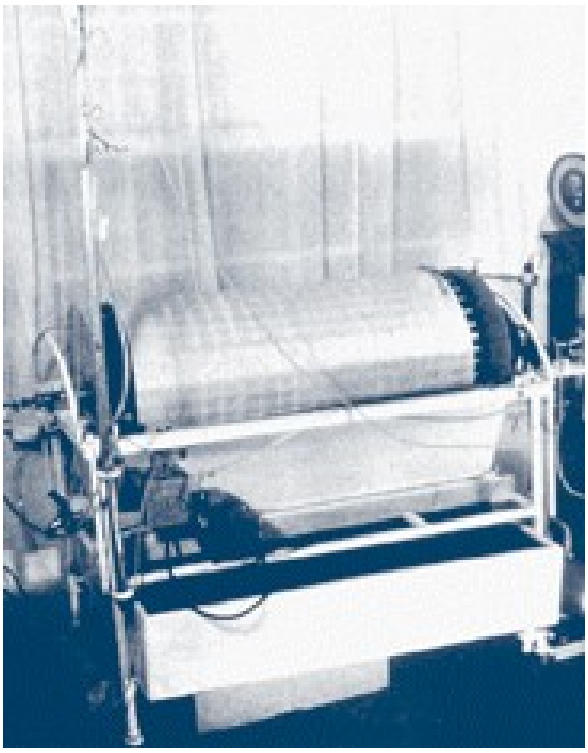

Figure 1.6 Kolff rotating drum kidney [10].

Kolff's rotating drum kidney used membranous tubes made from a new material known as cellophane that was actually used in the packaging of food [10]. During the treatment, the blood-filled tubes were wrapped around a wooden drum that rotated through an electrolyte solution known as "dialysate" [10]. As the membranous tubes passed through the bath, the uremic toxins would pass into this rinsing-liquid using the above mentioned physical principles.

Significant improvements in dialyzer and equipment design occurred during the 1940's and 50's. Nils Alwall developed a new system with a vertical stationary drum kidney and circulating dialysate around the membrane. He was also responsible for applying hydrostatic pressure to achieve ultrafiltration [10]. Kolff in turn developed the coil dialyzer using a tubular membrane wrapped around a solid core for use with a single

pass dialysis fluid delivery system. In 1960, Kiil developed the plate dialyzer which consisting of multiple polypropylene boards supporting flat cellulosic membranes [10]. This type of dialyzer could be used without a blood pump due to its low resistance as seen in Figure 1.7.

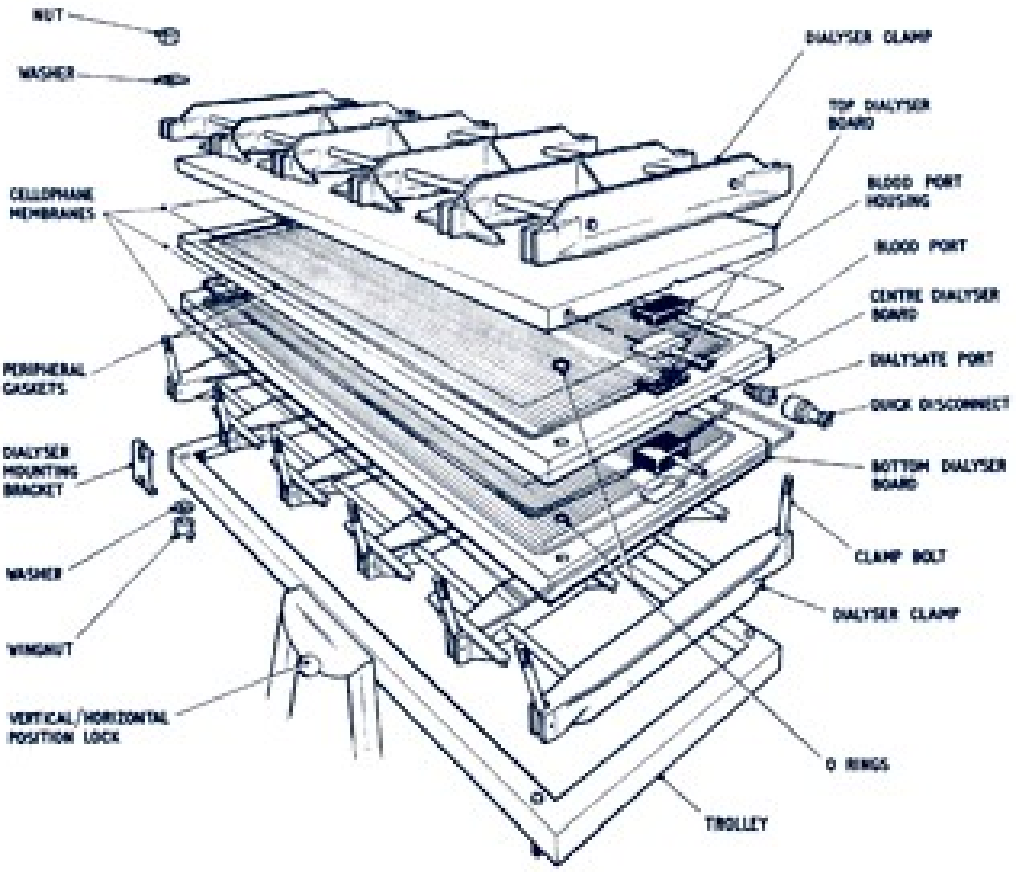

Figure 1.7 Schematic construction of a Kiil dialyzer [10].

After the invention of the arteriovenous (AV) shunt by Quinton and Scribner the door to chronic renal replacement therapy was opened [11].

The major developments over the past four decades related to improvements in membrane biocompatibility and dialyzer design, volumetric control, sophisticated monitoring systems that provide online clearances, isothermal dialysis, high flux membranes and convective modalities [10,11].

A major step forward was the development of the hollow-fiber dialyzer by Richard Stewart in 1964. This technology replaced the traditional membranous tubes and flat membranes with a number of capillary-sized hollow membranes. This procedure allows the production of dialyzers with a surface area large enough to fulfill the demands of efficient dialysis treatment [10].

The development of the related industrial manufacturing technology was completed by Dow Chemical between 1964 and 1967, with Dr. Ben Lipps [10]. This new technology allowed the production in subsequent years of large numbers of dialyzers at a reasonable price. The typical hollow-fiber dialyzers are still based on these concepts as seen in Figure 1.8.

Figure 1.8 The first family of hollow-fiber dialyzers [10].

As the clinical use of hemodialysis became increasingly widespread, scientists were better able to investigate the unique attributes of patients with chronic kidney disease. Although most hollow fiber dialyzers today resemble to those devices over 30 years ago, a number of variations in design have been established in order to optimize dialyzer performance.

1.3 Principles Of Modern Hemodialysis

Hemodialysis is a blood purifying therapy in which the blood of a patient is circulated through an artificial kidney, also called hemodialyzer [13]. This procedure was realized in an extracorporeal circuit as seen in Figure 1.9, where one or two needles (or catheters) can be used as the patient's vascular access. A general hemodialysis therapy lasts about 9-15 hours a week. Three hemodialysis sessions per week is the most common used type of dialysis therapy. The hemodialysis therapy takes place in the hospital, in a low care unit or at home.

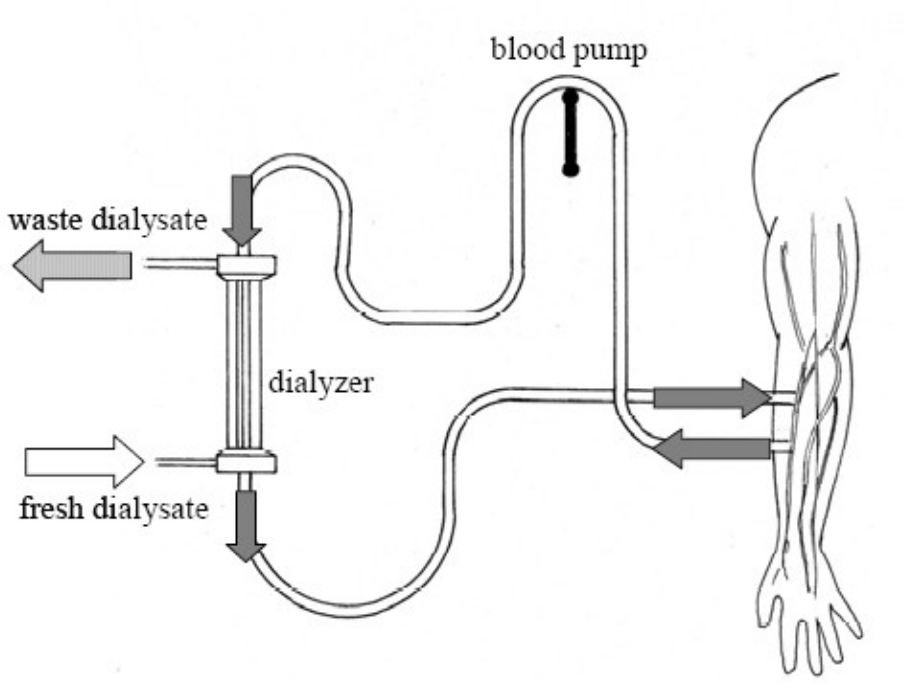

Figure 1.9 The extracorporeal circuit in hemodialysis [14].

A schematic diagram of a typical hemodialysis system is shown in Figure 1.10. The blood from the patient is circulated through a synthetic extracorporeal membrane and returned to the patient. The opposite side of that membrane is washed with an electrolyte solution (dialysate) containing the normal constituents of plasma. The apparatus contains a blood pump to circulate the blood through the system, proportioning pumps that mix a concentrated salt solution with water purified by reverse osmosis and/or deionization to produce the dialysate, a means of removing excess fluid from the blood (mismatching dialysate inflow and outflow to the dialysate compartment), and a series of pressure,

conductivity, and air embolus monitors to protect the patient. Dialysate is warmed to body temperature by a heater.

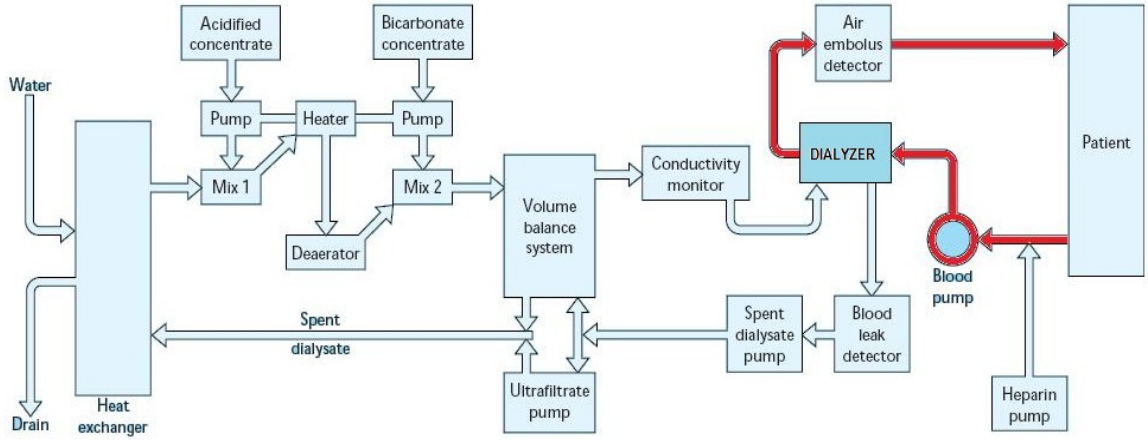

Figure 1.10 A schematic diagram of a of typical hemodialysis system [15].

A hollow fiber dialyzer consists of small capillaries as seen in Figure 1.11 [14]. Blood flows inside the capillaries whereas dialysate flows counter currently around them. Depending on the type of dialyzer used blood flow rates changes, while dialysate flows are preferably twice the blood flow on the other side of the dialysis membrane in the opposite direction of the blood flow. With respect to the membrane characteristics, distinction can be made between low, medium and high flux dialyzers . The ultrafiltration coefficient is lower than 15 mL/h/mmHg in low flux dialyzers [14, 16]. Medium flux dialyzers have an ultrafiltration coefficient between 15 mL/h/mmHg and 40 mL/h/mmHg. The ultrafiltration coefficient of high flux dialyzers is higher than 40mL/h/mmHg. Membrane surface area is lower than 1.5 m² in low area dialyzers and higher than 1.5 m² in high area dialyzers [16].

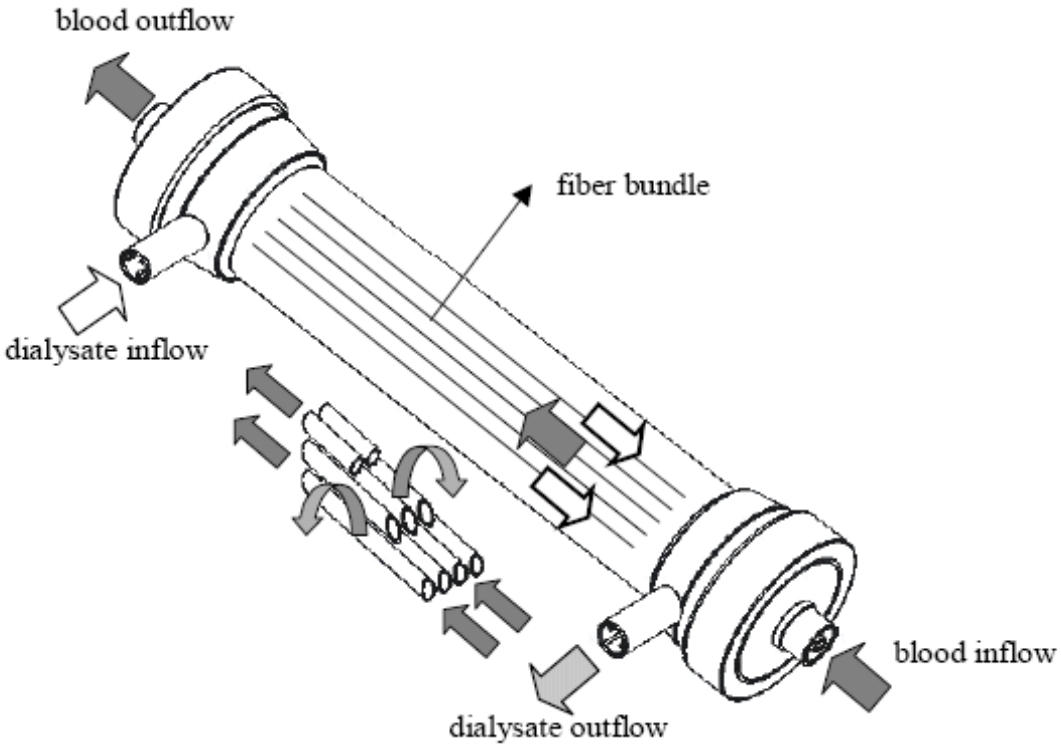

Figure 1.11 The hollow fiber dialyzer [14].

An adequate vascular access has always been an important issue for hemodialysis. Catheters are used for acute short phase of renal failure. The original subcutaneous internal arteriovenous fistula, described by Brescia and Cimino, between the arteria radialis and the vena cephalica is still the most successful vascular access method. In the latter, arterial flow and pressure dilates the vein, facilitating repetitive puncture. In case vessel conditions are inadequate or fail to dilate (10-30% of the patients), bridge grafts between an artery and a suitable vein are used. Several types of graft material are used, including autologous veins, allografts , and synthetic grafts . As hemodialysis implies a repeated and compulsory contact of blood with foreign materials, biocompatibility problems are unavoidable. Traditionally, biocompatibility is defined as the absence of functional and/or biochemical reaction during or after the contact of the body, a body fluid or an organ with an artificial device or a foreign material. Dialysis related biocompatibility problems are mainly due to the intermittent nature, the application of high blood flows, and the use of dialysis fluid and of semi-permeable membranes. They can be summarized as problems related to clotting phenomena, complement and leukocyte activation, susceptibility to bacterial and

tuberculosis infection, leaching, surface alterations, allergic reactions, shear, and inverse transfer of electrolytes, or endotoxins from the dialysate towards the blood .

Most membranes for hemodialysis are derived from cellulose. The most commonly used materials as low flux membranes were cuprophane, hemophan and cellulose acetate [15, 16]. These membranes are relatively porous to fluid and solute but do not allow large molecules like albumin and vitamin B12 to pass freely. Polysulfone, polyacrylonitrile, polymethylmethacrylate and polyamide membranes are more porous. These types of membranes or the membranes commonly used as high flux membranes in the dialyzers [15, 16]. The ideal properties of a hemodialysis membrane are summarized in Figure 1.12.

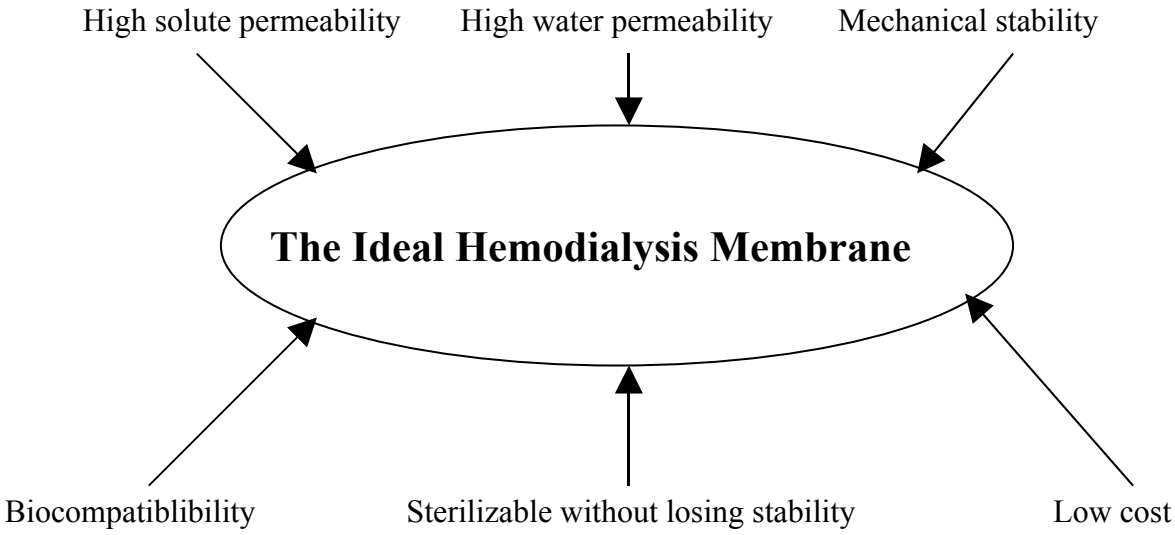

Figure 1.12 The ideal properties of a hemodialysis membrane.

1.4 High Flux Hemodialysis

Since the 1970s the need for shorter dialysis time with higher urea clearance rates has been the major cause for the development of high-flux hemodialysis. In the last decade the use of high-efficiency and high-flux membranes has increased and use of conventional low flux membrane has declined [17].

As high-flux membranes have larger pores, clearance of middle molecular weight molecules is usually high. Improved survival for hemodialysis patients has been reported for synthetic high flux biocompatible membranes [18, 19, 20]. With respect to previous method high flux dialysis has many advantages [20, 21]. Among them the best well known advantages of high flux hemodialysis are delayed onset and risk of dialysis-related amyloidosis because of enhanced ß2-microglobulin clearance, increased patient survival resulting from higher clearance of middle molecular weight molecules, reduced morbidity and hospital admissions, improved lipid profile, higher clearance of aluminum, improved nutritional status, reduced risk of infection and preserved residual renal function [21].

1.5 Objective Of The Thesis

As high flux membranes are facing a much more harsh environment compared to low flux hemodialysis membranes during hemodialysis, both virgin and used hollow fibers from two different dialyzers were compared in terms of the possible structural changes, chemical degradations, the effect of temperature, changes in the mechanical properties and alterations in the degree of crystallinity. The possible clinical effects of these changes and the reuse issue with these membranes were discussed.

2. MATERIALS, METHODS AND RESULTS

To our knowledge, there is no study performed about the effect of high flux dialysis on membrane stability. Also, there is no information in the open literature related to membrane stability by the help of analytical techniques used in this thesis.

Virgin and used hollow fibers used for this study originate from two dialyzers with two different membrane types. The first type of dialyzer consisted of hollow fibers made of polysulfone membrane and the other one consisted of hollow fibers made of polyamide membrane. Chemical structures of these polymers are given in Figures 2.1 and 2.2.

Used dialyzer membranes were obtained after the hemodialysis sessions of eight different patients with dialysis ages less than two years and without any accompanying systemic disease. The high flux hemodialysis sessions with these patients were performed at the Hemodialysis Department of Haydarpaşa Numune Hospital, because this hospital owns the necessary water treatment system designed for high flux hemodialysis.

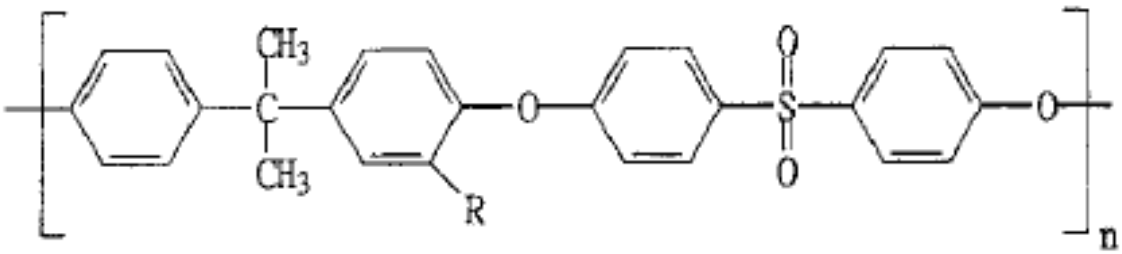

Figure 2.1 Chemical structure of polysulfone [22].

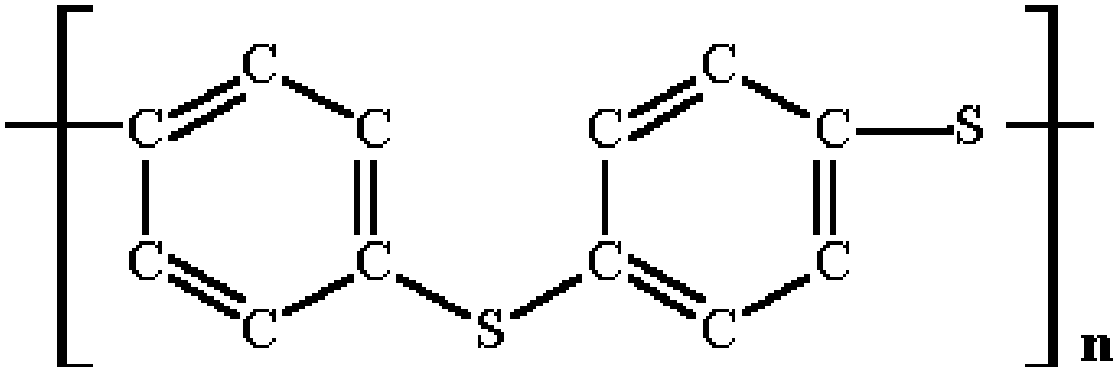

Figure 2.2 Chemical structure of polyamide [23].

Experimental methods used were selected to reveal mechanical and structural stability. Mechanical stability was studied by using Universal Mechanical Testing Machine. To get the idea about the effect of high flux dialysis on the structural stability of the membrane, microscopical, thermal, x-ray diffraction techniques and FTIR spectroscopy were used.

Both optical stereo microscopy and scanning electron microscopy studies were performed to reveal structural differences between two types of polymeric hollow fibers used in hemodialysis systems. X-Ray diffraction studies were performed in order to compare virgin and used dialysis membranes in terms of the degree of crystallinity. Differential scanning calorimetric studies were performed in order to reveal the effect of temperature on the chemical structure of hollow fibers used for dialysis. Mechanical tests were performed to compare mechanical properties of dialysis membranes before and after dialysis. The aim of using FTIR Spectroscopy in this study was to reveal the chemical degradation of dialysis membranes after dialysis if there is any.

2.1 Optical Microscopic Studies

Optical microscopical studies focus on the bundle configuration and the outer diameters of each hollow fiber [24].

2.1.1. Specimen Preparation For Optical Stereo-Microscopy

In order to evaluate the distribution of the hollow fibers, the dialyzers were cut at their upper part as seen in Figure 2.1.1. The pieces obtained by cutting procedure performed at Istanbul Technical University are shown on the following figures.

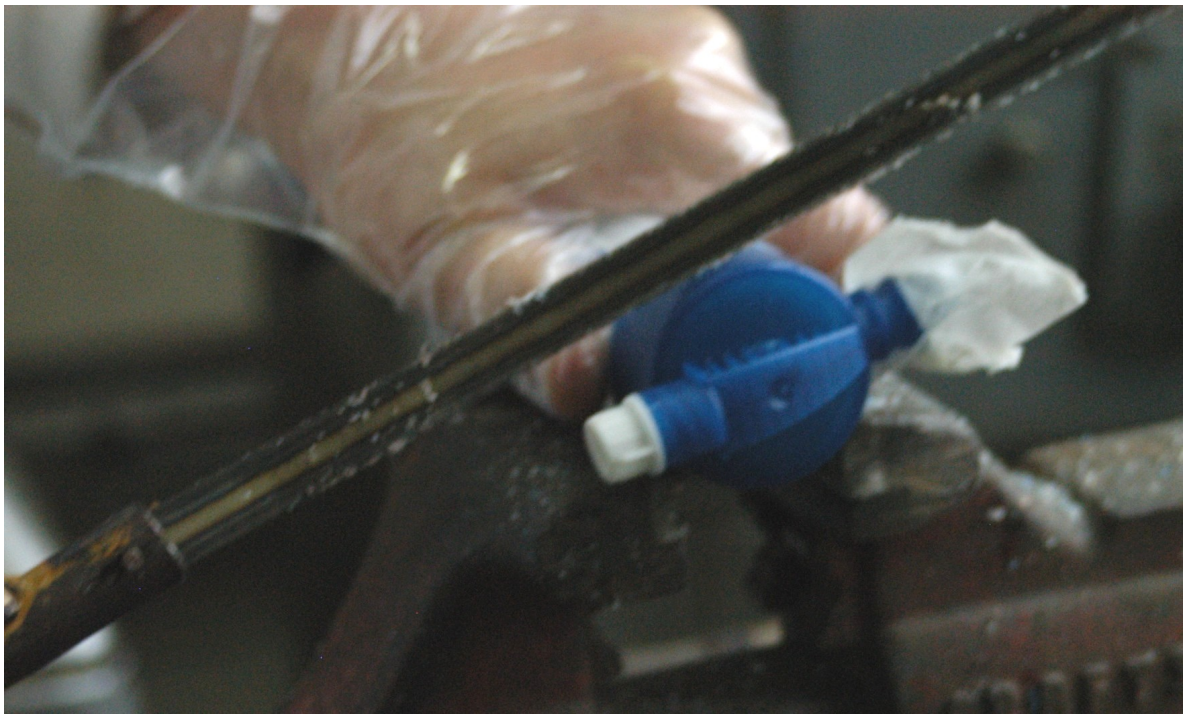

Figure 2.1.1 Cutting procedure of a dialyzer.

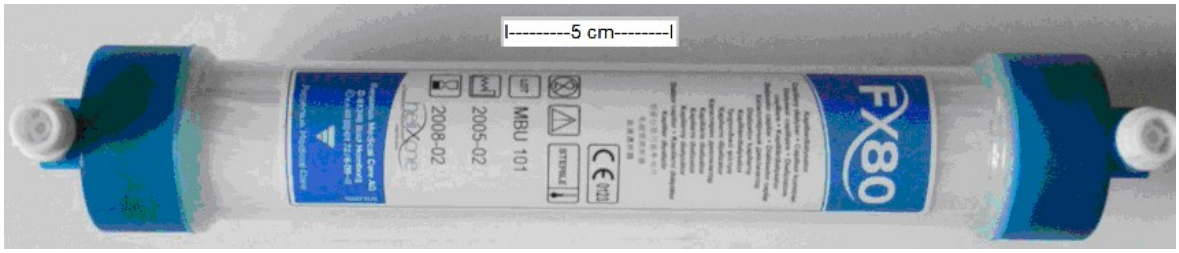

Figure 2.1.2 Virgin high flux type dialyzer with polysulfone membrane.

Virgin dialyzers manufactured by the Fresenius and Gambro are shown in Figures 2.1.2 and 2.1.3 respectively.

Figure 2.1.3 Virgin high flux type dialyzer with polyamide membrane.

2.1.2. Optical Stereo-Microscopic Studies Of Virgin Dialyzers

Optical microscopical studies were carried with Olympus stereomicroscope and Zeiss light microscope. The cross section of the dialyzer head originating from a dialyzer with polysulfone membrane is shown in Figure 2.1.4.

Figure 2.1.4 Cross section of a head section of a dialyzer with virgin polysulfone hollow fibers.

Figure 2.1.5 shows the cross section of the dialyzer head originating from a dialyzer with polyamide membrane.

Figure 2.1.5 Cross section of a head section of a dialyzer with virgin polyamide hollow fibers.

A homogeneous blood and dialysate flow distribution improve small solute clearances, which can be achieved by modifying the configuration of the filter bundle [25]. The different bundle configurations of hollow fibers in two different virgin dialyzers are shown in Figures 2.1.6 and 2.1.7.

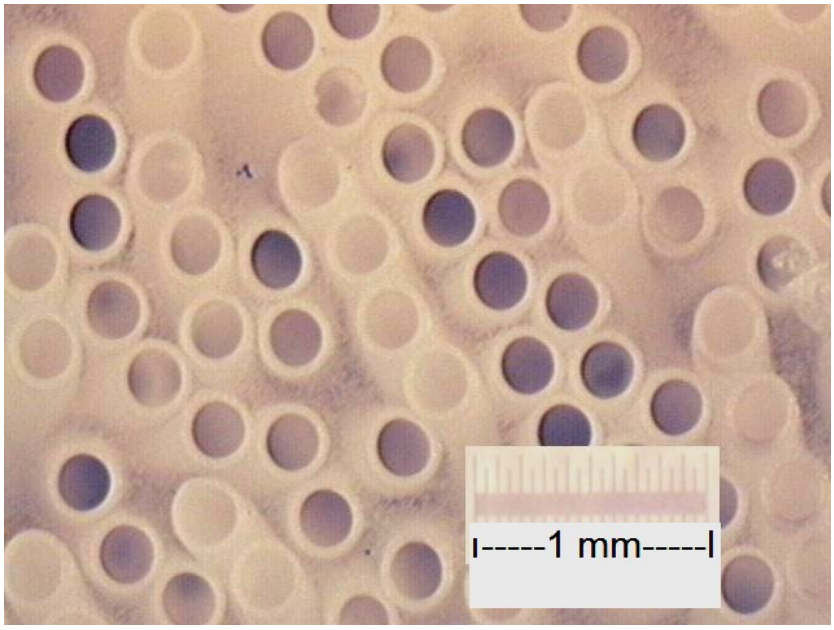

Figure 2.1.6 Stereomicroscopic view of the hollow fiber distribution from a dialyzer with polysulfone membrane .

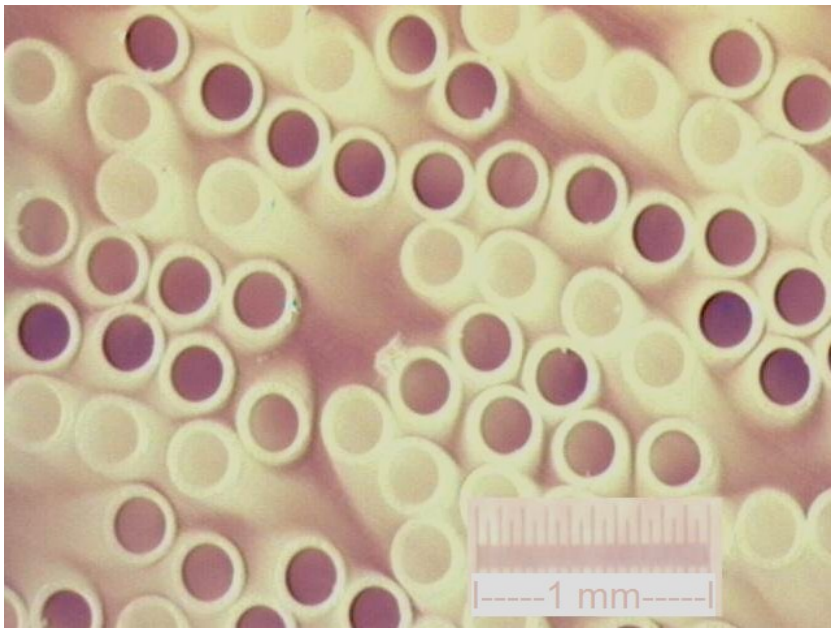

Figure 2.1.7 Stereomicroscopic view of the hollow fiber distribution from a dialyzer with polyamide membrane.

In order to obtain the outer diameters of polyamide and polysulfone fibers, the pictures of these fibers were taken from the lateral side using optical stereo microscopy.

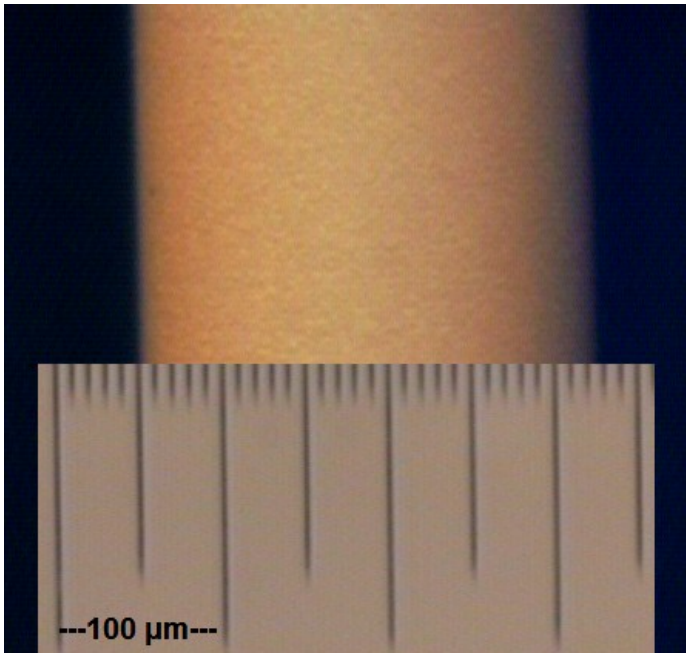

Figure 2.1.8 Stereo microscopic view of a virgin hollow fiber from a dialyzer with polysulfone membrane from the lateral side.

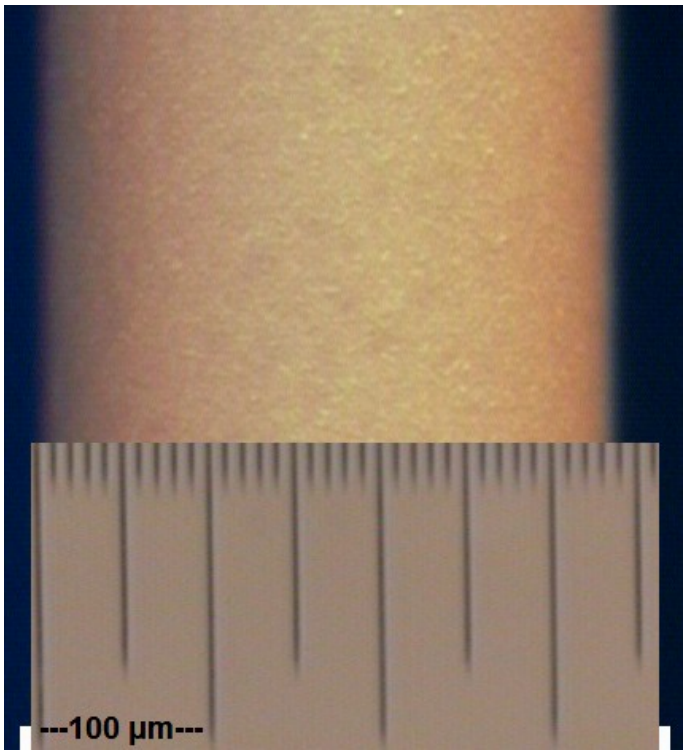

Figure 2.1.9 Stereo microscopic view of a virgin hollow fiber from a dialyzer with polyamide membrane from the lateral side.

Figures 2.1.8 and 2.1.9 show that the outer diameter of a virgin polysulfone fiber is approximately 265 μm and the outer diameter of a virgin polyamide fiber is approximately 320 μm. Data obtained from the optical microscopic studies have been compared with the data from the Scanning Electron Microscopy studies.

2.1.3. Optical Stereo-Microscopic Studies Of Used Dialyzers

Dialyzer upper parts of dialyzers with used polysulfone hollow fibers are shown in Figure 2.1.10.

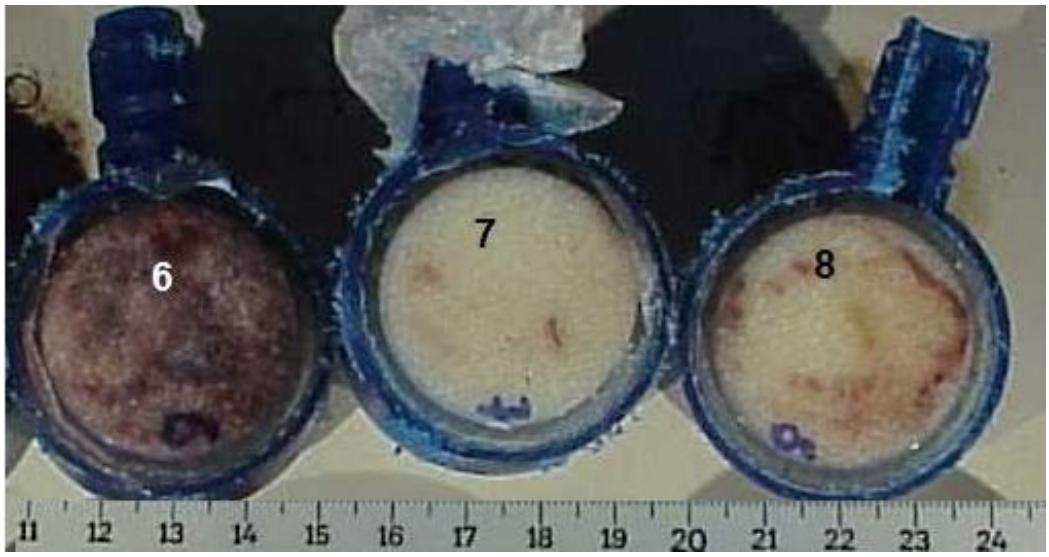

Figure 2.1.10 Upper parts of used polysulfone dialyzers after cutting.

Dialyzer upper parts of dialyzers with used polyamide hollow fibers are shown in Figure 2.1.11.

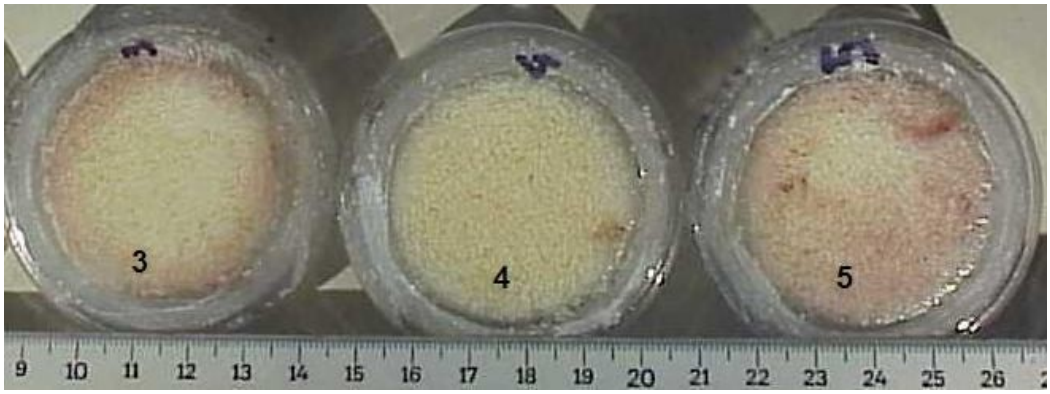

Figure 2.1.11 Upper parts of used polyamide dialyzers after cutting.

The hollow fibers of a used dialyzer are observed in Figure 2.1.12.

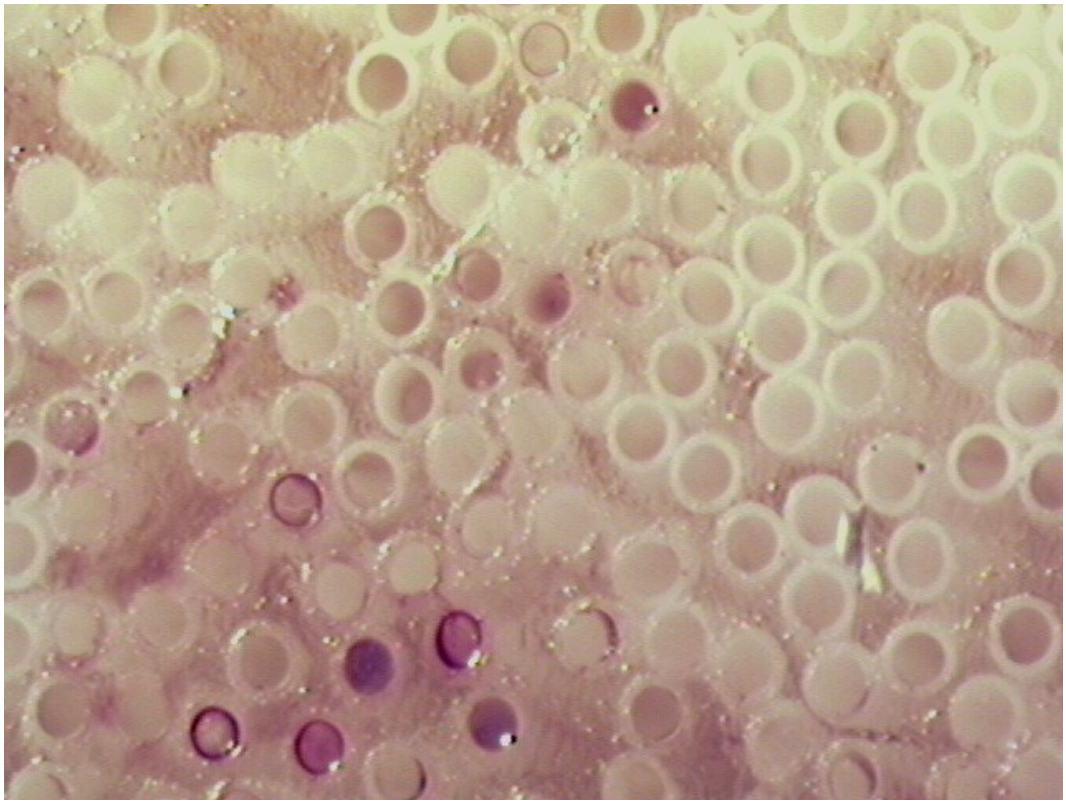

Fig 2.1.12 Hollow fibers of a used dialyzer with polyamide hollow fibers.

As seen on Figures 2.1.10, 2.1.11 and 2.1.12 blood residues are seen in some hollow fibers. These blood residues may be caused either by improper rinsing or insufficient use of anticoagulants during dialysis.

2.2. Scanning Electron Microscopy (SEM)

Scanning Electron Microscopy (SEM) studies were performed by using both Philips XL30 SFEG Scanning Electron Microscope and with JEOL JSM-6400 Scanning Electron Microscope. Philips XL30 SFEG Scanning Electron Microscope is shown in Figure 3.2.1 and JEOL JSM-6400 Scanning Electron Microscope is shown in Figure 2.2.2.

Figure 2.2.1 Philips XL30 SFEG Scanning Electron Microscope.

Fig 2.2.2 JEOL JSM-6400 Scanning Electron Microscope.

SEM studies of both polysulfone and polyamide hollow fibers were performed on lateral and fracture surfaces of used and virgin dialyzers. Fracture surfaces were obtained via rupturing of the samples in liquid nitrogen, after tensile tests and loading-unloading-reloading cycle.

2.2.1. Results Of SEM Studies On Virgin Polysulfone Membranes

The major observation from SEM studies on lateral surfaces of the membrane is the diameter measured relatively with low magnification. This is also kind of confirmation what is obtained by using stereomicroscope as seen in Figure 2.1.8 in the section of optical microscopical studies. Figure 2.2.3 shows clearly that the diameter of polysulfone membrane is around 250 microns.

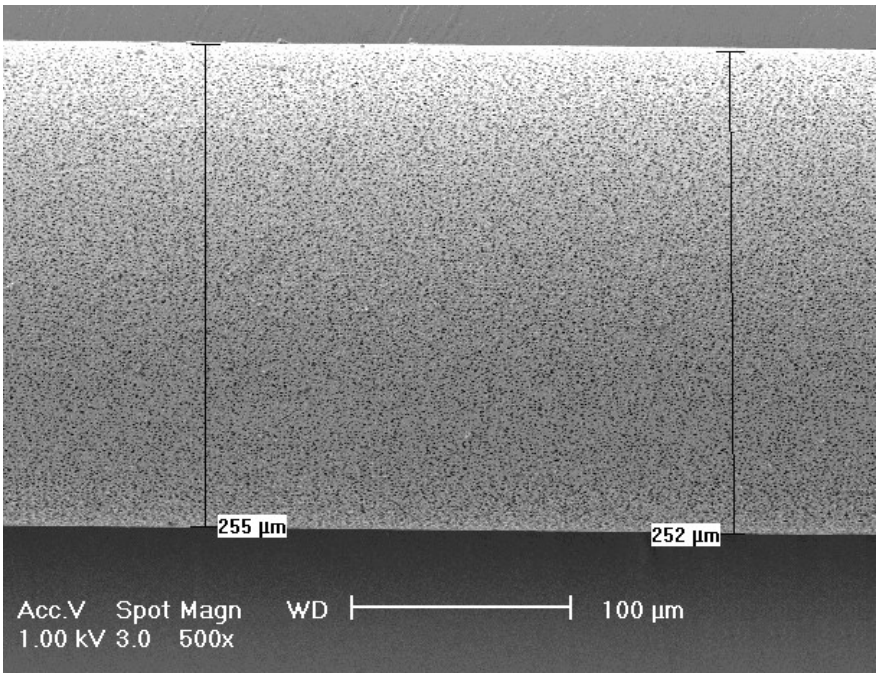

Figure 2.2.3 Lateral view of a polysulfone membrane .

These values were compared with the data on the original datasheet of the dialyzer with polysulfone membrane [26]. On the original technical datasheet and the outer diameter of the hollow was given as 255 µm.

SEM image taken from the lateral wall surface of a virgin polysulfone membrane is seen in Figure 2.2.4. Another SEM image of the same specimen with a relatively higher magnification is shown in Figure 2.2.5. The diameters of the pores at the dialysate side of the virgin polysulfone membrane vary from 565 nm up to 2,14 µm.

In both Figures 2.2.4 and 2.2.5 pores with variable diameters are observable.

Although pores on the outer surface of the dialysis membrane are not exactly spherical, they are elliptic with the axes close to each other in terms of dimensionally.

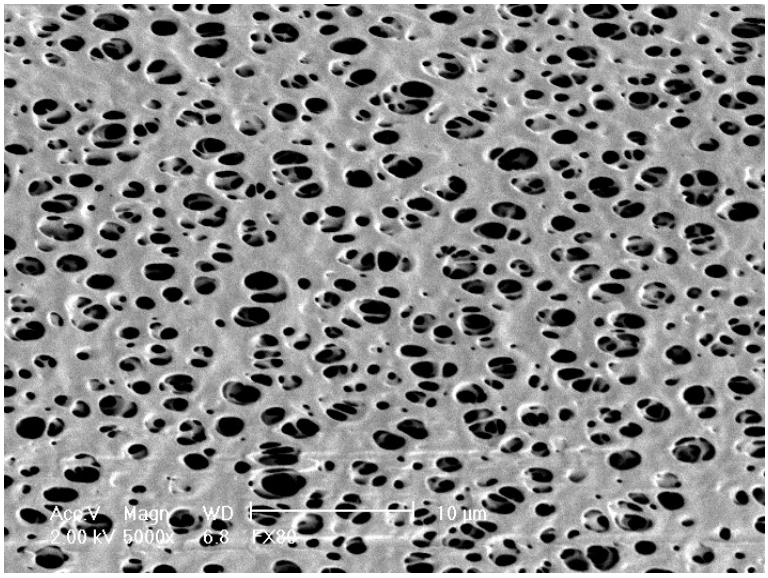

Figure 2.2.4 Lateral surface a virgin polysulfone membrane and pore distribution.

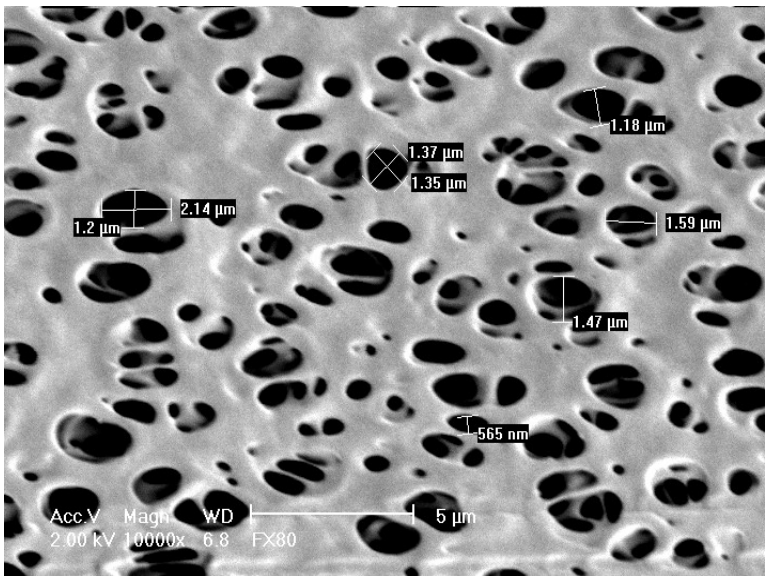

Figure 2.2.5 Lateral surface of a virgin polysulfone membrane and pore distribution.

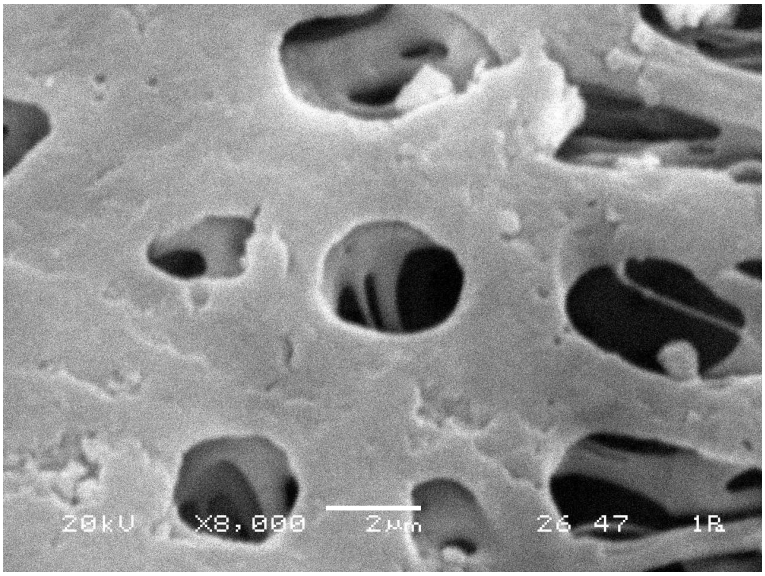

Figure 2.2.6 Lateral surface of a virgin polysulfone membrane.

Figure 2.2.6 shows inner morphology of the pore. The size and morphology from the surface to the inside show changes and different type of continuation such as some ligaments are observed.

Fracture surfaces of virgin polysulfone membranes after rupturing in liquid nitrogen are shown on Figure 2.2.7.

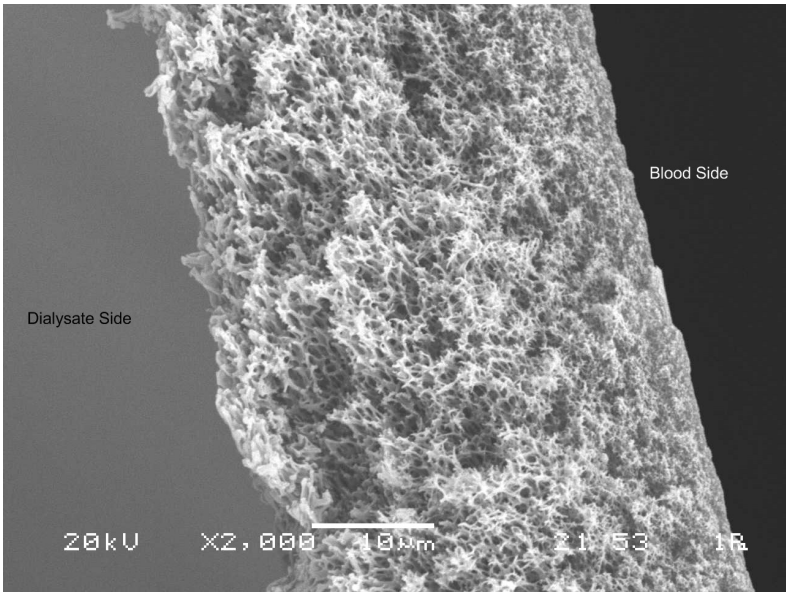

Figure 2.2.7 Fracture surface of a virgin polysulfone membrane obtained by rupturing in liquid nitrogen.

Figure 2.2.7. shows fracture surface of hollow fiber; a lot of pores with different sizes are clearly visible. From the outside to the inside especially the places being close to the wall have pores with the sizes decreasing. These features can be observed in a more distinct way on the Figure 2.2.8, that has higher magnification. Even in addition to the trend mentioned above, greater holes, which possibly were created due to ruptures of the ligaments, are observed.

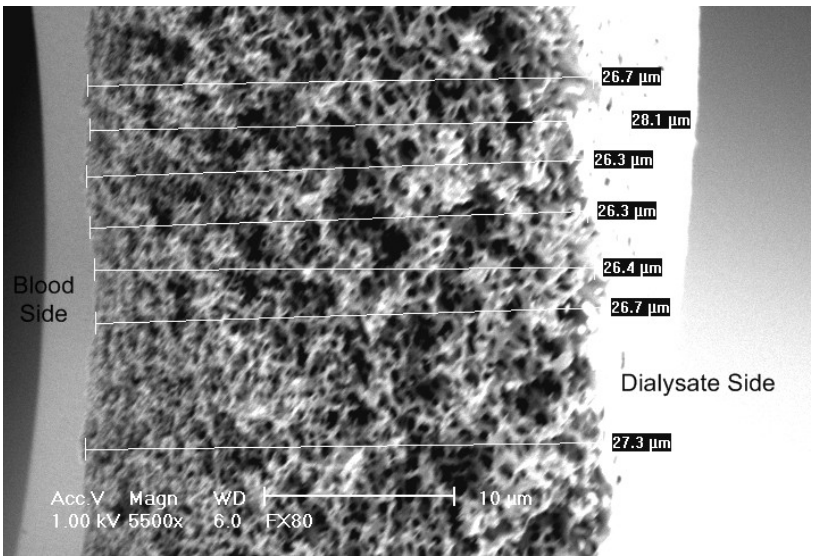

Figure 2.2.8 Fracture surface of a virgin polysulfone hollow fiber obtained by rupturing in liquid nitrogen. The wall thickness values are marked on the picture.

The wall thickness of a virgin polysulfone hollow fiber was measured as between 26 µm and 28 µm as seen in Figure 2.2.8. On the original technical datasheet the wall thickness of the hollow fiber was given as 35 µm [26]. The membrane wall consists of a sponge like structure which becomes much denser from the dialysate side to the blood side of the polysulfone hollow fiber.

After tensile test surface of polysulfone membrane is changed; Figure 2.2.9 shows that pores outside of the fiber are elongated, i.e. the axes of ellipse have greater differences comparing with the unstressed fiber surfaces.

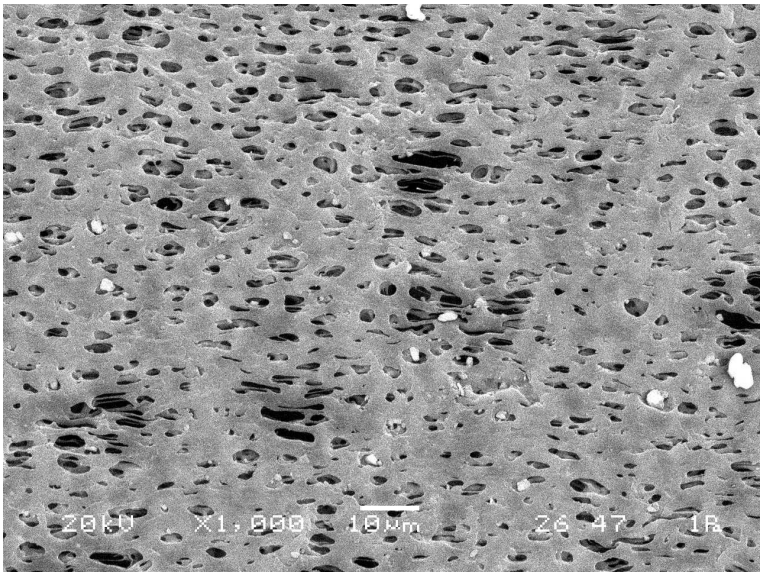

Figure 2.2.9 Elongated pores outside of a virgin hollow fiber after tensile test.

After tensile test, surface of polysulfone membrane is changed; Figure 2.2.9 shows, that pores outside of the fiber are elongated, i.e. the axes of ellipse have greater differences comparing with unstressed fiber surfaces. SEM images on Figure 2.2.10 were taken from used membranes after tensile test in order to show the fracture surface.

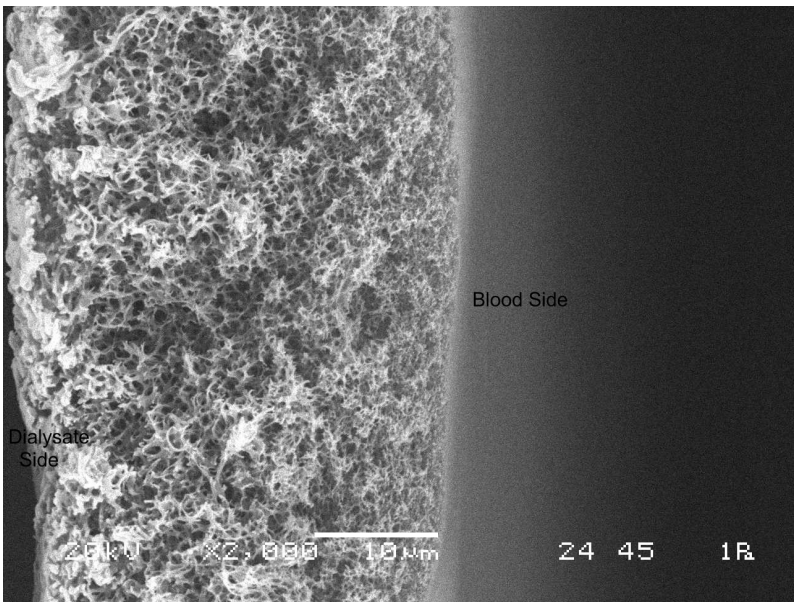

Figure 2.2.10 Fracture surface of a virgin polysulfone membrane after tensile test.

Loading-unloading-reloading cycle caused more merging of the pores so that

greater holes are created as seen on Figure 2.2.11.

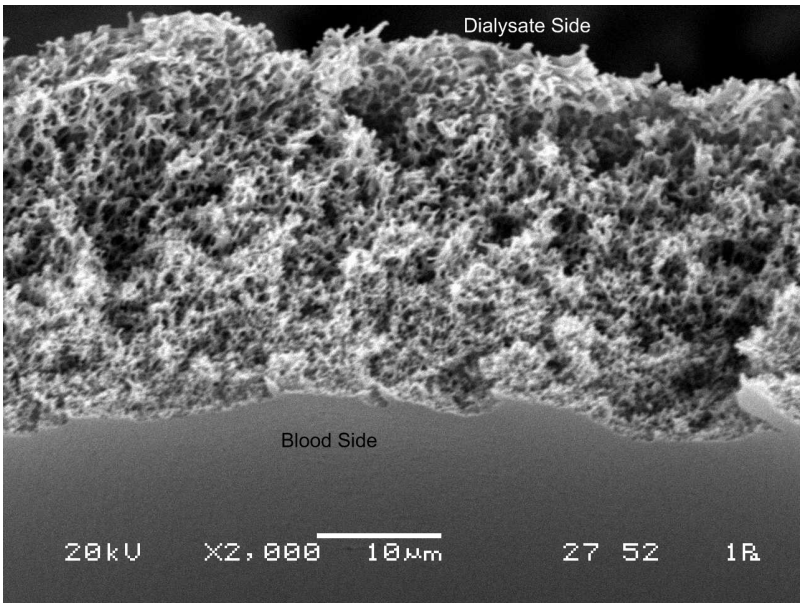

Figure 2.2.11 Fracture surface of a virgin polysulfone membrane obtained by loading-unloading and reloading.

2.2.2. Results Of SEM Studies On Used Polysulfone Membranes

SEM Studies on lateral surfaces of used polysulfone membranes are shown in Figures 2.2.12 and 2.2.13.

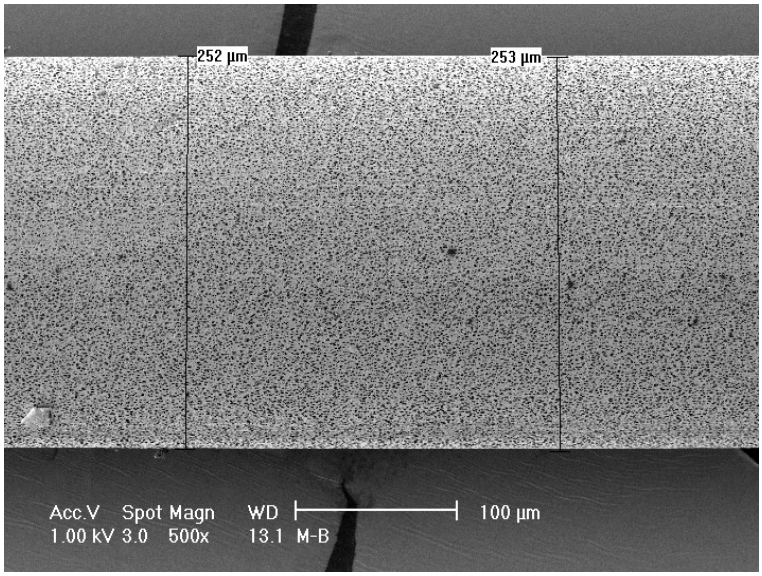

Figure 2.2.12 Lateral surface of a used polysulfone membrane (Dialysate side).

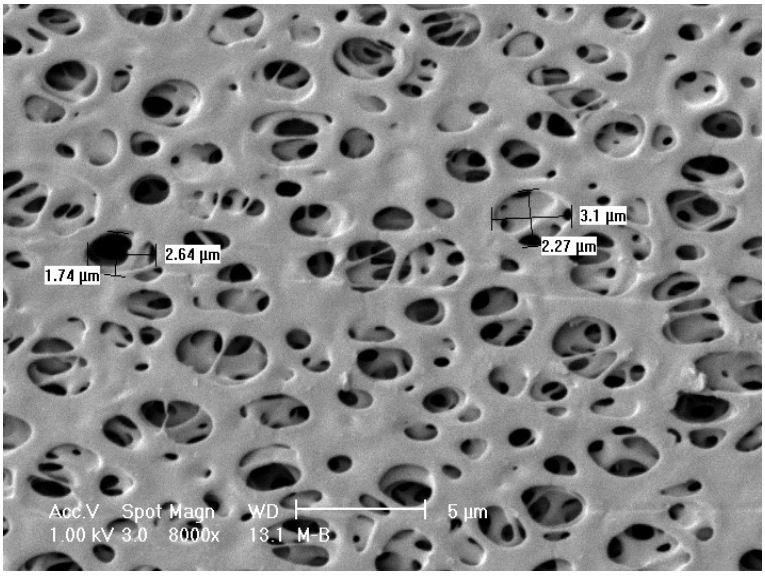

Figure 2.2.13 Lateral surface of a used polysulfone membrane (Dialysate side).

As seen on these SEM images, there is no remarkable change in the value of outer diameters of virgin and used polysulfone hollow fibers. Figure 2.2.13 shows the pores of the membrane on both surface and partially inside of the surface. Inside of the pore comparing to what is observed on the virgin membrane has different morphology depicting changes inside of the pore.

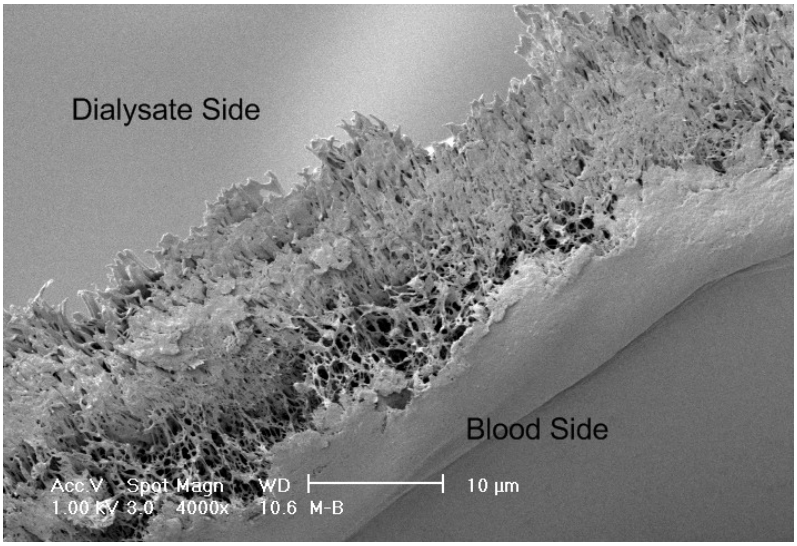

Figure 2.2.14 Fracture surface of the polysulfone used membrane after rupturing in liquid nitrogen.

Fracture surface studies by using SEM were also performed on used polysulfone membranes. The sample ruptured in liquid nitrogen shows extensive damage and smearing. This kind of SEM picture gives information together with sudden increase in pore size and many mergings of the pores close to inside of the lateral surface at the dialysate side as seen in Figure 2.2.14.

Figure 2.2.15 shows fracture surface of the polysulfone used membrane after tensile test; on the fracture surface merging of the pores are clearly visible. There are residues from dialysis inside of the surface of the membrane (blood side).

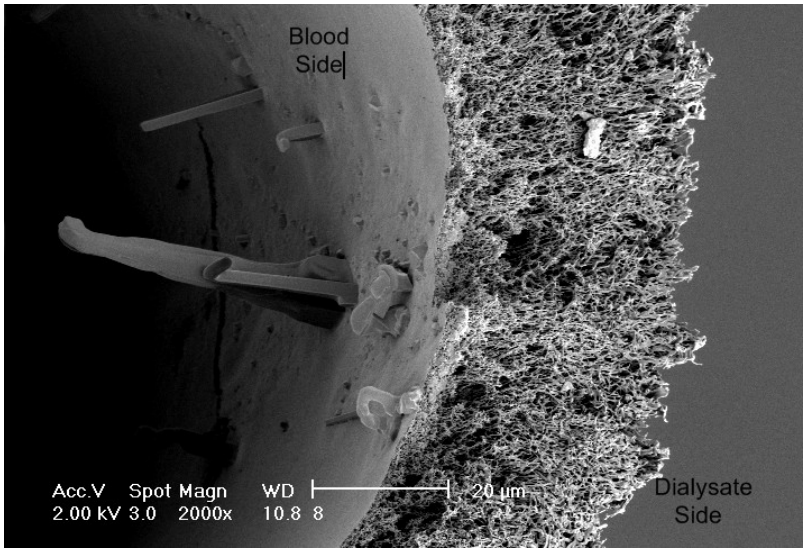

Figure 2.2.15 Fracture surface of the polysulfone used membrane after tensile test.

2.2.3. Results Of SEM Studies On Virgin Polyamide Membranes

In order to reveal the wall structure, changes in the fracture surface, pore distribution and outer wall diameters SEM studies were performed on virgin and used polyamide hollow fibers.

The SEM image from the lateral wall of the virgin polyamide hollow fiber is shown on Figure 2.2.16 - 2.2.18. SEM picture of polyamide membrane shows that the diameter of the fiber is 300 µm and confirms roughly what is measured by the help of stereo microscope.

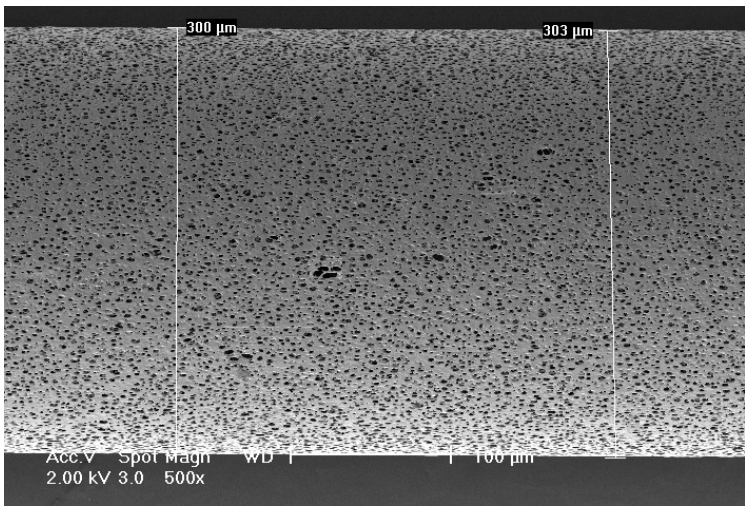

Figure 2.2.16 Lateral view of a virgin polyamide membrane.

Diameters of virgin polyamide hollow fibers were measured as around 300 μm as seen on Figure 2.2.16. This value was compared with the data on the original datasheet of the dialyzer with polyamide membrane [27]. On the original technical datasheet the wall the outer diameter of the hollow was given as 315 μm [27].

Figure 2.2.17 and 2.2.18 give information about the pore sizes and pore distribution at the dialysate side of the polyamide hollow fiber. There are elliptic pores with diameters varying between 529 nm and 5,05 μm.

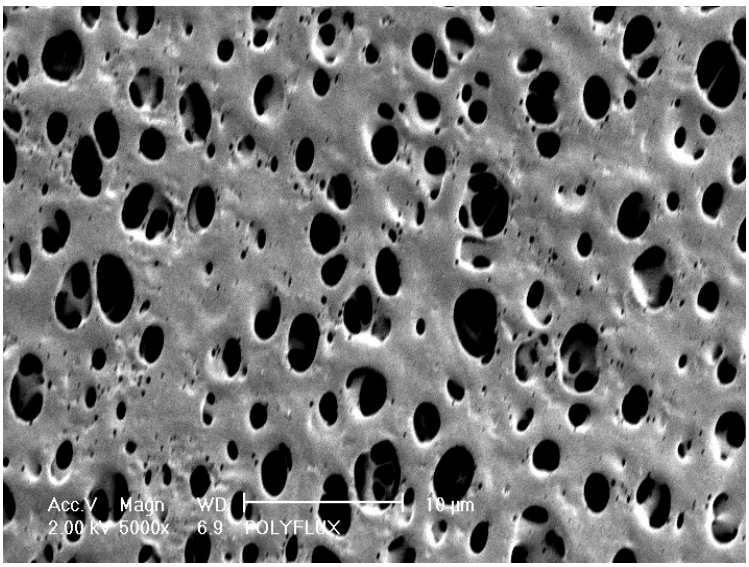

Figure 2.2.17 Lateral surface of a virgin polyamide membrane and pore distribution.

Figures 2.2.19 and 2.2.20 give information on the pore morphology and the distribution of pores on the surface of polyamide hollow fiber. Geometrical axes of the pores do not have relatively big differences as seen in Figure 2.2.20.

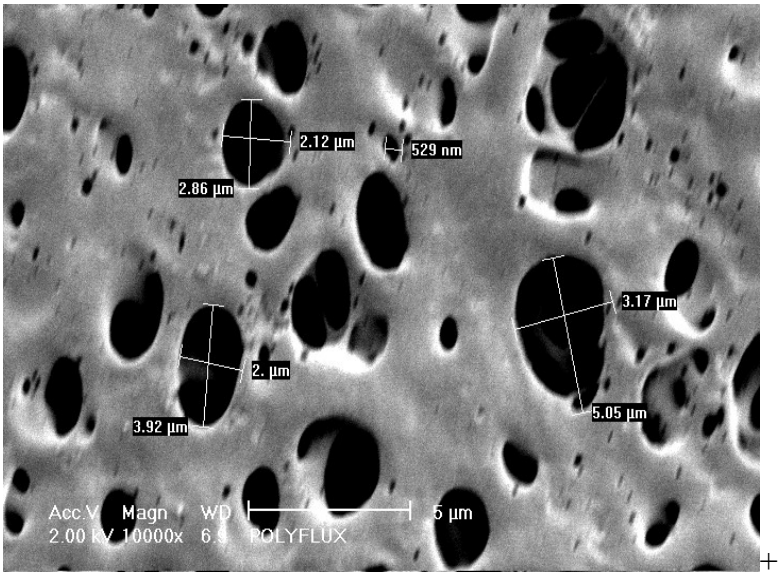

Figure 2.2.18 Lateral surface of a virgin polyamide membrane and pore distribution.

Figure 2.2.19 depicts elongated pores on the surface of virgin polyamide after tensile test. Tensile test also affects on the changing of the morphology below the pores as seen in Figure 2.2.19.

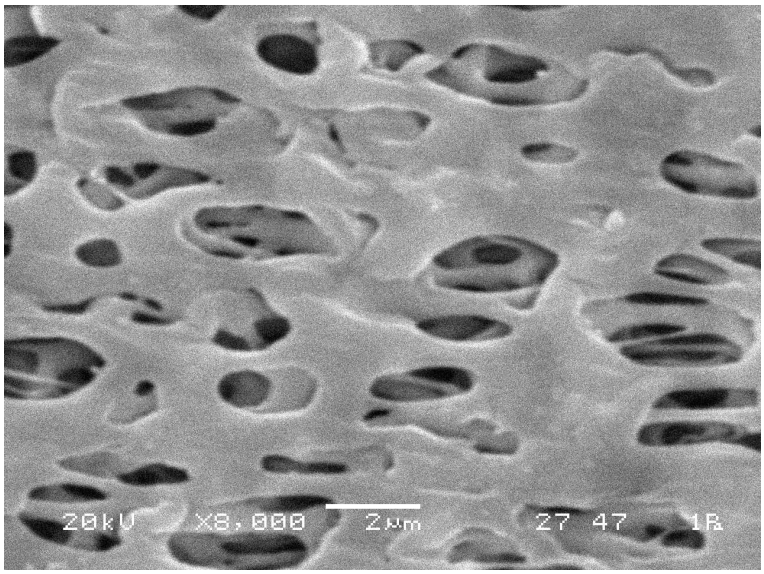

Figure 2.2.19 Lateral surface of a virgin polyamide membrane after tensile test.

Fractographical studies were also performed with virgin polyamide hollow fibers. Virgin polyamide hollow fibers were ruptured in liquid nitrogen in order to obtain detailed information about the wall structure of the membrane.

Figure 2.2.20 shows fracture surface of the polyamide virgin membrane ruptured in liquid nitrogen. On the fracture surface, pores are visible but the pores on the blood side are not visible inside of the capacity of the microscope used. In the same time merging of the pores causing holes is visible.

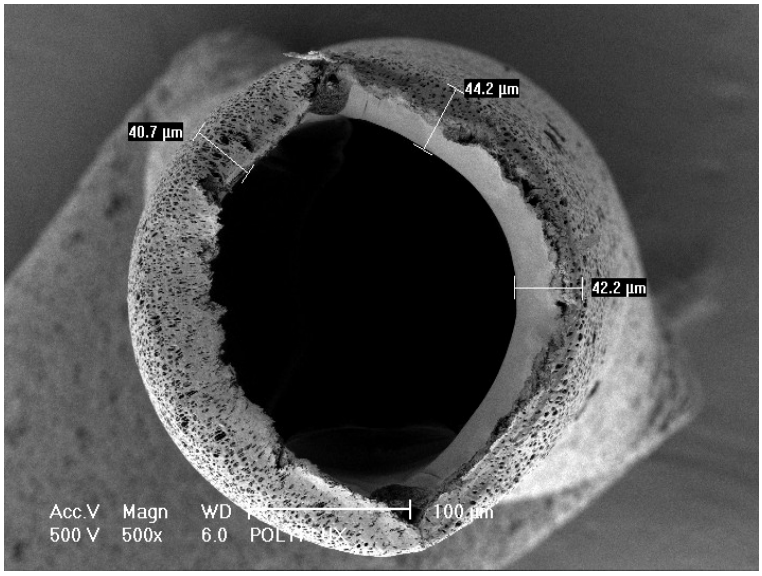

Figure 2.2.20 Fracture surface (ruptured in liquid nitrogen) of a virgin polyamide membrane .

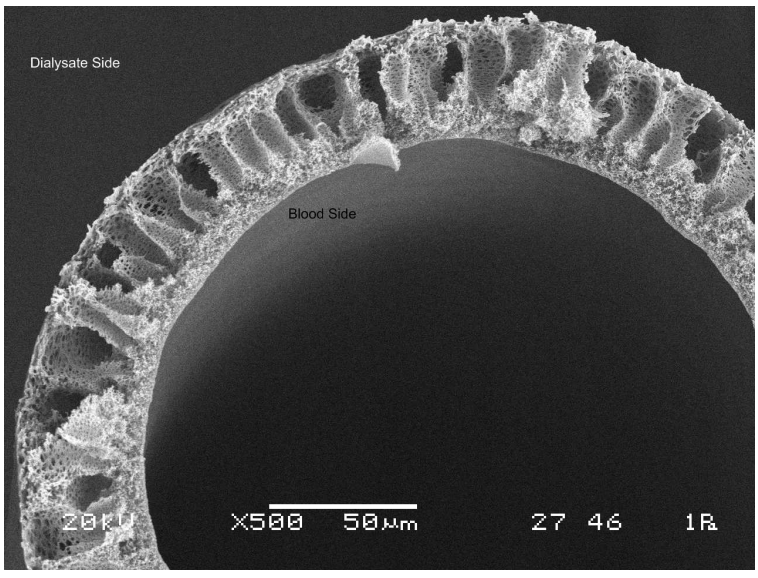

Figure 2.2.21 Fracture surface of a virgin polyamide membrane after tensile test.

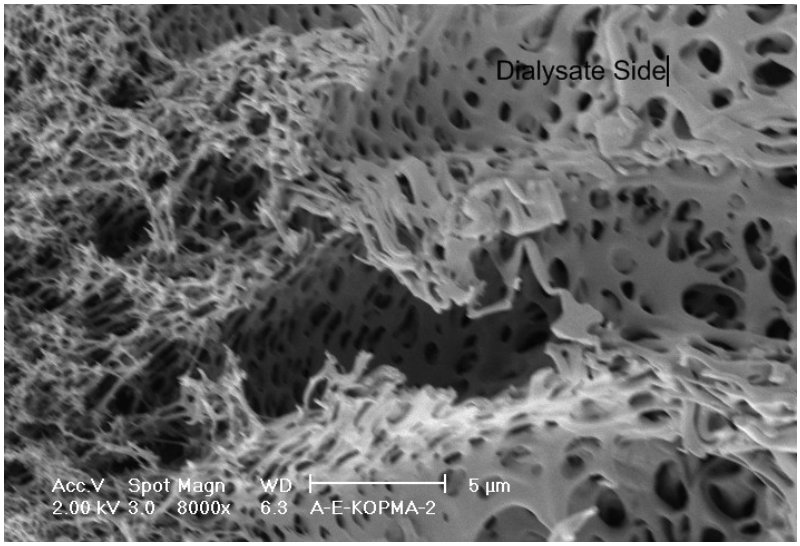

Figure 2.2.22 A side lateral view of the fracture surface of a virgin polyamide membrane after tensile test.

Stressing under monotonic tensile loading caused creation of greater holes which can be considered as merging of many pores into each other as seen in Figures 2.2.21 and 2.2.22.

2.2.4. Results Of SEM Studies On Used Polyamide Membranes

SEM studies were performed on used polyamide membranes before and after tensile test.

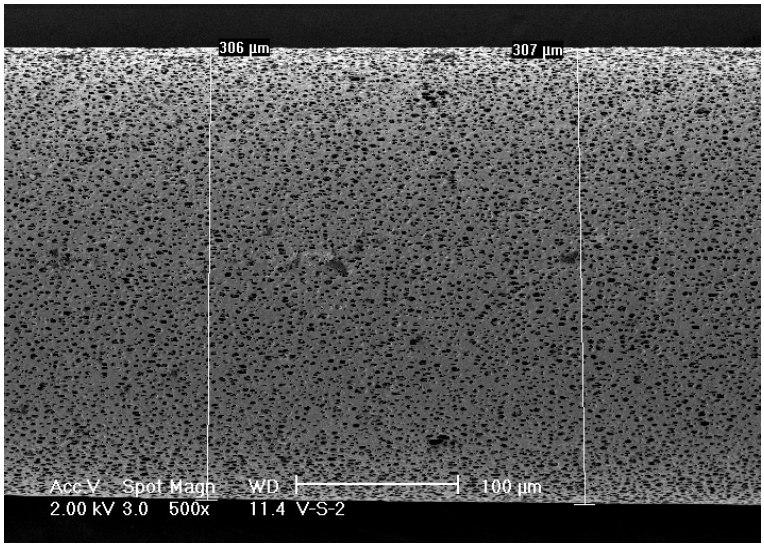

Figure 2.2.23 Lateral surface of a used polyamide membrane (Dialysate side).

Lateral surface of the used polyamide fibers is seen on Figures 2.2.23 - 2.2.24. Elongated pores and morphological changes below the pores are visible in Figure 2.2.24.

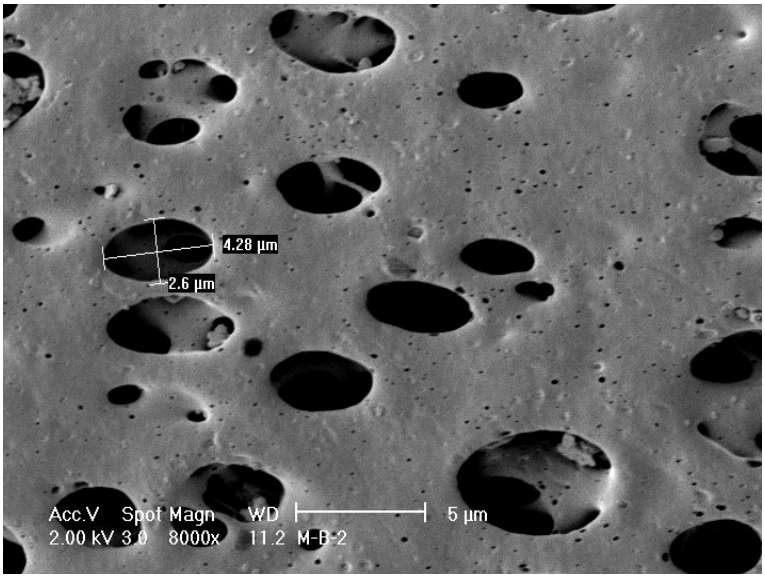

Figure 2.2.24 Pores on the lateral surface of a used polyamide membrane .

SEM studies of used polyamide membranes were first performed after monotonic loading of the used polyamide hollow fibers. SEM Studies on lateral surface of polyamide stressed by monotonic tensile test clearly show many mergings of the pores so that a lot of holes are clearly visible on the surface as seen in Figures 2.2.25 - 2.2.26.

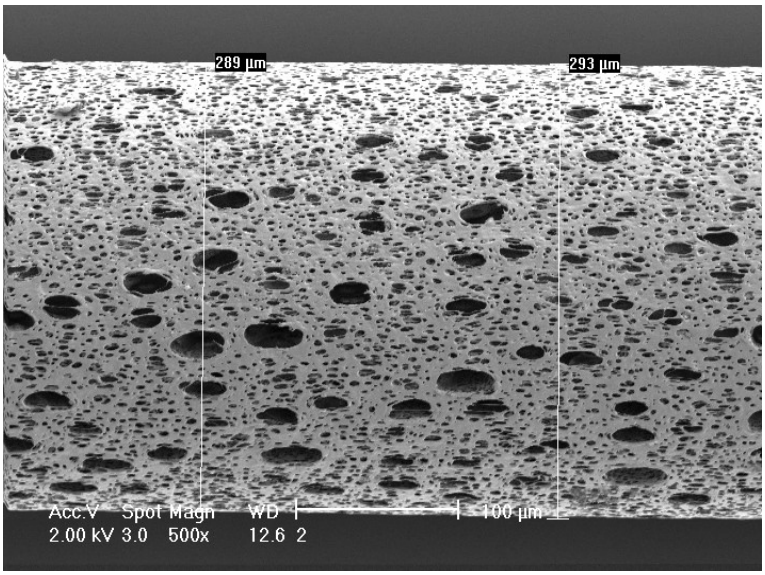

Figure 2.2.25 Lateral surface of a used polyamide membrane after tensile test.

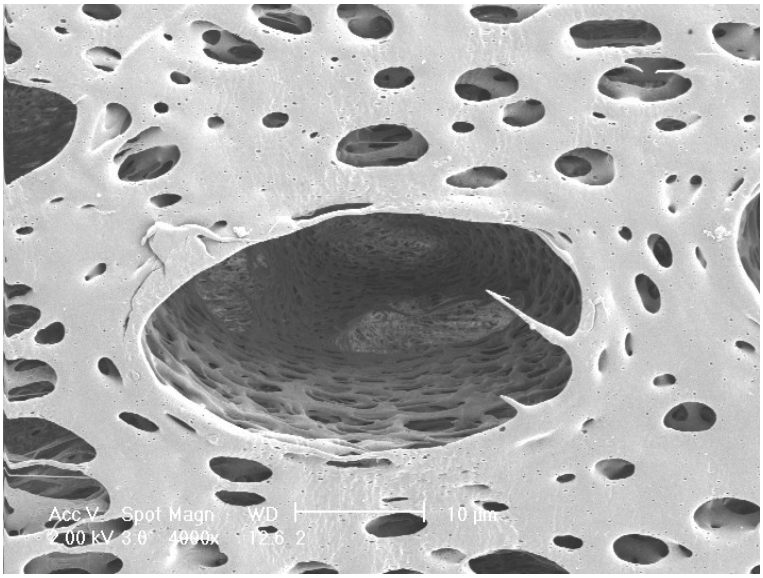

Figure 2.2.26 Pores of polyamide membrane merging into each other and rupturing of the ligaments during tensile test.

Figure 2.2.26 includes one of the holes created by merging as mentioned above; inside of the hole there ruptured ligaments and pores which may represent interconnection of the pores on the dialysis membrane.

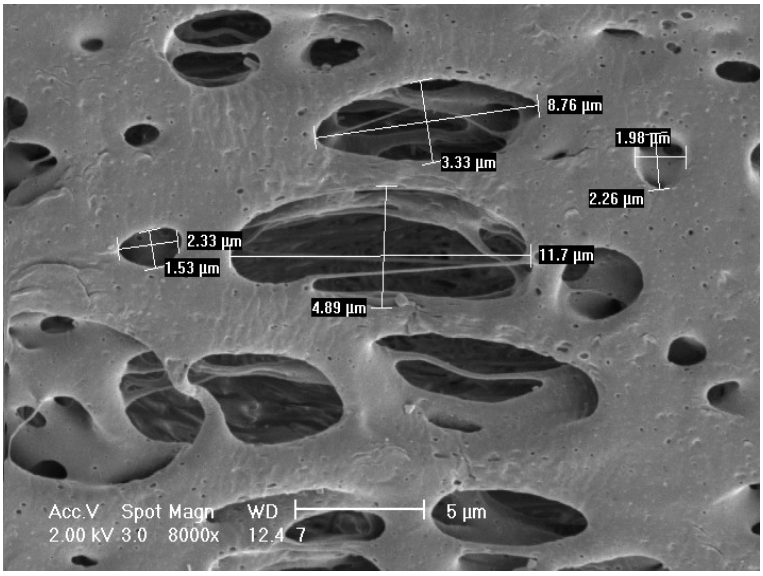

Figure 2.2.27 Elongated pores of a used polyamide membrane after tensile test.

Figure 2.2.27 shows elongated pores together with morphological changes below the pores after tensile test.

2.3 Mechanical Tests

During dialysis internal and external pressures are applied to the dialysis fibers by the pump of the hemodialysis machine, dialysate and blood. The dialysis membrane has to withstand these pressures during hemodialysis, because any damage in any part of the hemodialysis membrane will cause blood leakage from the blood side of the membrane into the dialysate side of the membrane. If it is not noticed by medical staff or if there is any failure in the blood leakage alarm system of the hemodialysis machine, this leakage would cause fatal results. In this context, the mechanical properties of dialysis membranes become important and should be investigated.

In order to make the analysis of a mechanical test independent of the materials size, it is useful to define a quantity called stress (σ) [28, 29, 30]. Stress is defined as the force (*F*) divided by the cross-sectional area (*A*) of the material where force is acting (units N/m2 = Pa). The elongation is mostly quantified as engineering tensile strain (ε) which is defined as the length change (Δl) divided by the initial length (l_0) [28, 29, 30].

In order to calculate the cross-sectional area, which is imperative for the calculation of engineering stress of the fibers, the following formula was used:

The value of engineering stress was calculated as;

$$\textit{Stress } (\sigma) = \textit{Applied Force } (F) \,/\, \textit{Cross sectional area of a fiber } (A) \qquad (2.3.1)$$

The value of engineering strain (%) was calculated as;

$$\textit{Strain } (\%) = \Delta l / l_0 \times 100 \; (\Delta l = \textit{elongation}, \; l_0 = \textit{initial gauge length}) \qquad (2.3.2)$$

Tensile tests were performed by using Instron Universal tensile test machine shown in Figure 2.3.1.

Figure 2.3.1 Instron 5565 Universal tensile test machine.

Each mechanical test was performed for five times. All tests were run at room temperature in laboratory environment. Crosshead speed was kept constant (50mm/min) and the gauge length was 40 mm for all tensile tests. In addition to monotonic tensile test another kind of tensile loading until fracture following unloading from the stress value being 90% of fracture stress value obtained by prior tensile tests was performed on used hollow fibers. The reason for this kind of test is to observe what may happen before going to cyclic loading.

2.3.1 Tensile Test Results On Virgin Polysulfone Membranes

Figure 2.3.2 shows a graph prepared by using average values of typical tensile test results for virgin polysulfone membranes after monotonic loading until fracture.

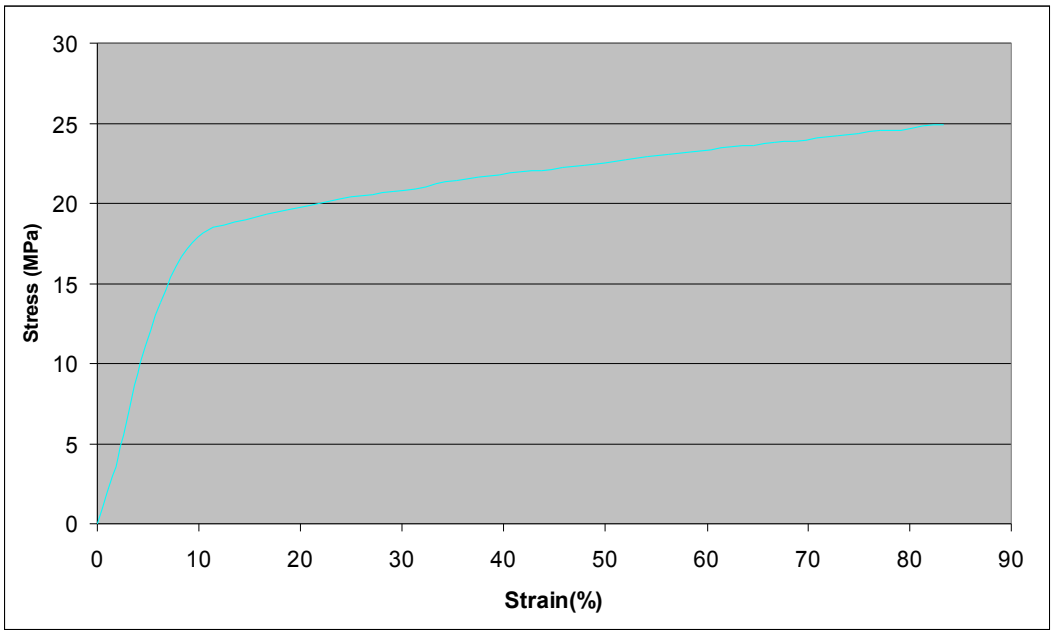

Figure 2.3.2 Tensile test results of a hollow fiber consisting of virgin polysulfone membrane.

2.3.2 Tensile Test Results On Used Polysulfone Membranes

Tensile test results of used polysulfone membrane are given below. Tensile test results of the hollow fibers from the dialyzer used for patient M.K. and virgin polysulfone hollow fibers are shown in Figures 2.3.3 - 2.3.4.

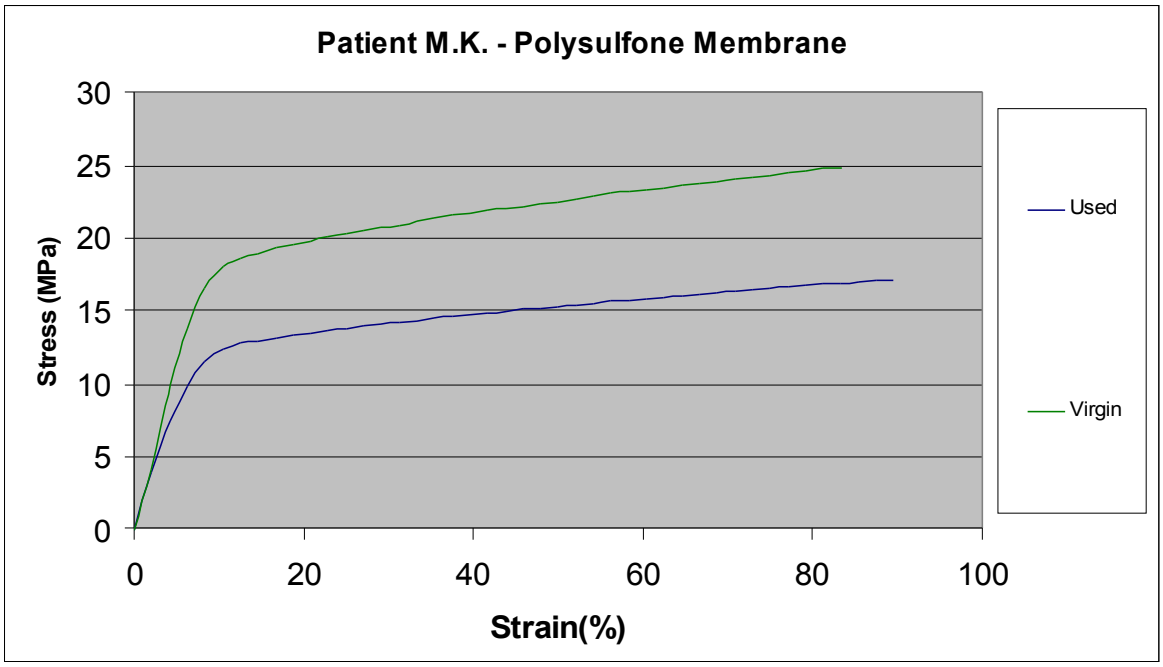

Figure 2.3.3 Tensile test result of virgin and used polysulfone hollow fibers (Patient M.K.).

Tensile test results of the hollow fibers from the dialyzer used of the patient I.C. and virgin polysulfone fibers can be observed in Figure 2.3.4.

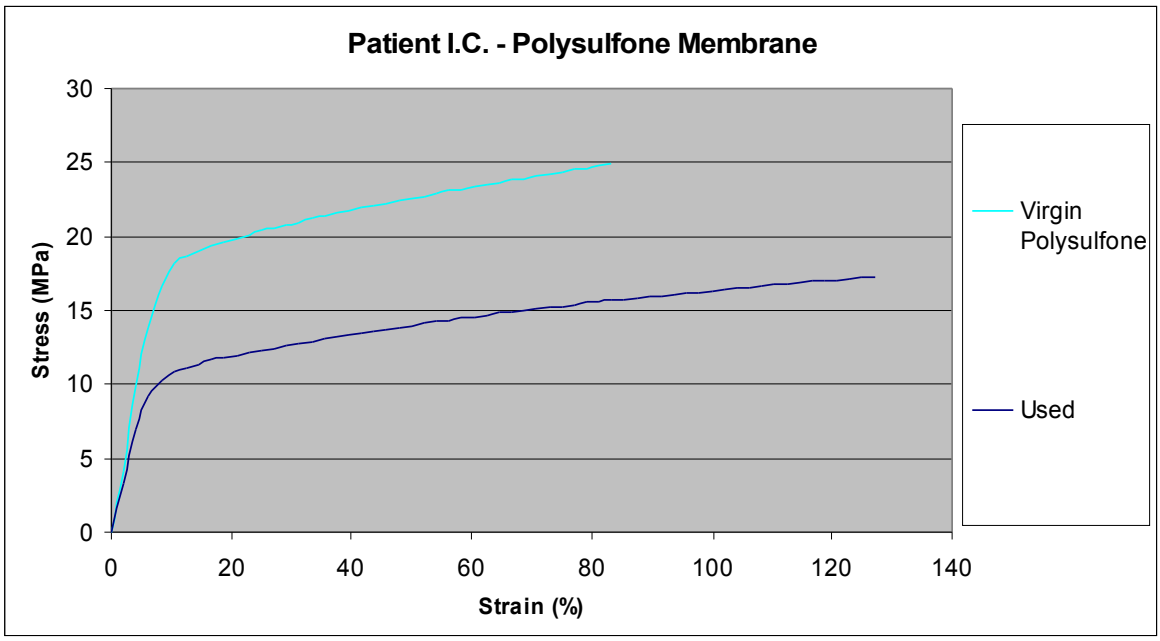

Figure 2.3.4 Tensile test result of virgin and used polysulfone hollow fibers (Patient I.C.).

Tensile test curves of the hollow fibers from the dialyzer used of the patient A.F.K. and virgin polysulfone fibers are shown in Figure 2.3.5.

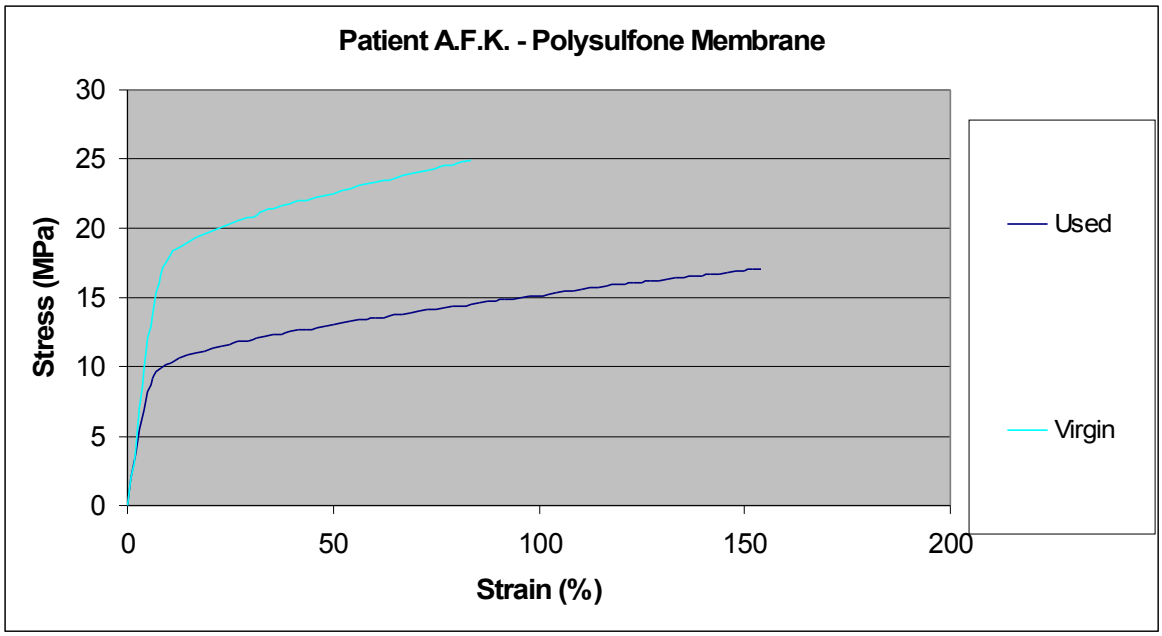

Figure 2.3.5 Tensile test result of virgin and used polysulfone hollow fibers (Patient A.F.K.).

2.3.3 Results Of Load-Unload-Reload Experiments On Used Polysulfone Membranes

Engineering stress-strain curves obtained during reloading following loading until 90% of ultimate tensile strength of a used polysulfone hollow fiber and then unloading from dialyzers used for three different patients were given in Figures 2.3.6 - 2.3.8.

Figure 2.3.6. shows the tensile test data obtained from used polysulfone hollow fibers and used polysulfone fibers from patient M.K. after loading-unloading-reloading cycle.

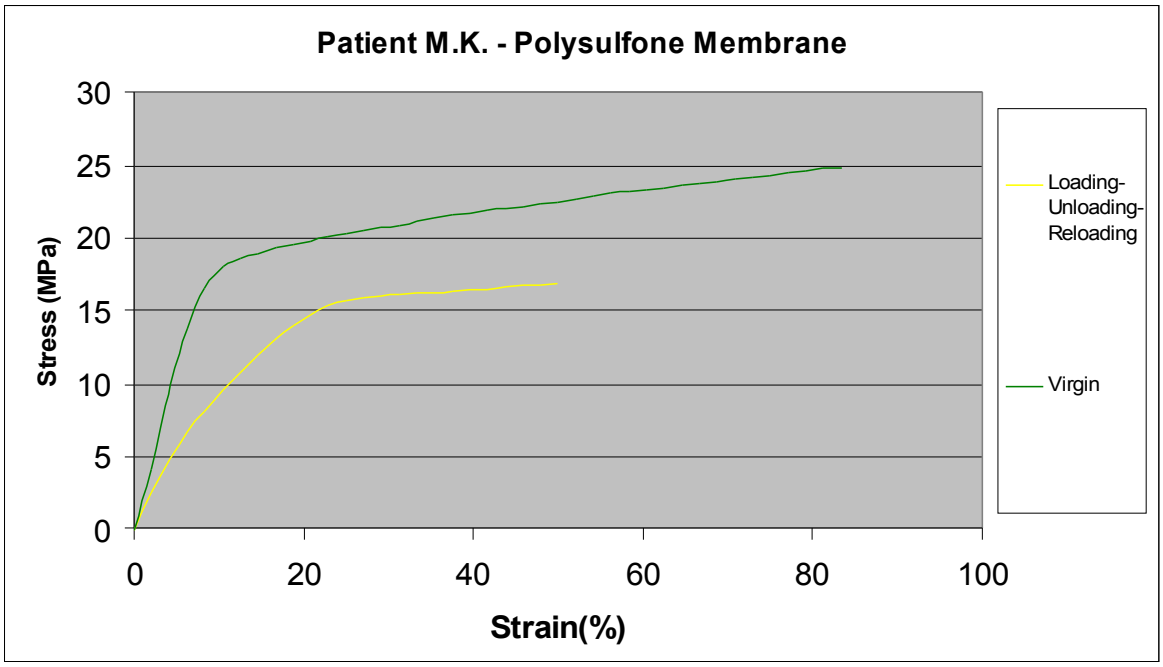

Figure 2.3.6. Tensile test results of virgin and used polysulfone hollow fibers after loading-unloading-reloading (Patient M.K.).

The comparison of tensile test results of virgin polysulfone hollow fibers and used hollow fibers from patient I.C after loading-unloading-reloading can be observed in Figure 2.3.7.

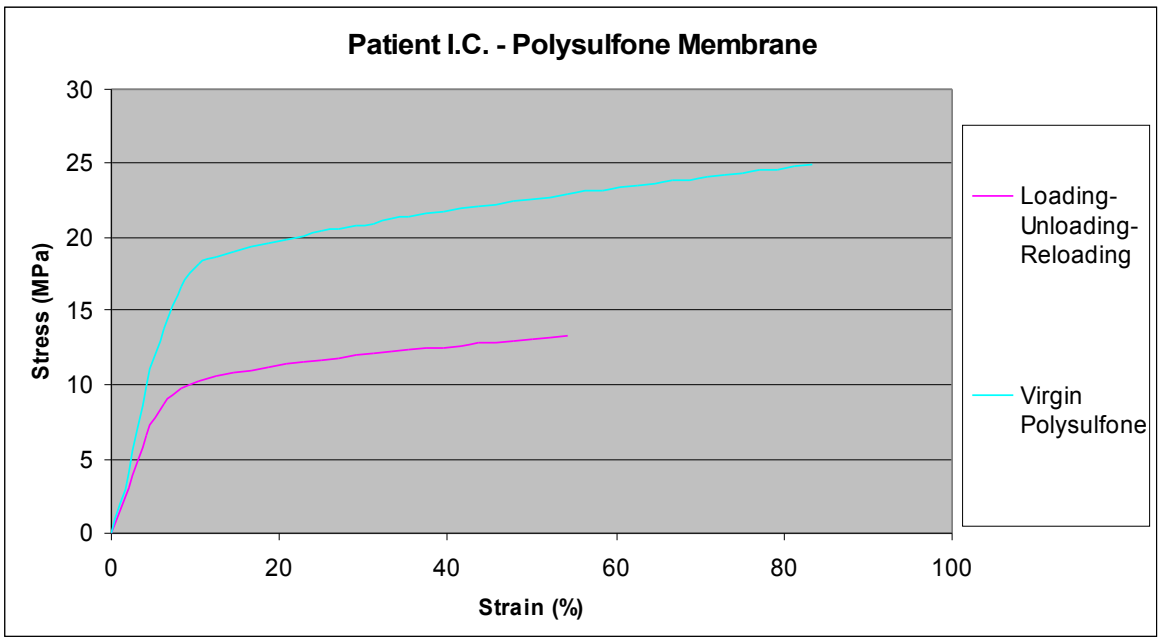

Figure 2.3.7 Tensile test results of virgin and used polysulfone hollow fibers after loading-unloading-reloading (Patient I.C.).

Figure 2.3.8 shows tensile test data of used fibers from patient A.F.K. after dialysis and used polysulfone hollow fibers from patient A.F.K. after loading-unloading-reloading.

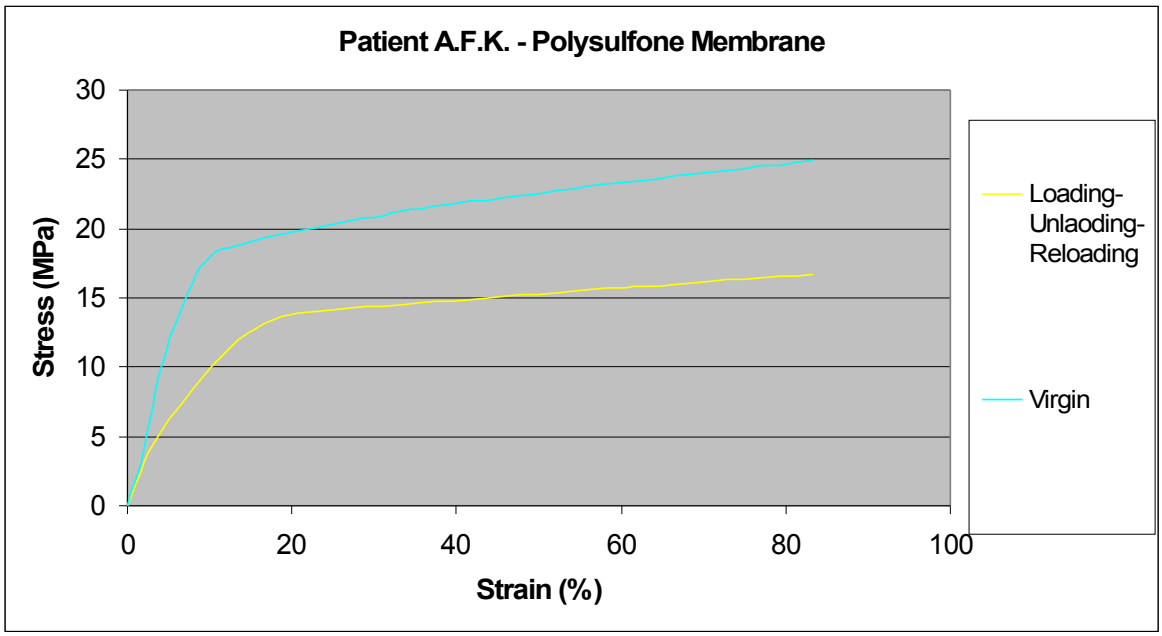

Figure 2.3.8 Tensile test results of virgin hollow fibers after dialysis and used polysulfone hollow fibers after loading-unloading-reloading (Patient A.F.K.).

Depending on the results of tensile test studies, it was concluded that virgin polysulfone membranes can resist higher stresses compared to used membranes. Fracture stress of a used polysulfone membrane decreases compared to the values of the virgin membranes. The toughness of polysulfone membranes, which can be represented with the area under stress-strain curve, after single use is also decreased compared to virgin polysulfone membrane. After loading-unloading-reloading procedure both toughness and ultimate tensile strength values of used polysulfone membranes decrease when compared to that of virgin polysulfone membranes.

Tensile test data reveal that polysulfone membranes are becoming more brittle with loading-unloading and reloading processes.

2.3.4 Tensile Test Results On Virgin Polyamide Membranes

Figure 2.3.9 shows graphs prepared by using average values of typical tensile test results belonging to polyamide membranes after monotonic loading until fracture.

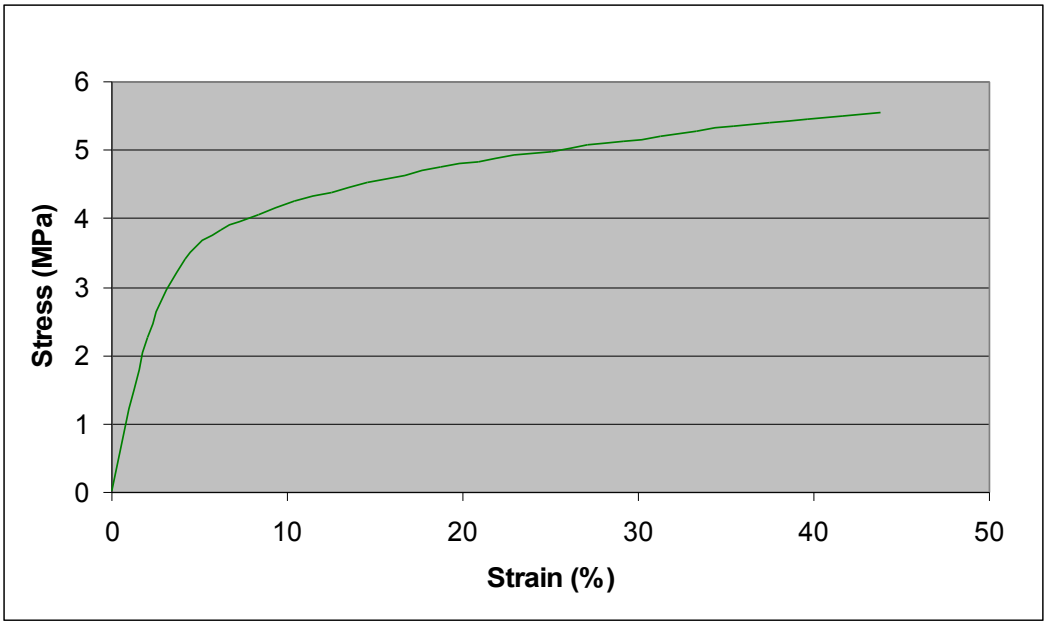

Figure 2.3.9 Tensile test results of a hollow fiber consisting of virgin polyamide membrane.

2.3.5 Tensile Test Results On Used Polyamide Membranes

Tensile test results of used polysulfone membrane of three different patients were given below. Tensile test results of the polyamide hollow fibers from the dialyzer used for patient H.O. and from a virgin dialyzer with a polyamide membrane are shown in Figure 2.3.10.

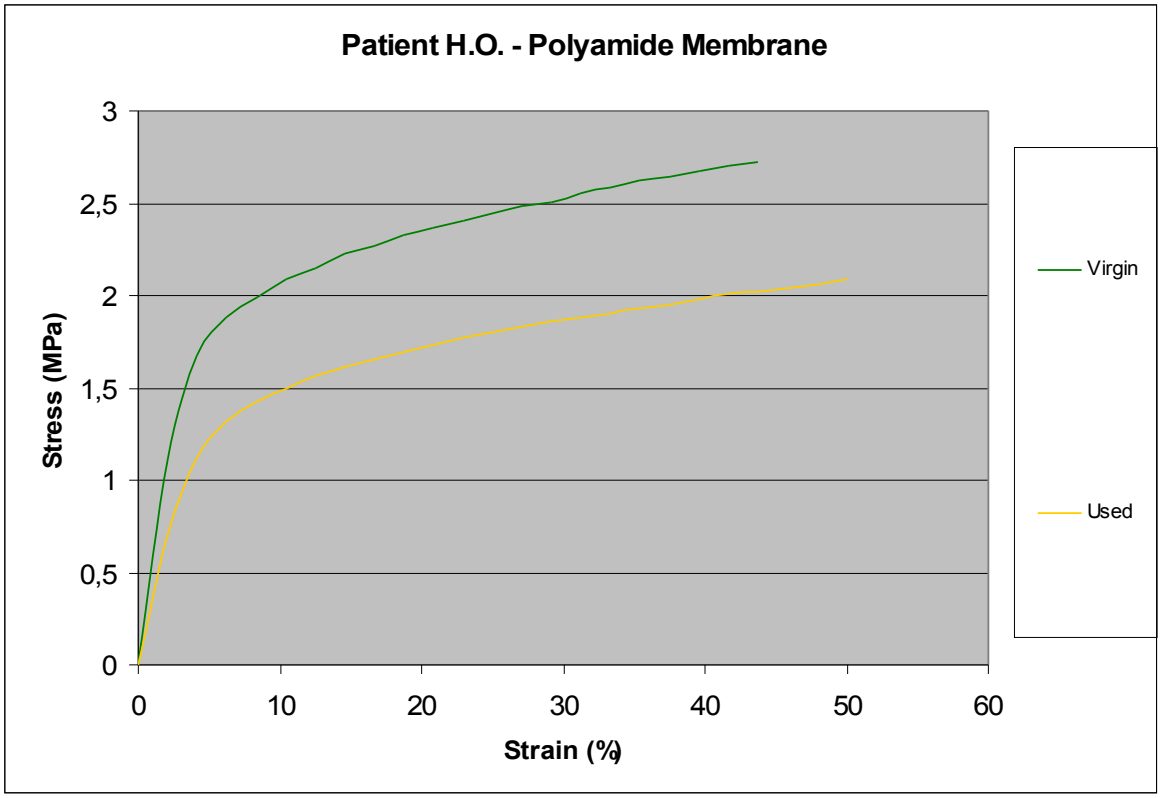

Figure 2.3.10 Tensile test results of virgin and used polyamide hollow fibers (Patient H.O.).

Tensile test results of the polyamide hollow fibers from the dialyzer used for patient R.U. and from virgin dialyzer with polyamide membrane are shown in Figure 2.3.11.

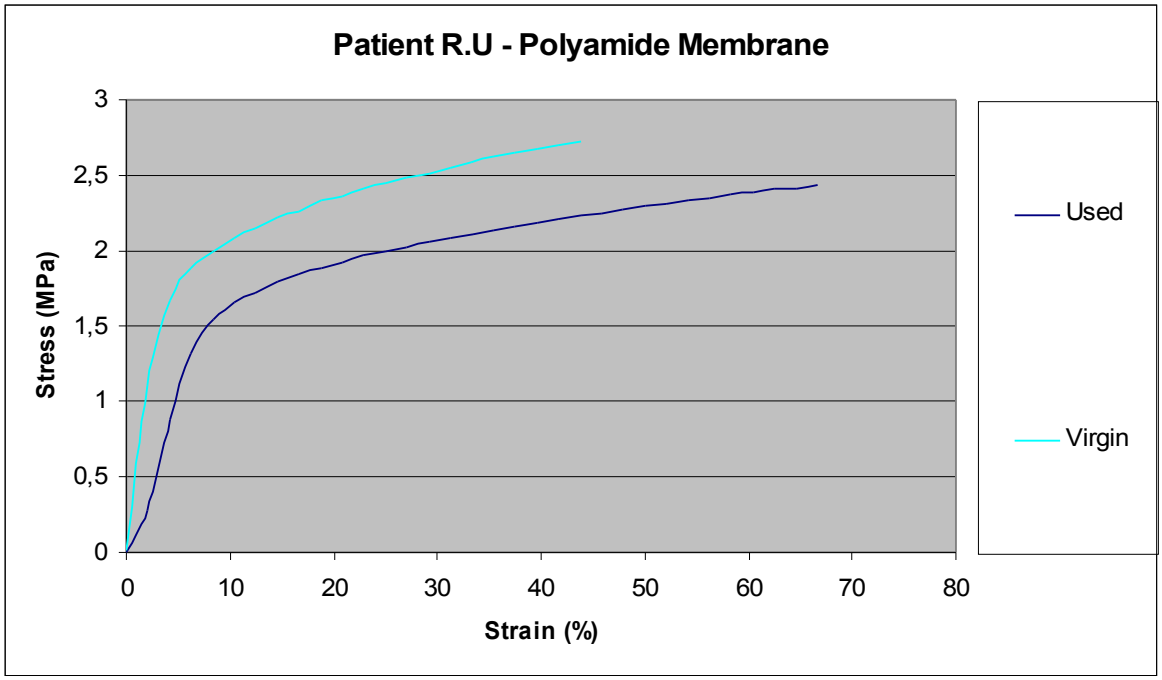

Figure 2.3.11 Tensile test results of virgin and used polyamide hollow fibers (Patient R.U.).

Tensile test results of the hollow fibers from the dialyzer used for Patient O.D. and a virgin dialyzer polyamide membrane are shown in Figure 2.3.12.

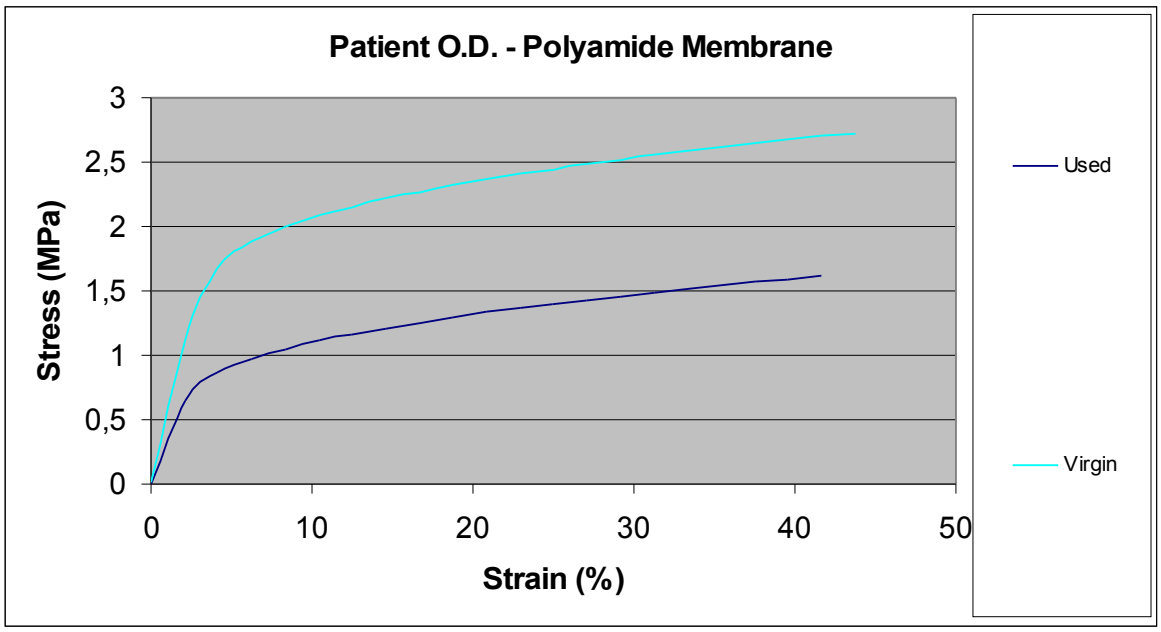

Figure 2.3.12 Tensile test result of virgin and used polyamide hollow fibers (Patient O.D.).

2.3.6 Results Of Load-Unload-Reload Experiments On Used Polyamide Membranes

Engineering stress-strain curves obtained during reloading following loading until 90% of ultimate tensile strength of a used polyamide hollow fiber and then unloading from the dialyzers used for three different patients were given in Figures 2.3.13 - 2.3.15. Figure 2.3.13 shows tensile test data of virgin polyamide fibers and used polyamide hollow fibers from the dialyzer used for patient H.O. after cyclic loading followed by tensile test.

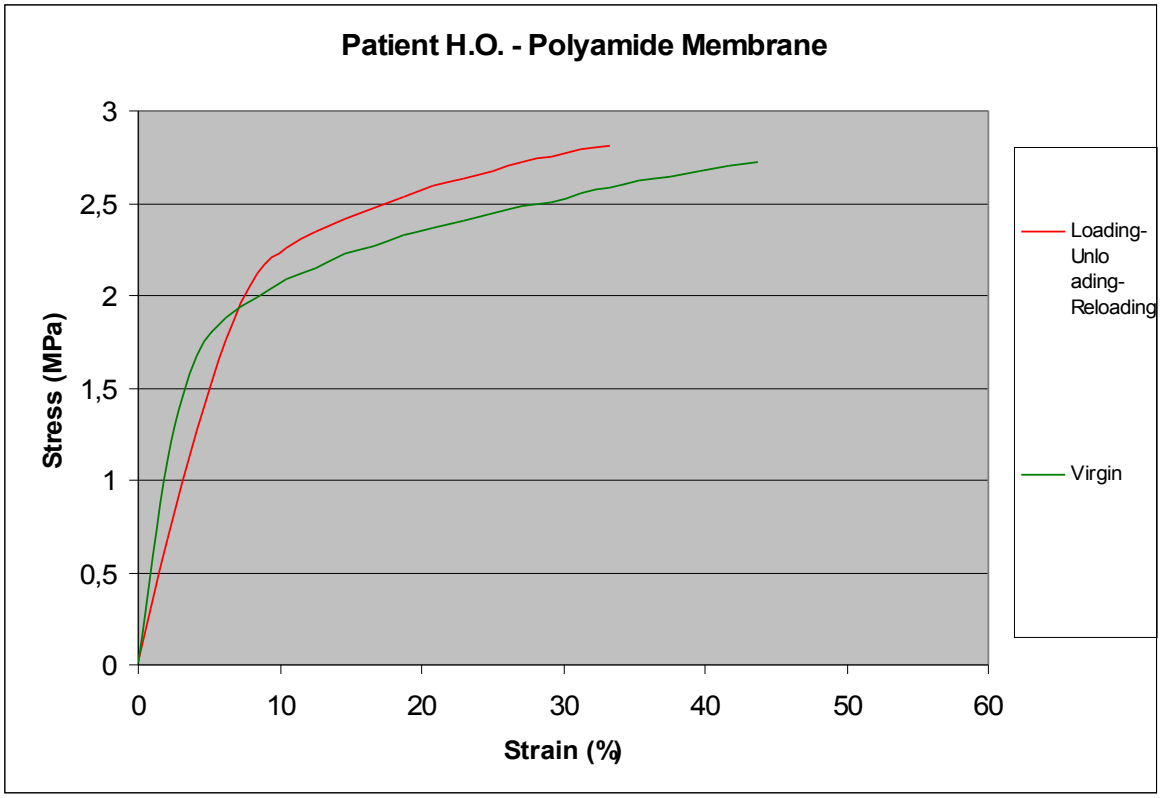

Figure 2.3.13 Tensile test results of virgin polyamide hollow fibers after dialysis and used polyamide hollow fibers after loading-unloading-reloading (Patient H.O.).

Figure 2.3.14 shows tensile test data of virgin and used fibers from the dialyzer used for patient R.U after cyclic loading followed by tensile test.

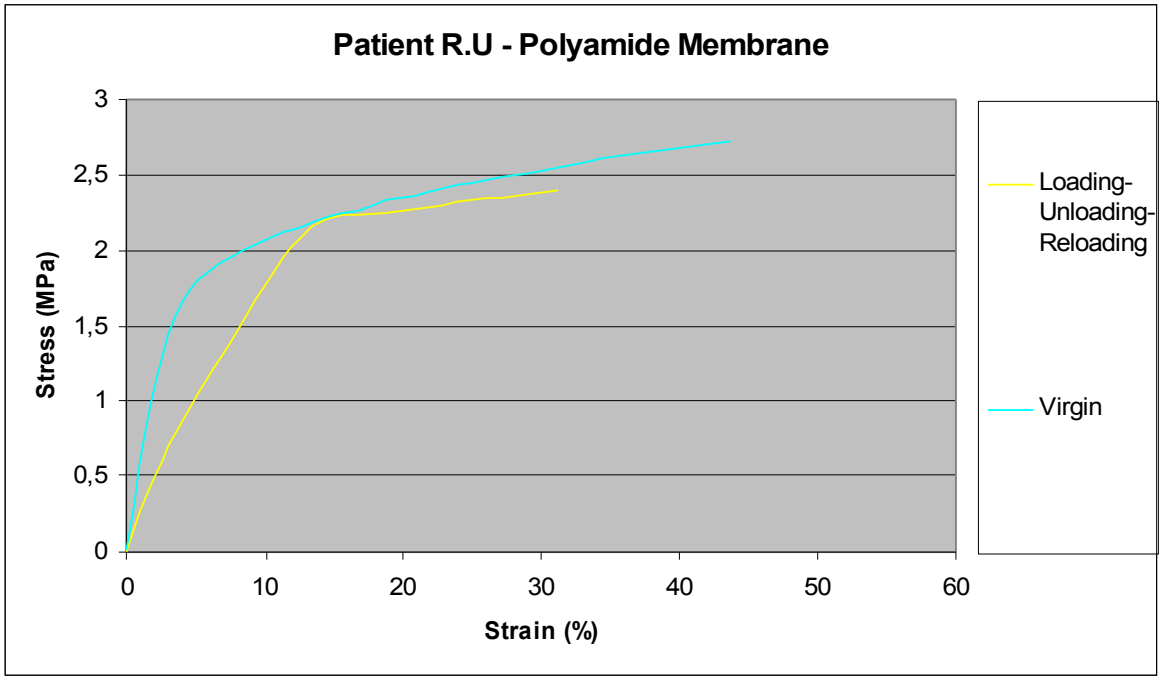

Figure 2.3.14 Tensile test results of virgin and used polyamide hollow fibers after loading-unloading-reloading (Patient R.U.).

Figure 2.3.15 shows the comparison between the tensile test curves of virgin and used polyamide hollow fibers after cyclic test followed by tensile test.

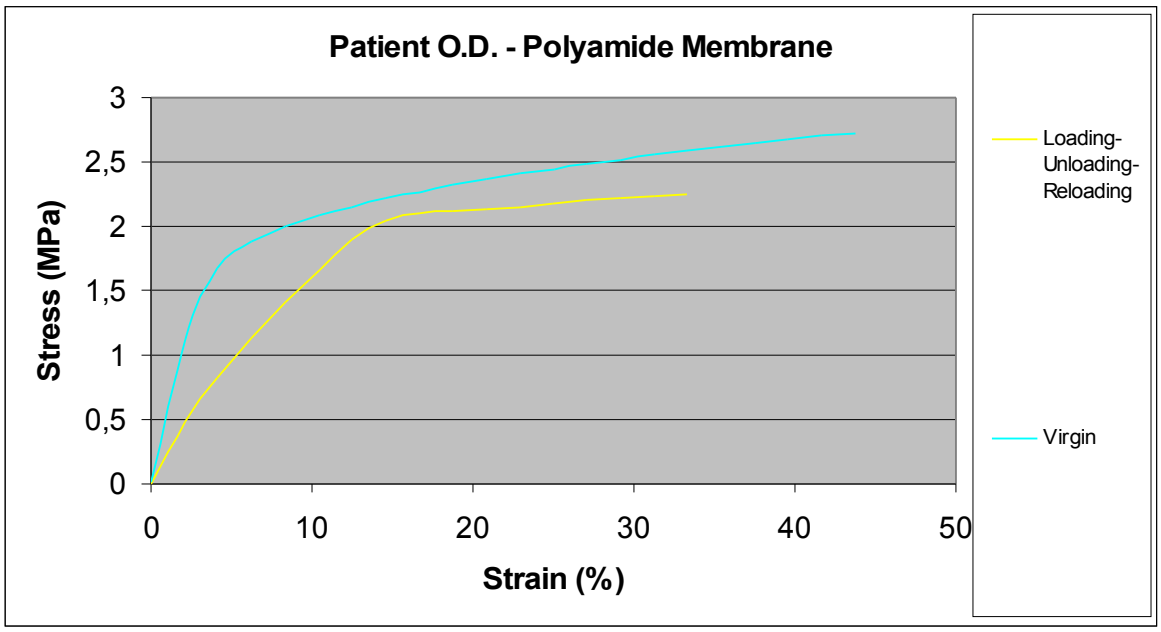

Figure 2.3.15 Tensile test results of virgin and used polyamide hollow fibers after loading-unloading-reloading (Patient O.D.).

After the tensile test studies it was concluded that virgin polyamide membranes can resist higher loads compared to used membranes. It was also concluded that both virgin polysulfone and polyamide have higher ultimate tensile strength compared to the used membranes. Same trend was observed for toughness and yield strength. For the one cycle "Loading-unloading from 90% ultimate tensile strength – Reloading until fracture caused the decrease drastically in toughness and ultimate tensile strength values. For the polyamide membranes the one cycle loading showed increase in yield strength.

When the tensile test curves of used polyamide membranes after dialysis and used polyamide membranes after cyclic loading followed by tensile test are compared, strain hardening after loading/unloading process can be observed in Figures 2.3.13, 2.3.14 and 2.3.15. These data show us that membranes are becoming more brittle with loading-unloading and reloading processes.

2.4 X-Ray Diffraction (XRD) Studies

X-ray diffraction (XRD) is one of the most powerful techniques for qualitative and quantitative analysis of crystalline compounds [31, 32]. A polymer can be considered partially crystalline and/or partially amorphous. Many polymers can be identified by using the XRD method. Polymers are, at least in part, crystalline or pseudo-crystalline with partially ordered structures [31, 32].

XRD studies have been performed on virgin and used both polysulfone and polyamide membranes. XRD studies also were performed on used membranes after two different types of mechanical test which are monotonic tensile loading until fracture and tensile stressing until 90% of ultimate tensile strength following unloading and reloading until fracture.

Used hollow fibers were obtained from 6 different patients. The patients were chosen among the patients with dialysis ages less than two years and without any accompanying disease.

XRD studies were performed by using Rigaku Dmax 2200 XRD instrument shown in Figure 2.4.1. X-ray diffraction of test materials were performed by using CuKα radiation with a wavelength of 1.5418 A over a 2θ range of 10^{o} to 80^{o}. X-Ray voltage and current values were 40kV and 40mA. Copper x-ray tube was used for the experiments.

Figure 2.4.1 Rigaku Dmax 2200 XRD instrument.

2.4.1 XRD Results Of Virgin Polysulfone Hollow Fibers

The result of the XRD experiment performed on virgin polysulfone membrane is shown in Figure 2.4.2.

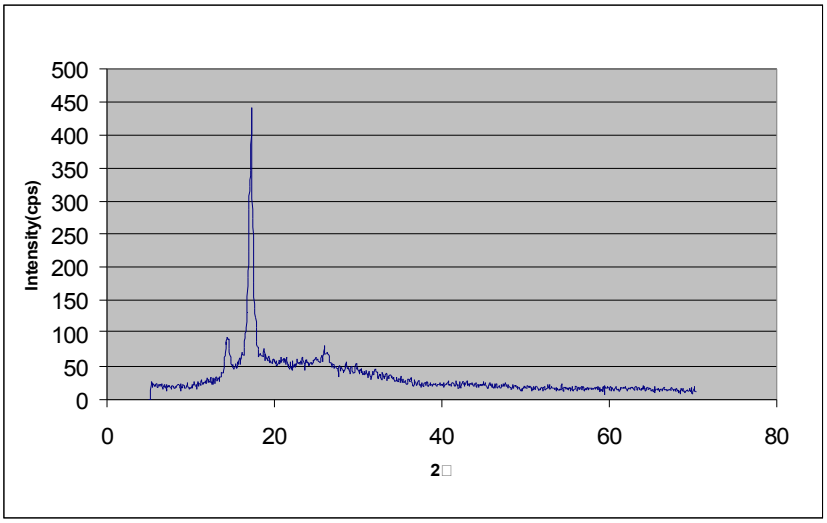

Figure 2.4.2 XRD result of a virgin polysulfone membrane.

As it can be seen in Figure 2.4.2, there are three major intensity peaks on the XRD result of a virgin polysulfone membrane. These intensity peaks can be observed at 14 (2□) with an intensity of 94 cps. The second peak can be seen at 17 (2□) with an intensity of 440 cps. The third peak is seen at 27 (2□) with an intensity of 78 cps.

2.4.2 XRD Results Of Used Polysulfone Hollow Fibers After One Dialysis Session

The results of the XRD experiments performed on used polysulfone membranes of patient A.F.K. is shown in Figure 2.4.3. XRD results of virgin and the used membranes of patient M.K. after a dialysis session are shown in Figure 2.4.4.

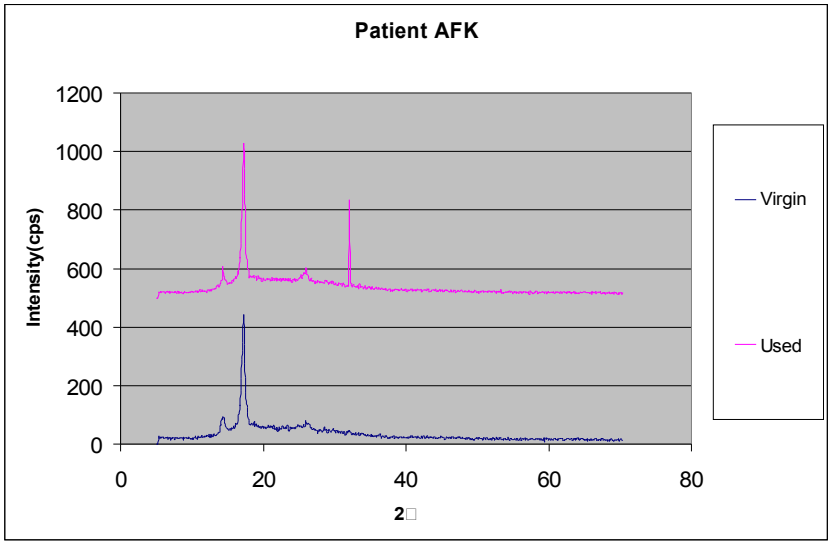

Figure 2.4.3 XRD results from the virgin and used polysulfone fibers of patient A.F.K.

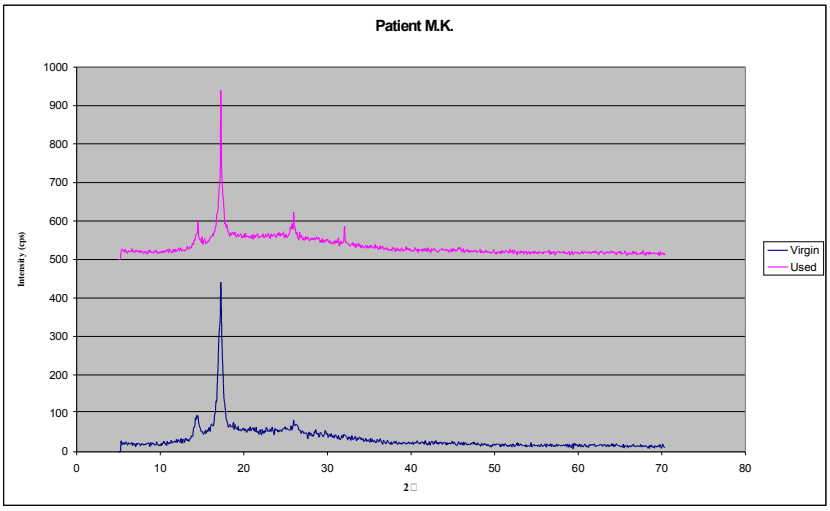

Figure 2.4.4 XRD results of the virgin and used polysulfone fibers of patient M.K.

The comparison of the XRD data obtained from virgin polysulfone membranes and used polysulfone membranes of patient M.D. are shown in Figure 2.4.5.

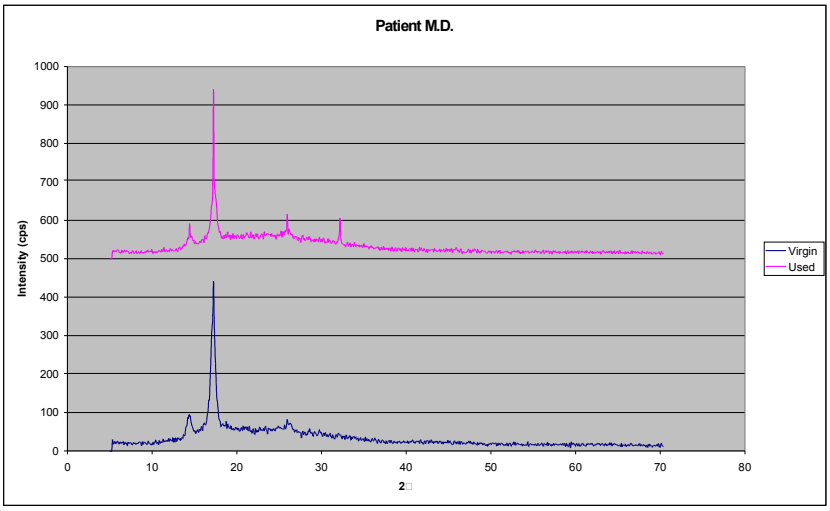

Figure 2.4.5 XRD results of the virgin and used polysulfone fibers of patient M.D.

There are four major intensity peaks in this used polysulfone membrane. These intensity peaks can be observed at 14 =2□ with an intensity of 110 cps. The second peak can be seen at 17=2□ with an intensity of 525 cps. The third peak is seen at 27=2□ with an intensity of 100 cps. There is a fourth peak that can be observed at 33=2□ with an intensity of 345 cps in only used polysulfone membranes.

When these data are compared with the results of virgin polyamide membranes, it is noticed that there is one more peak additional to the available peaks of which intensity are also increased.

2.4.3 XRD Results Of Used Polysulfone Hollow Fibers After Tensile Test

Figure 2.4.6 shows the comparison of the XRD results of virgin and used samples of patient A.F.K. after tensile test.

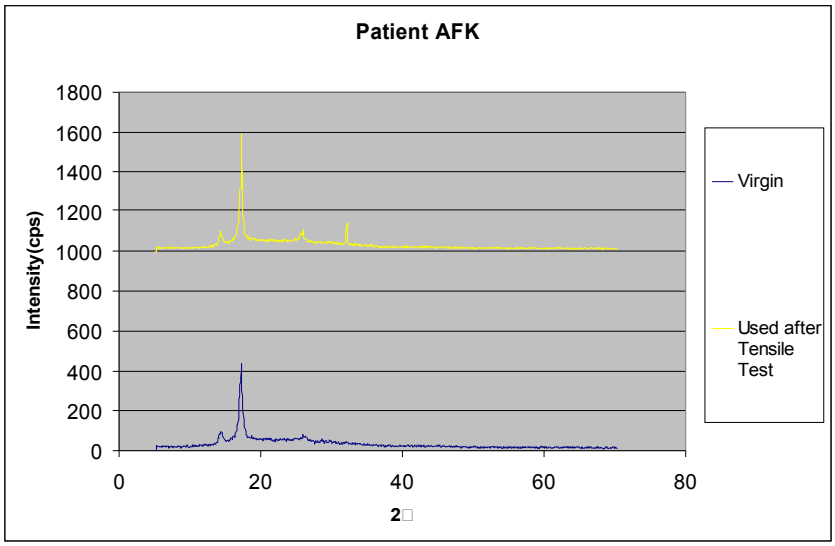

Figure 2.4.6 XRD results of the virgin and used polysulfone fibers of patient A.F.K. after tensile test.

2□

Figure 2.4.7 shows the XRD values of used polysulfone membranes(after tensile test) of patient M.D. in comparison with the XRD values of virgin polysulfone membranes.

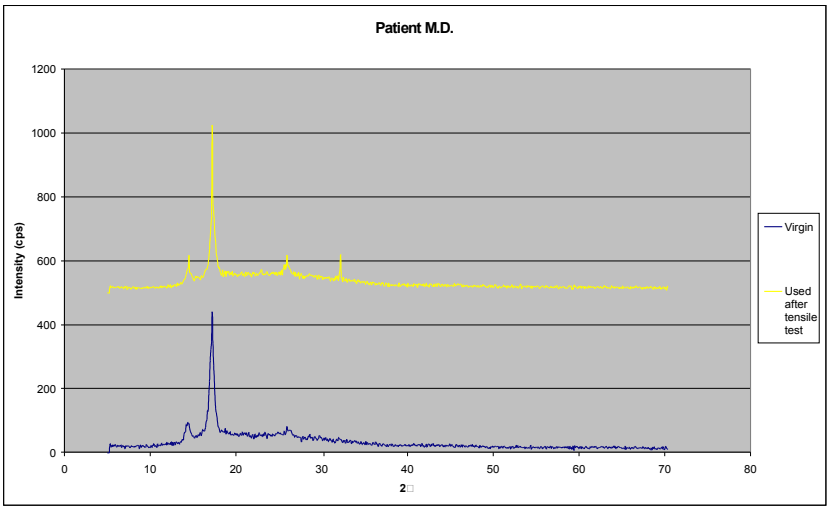

Figure 2.4.7 XRD results of virgin and used polysulfone fibers of patient M.D. after tensile test.

XRD results of the used membranes of patient M.K. after tensile test are shown in Figure 2.4.8.

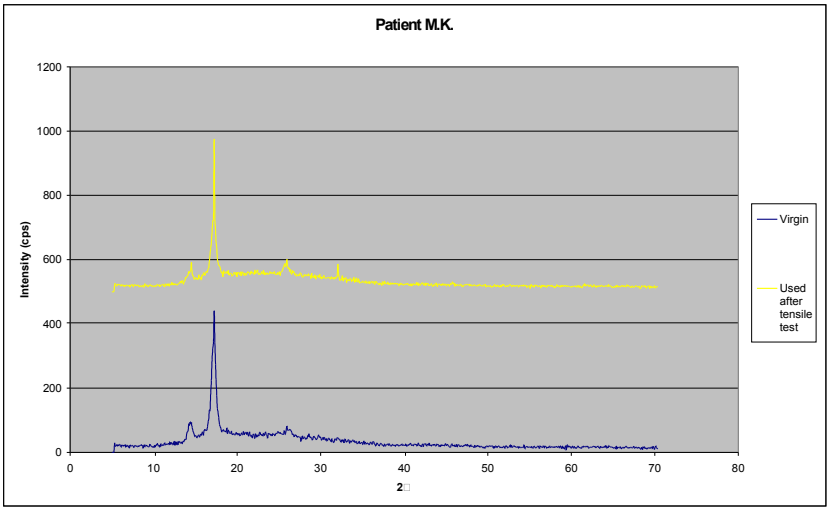

Figure 2.4.8 XRD results from virgin and used polysulfone fibers of patient M.K. (After tensile test).

2.4.4 XRD Results Of Used Polysulfone Hollow Fibers After Loading-Unloading Followed By Reloading Until Fracture

Figure 2.4.9 shows the comparison of the XRD results belonging to virgin and used samples of patient A.F.K. (after loading-unloading-reloading).

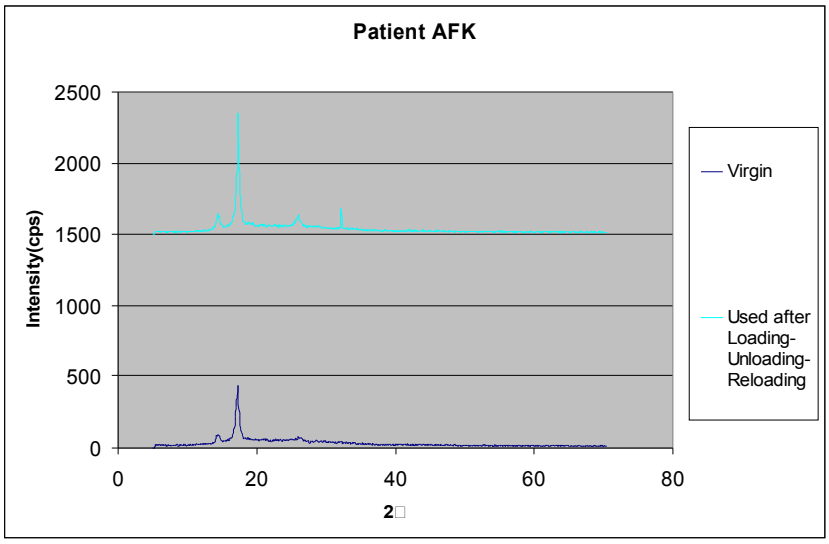

Figure 2.4.9 XRD results from the virgin used polysulfone fibers of patient A.F.K. (After loading-unloading-reloading until fracture).

The XRD results of virgin and used polysulfone membranes of patient M.K. (after loading-unloading-reloading) are shown in Figure 2.4.10.

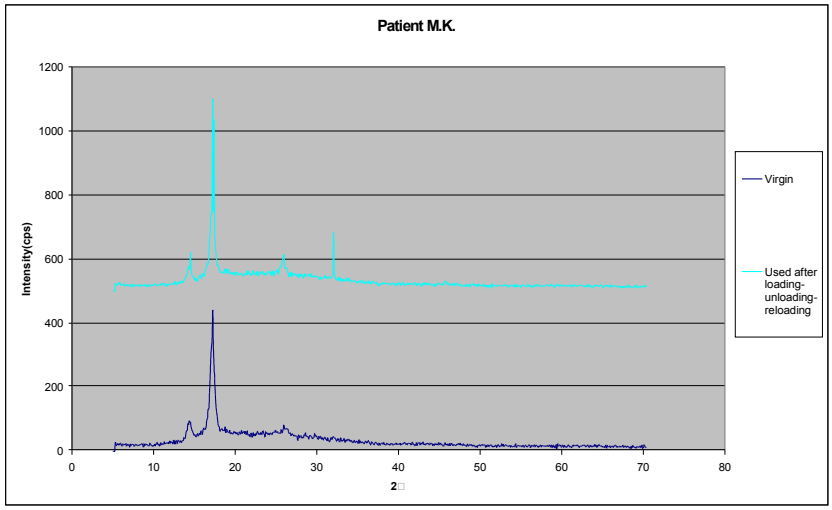

Figure 2.4.10 XRD results of virgin and used polysulfone fibers of patient M.K. (After loading-unloading-reloading until fracture).

Figure 2.4.11. shows the comparison of the XRD results belonging to virgin and used samples of patient M.D after loading-unloading-reloading.

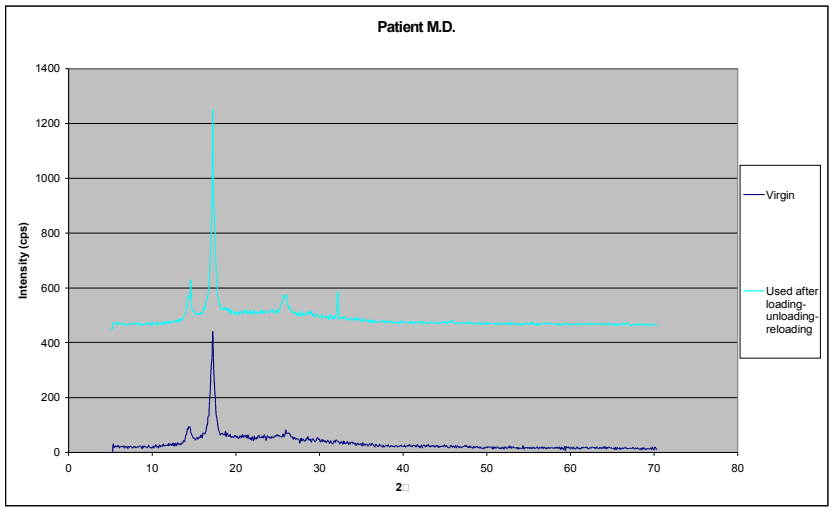

Figure 2.4.11 XRD results of virgin and used polysulfone fibers of patient M.D. (After loading-unloading-reloading).

It is remarkable that the number of peaks and the height of main peak are increased for the used membranes.

Table 2.4.1 Comparison of the XRD results of virgin, used, used after "tensile test" and used after "loading-unloading-reloading until fracture cycle" samples.

Polysulfone				
2□ = 14		**Intensity(cps)**	**Intensity(cps)**	**Intensity(cps)**
Virgin (cps)	**Patient**	**Used**	**After tensile test**	**After loading- unloading and reloading**
94	M.D.	85	120	180
	M.K.	95	90	120
	A.F.K.	110	105	150
	Mean	**96,66**	**105**	**150**
2□ = 17		**Intensity(cps)**	**Intensity(cps)**	**Intensity(cps)**
Virgin (cps)	Patient	**Used**	**After tensile test**	**After loading and unloading**
440	M.D.	440	525	800
	M.K.	440	470	605
	A.F.K.	525	590	850
	Mean	468,33	528,33	751,66
2□ = 27		**Intensity(cps)**	**Intensity(cps)**	**Intensity(cps)**
Virgin (cps)	Patient	**Used**	**After tensile test**	**After loading and unloading**
78	M.D.	118	115	120
	M.K.	120	105	110
	A.F.K.	100	110	140
	Mean	112,66	110	123,33
2□ = 33		**Intensity(cps)**	**Intensity(cps)**	**Intensity(cps)**
Virgin (cps)	Patient	**Used**	**After tensile test**	**After loading and unloading**
0	M.D.	105	110	135
	M.K.	85	85	187
	A.F.K.	345	105	180
	Mean	178,33	100	167,33

All the XRD results belonging both virgin and used polysulfone membranes were given in Table 2.4.1. As it can be seen in Table 2.4.1, there are three main intensity peaks in virgin polysulfone membrane and four main intensity peaks in used polysulfone membranes. The first three peaks at 2□=14, at 2□ = 17 and at 2□ = 27 are also present in the XRD data of both virgin and used polysulfone membranes, but the fourth peak at 2□ = 33 is only seen in used membranes. The intensity values of all the peaks are getting their

highest values when the membrane is imposed to loading-unloading-reloading test. In used membranes the mean intensity value at 2□ = 27 is 44,44% higher compared to the same intensity value of a virgin membrane. The mean intensity value of used polysulfone membranes (after tensile test) at 2□ = 17 is 20% higher than the XRD value of a virgin membrane. At the intensity of 2□ = 27 data obtained from XRD studies of used membranes after tensile test are 41% higher than the data from virgin membranes.

When loading-unloading-reloading test was applied to the used membranes, the intensity values for the first three peaks were increased between 59% - 70% with respect to the values of virgin membranes.

The intensity peaks obtained after the XRD studies from the hollow fibers of the dialyzers acquired after the dialysis sessions of three different patients change with different process such as the usage, monotonic loading and loading-unloading-reloading test.

2.4.5 XRD Studies On Virgin Polyamide Hollow Fibers

The result of the XRD experiments performed on virgin polyamide membrane is shown in Figure 2.4.12.

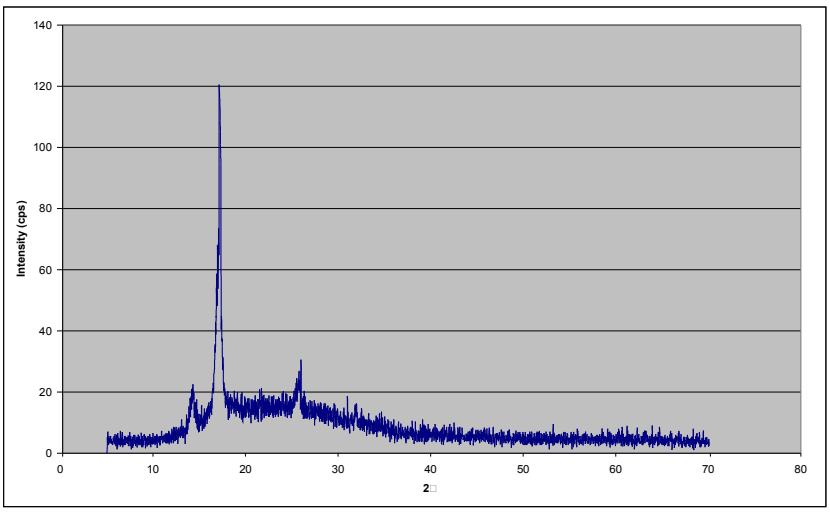

Figure 2.4.12 XRD result of a virgin polyamide membrane.

XRD studies on polyamide membranes revealed four intensity peaks at 2□ = 14 with an intensity of 22 cps, at 2□ = 17 with an intensity of 120 cps, at 2□ = 26 with an intensity of 31 cps and 2□ = 32 with an intensity of 18 cps.

2.4.6 XRD Studies On Used Polyamide Hollow Fibers After One Dialysis Session

XRD results from the used fibers of patient O.D. (Polyamide) and from virgin polyamide membrane are shown in Figure 2.4.13.

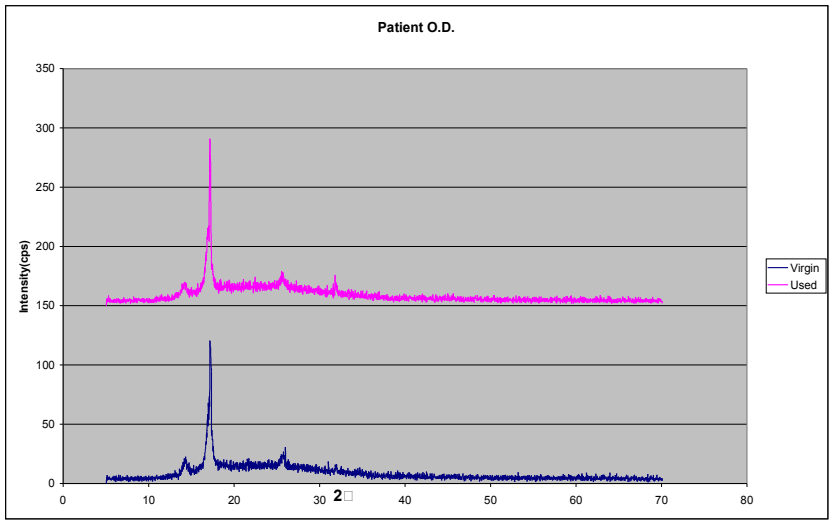

Figure 2.4.13 XRD results of virgin and used polyamide fibers of patient O.D.

XRD results of used polyamide fibers of patient R.U. and virgin polyamide fibers are shown in Figure 2.4.14.

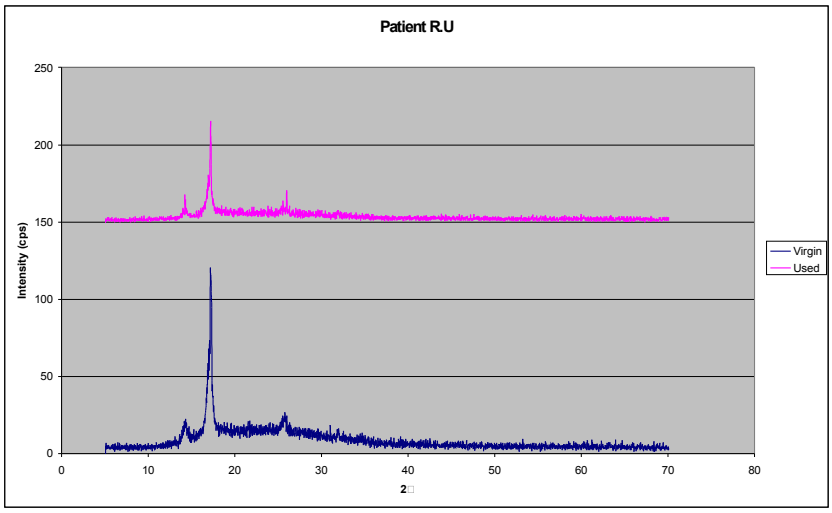

Figure 2.4.14 XRD results of virgin and used polyamide fibers of patient R.U.

XRD results of virgin and used polyamide fibers from the dialyzers used for patient H.A. are shown in Figure 2.4.15.

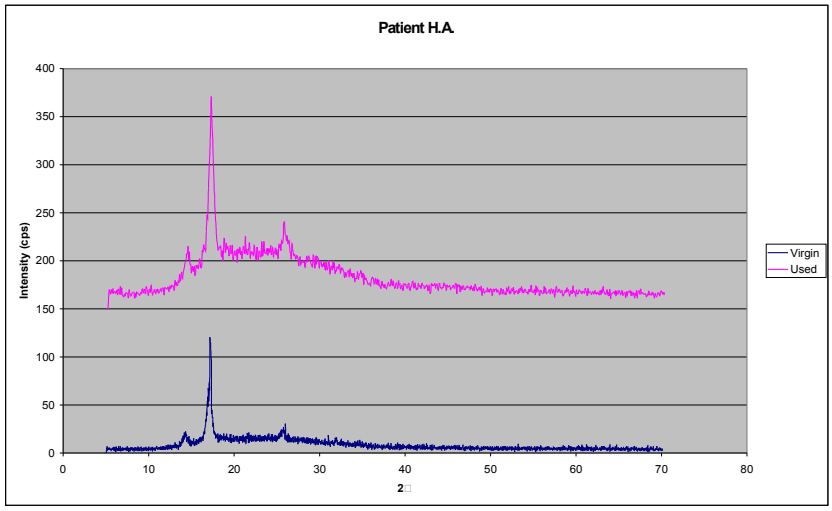

Figure 2.4.15 XRD results of virgin and used polyamide fibers of patient H.A.

2.4.7 XRD Studies on Used Polyamide Hollow Fibers After Tensile Test

XRD values obtained from virgin polyamide membranes and used polyamide membranes of patient O.D. after tensile test are shown in Figure 2.4.16.

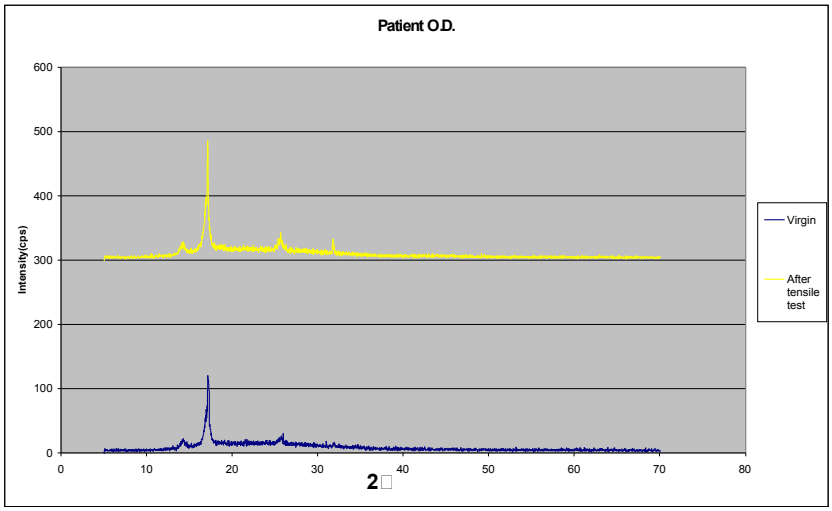

Figure 2.4.16 XRD results of virgin and used polyamide fibers of patient O.D. (After tensile test).

Figure 2.4.17 shows the XRD data acquired from virgin and used polyamide membranes of patient R.U. after tensile test.

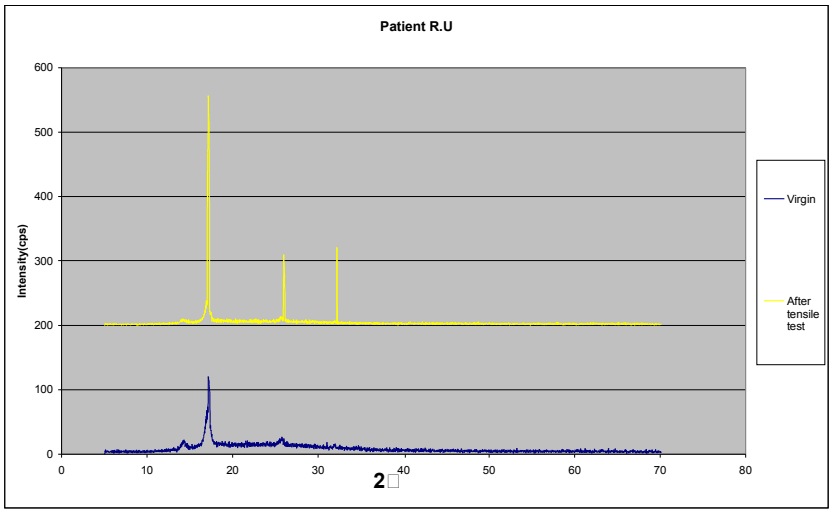

Figure 2.4.17 XRD results of virgin and used polyamide fibers of patient R.U. (After tensile test).

XRD values obtained from virgin and used polyamide membranes of patient H.A. after tensile test are shown in Figure 2.4.18.

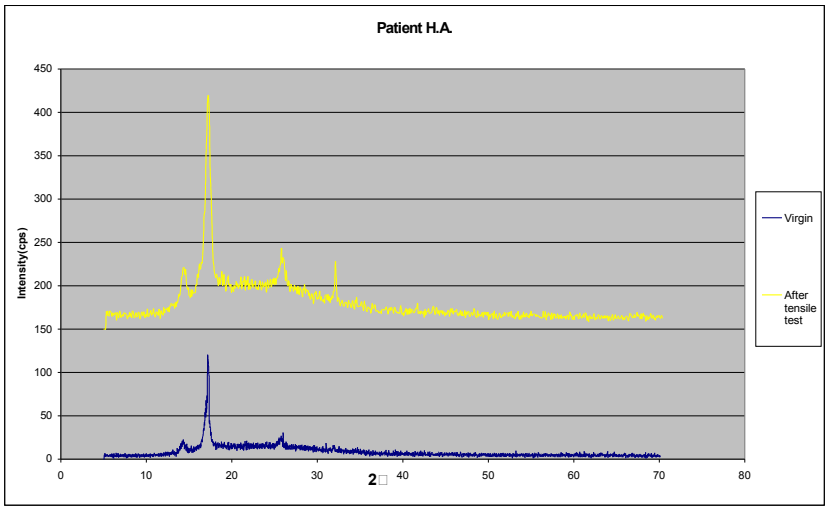

Figure 2.4.18 XRD results of virgin and used polyamide fibers of patient H.A. (After tensile test).

2.4.8 XRD Studies On Used Polyamide Hollow Fibers After Loading-Unloading Followed By Reloading Until Fracture

Figure 2.4.19 shows the results of the XRD studies performed on virgin polyamide membranes and used polyamide membranes (after loading-unloading and reloading) from the dialyzer used for patient O.D.

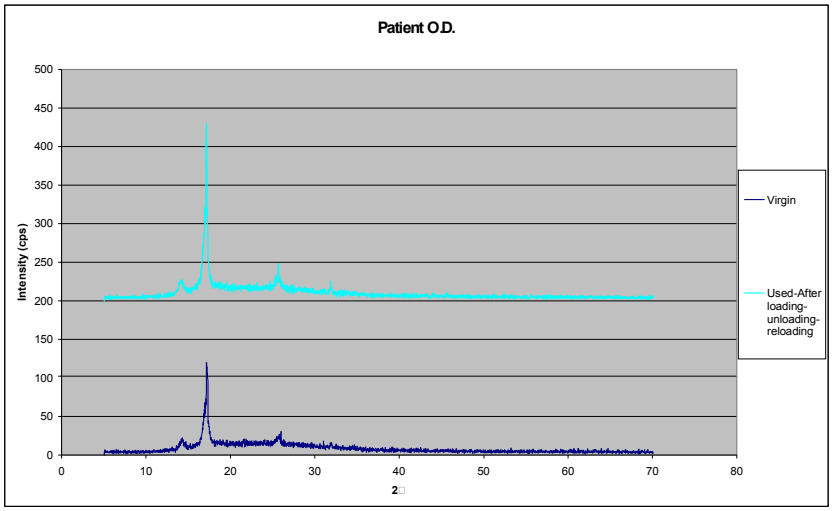

Figure 2.4.19 XRD results of virgin and used polyamide fibers of patient O.D. (After loading-unloading and reloading).

XRD values obtained from virgin polyamide membranes and used polyamide membranes of patient H.A. after loading-unloading and reloading test are shown in Figure 2.4.20.

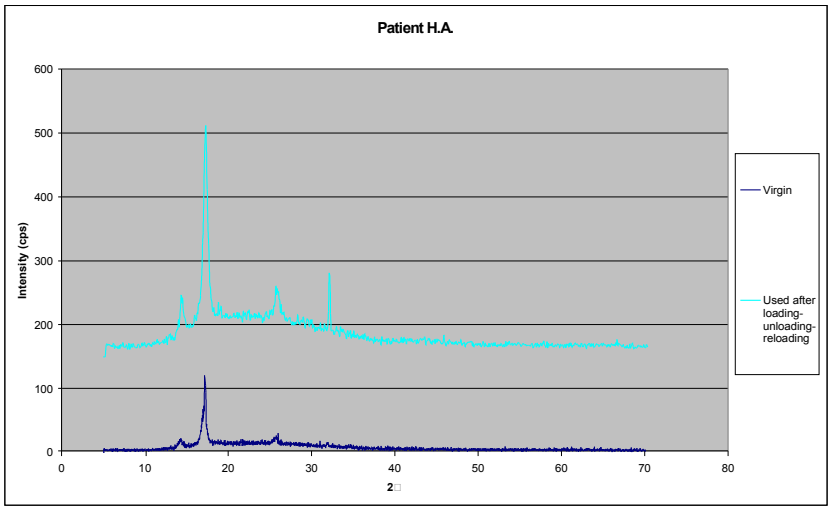

Figure 2.4.20 XRD results of virgin and used polyamide fibers of patient H.A. (After loading-unloading and reloading).

Table 2.4.2 Comparison of the XRD results of used polyamide membranes with the XRD result of virgin polyamide membranes.

Polyamide				
2□ = 14		**Intensity**	**Intensity**	**Intensity**
Virgin (cps)	**Patient**	**Used**	**After tensile test**	**After loading- unloading and reloading**
22	O.D.	20	12	24
	R.U.	18	90	86
	H.A.	65	70	98
	Mean	***34***	***57***	***69***
2□ = 17		**Intensity**	**Intensity**	**Intensity**
Virgin (cps)	Patient	**Used**	**After tensile test**	**After loading- unloading and reloading**
120	O.D.	140	355	238
	R.U.	66	470	530
	H.A.	222	270	360
	Mean	***143***	***365***	***376***
2□ = 26		**Intensity**	**Intensity**	**Intensity**
Virgin (cps)	Patient	**Used**	**After tensile test**	**After loading- unloading and reloading**
31	O.D.	28	42	48
	R.U.	21	110	120
	H.A.	90	93	110
	Mean	***46***	***82***	***93***
2□ = 32		**Intensity**	**Intensity**	**Intensity**
Virgin (cps)	Patient	**Used**	**After tensile test**	**After loading- unloading and reloading**
18	O.D.	25	33	24
	R.U.	8	120	45
	H.A.	45	78	135
	Mean	***26***	*77*	***68***

There are four intensity peaks at 2□=14, at 2□ = 17, at 2□ = 26 and at 2□ = 32 that are also present in the XRD data of both virgin and used polyamide membranes as seen on Table 2.4.2. After loading-unloading and reloading test the intensity values of all the peaks are getting their highest values . The mean intensity value of used polyamide membranes at 2□ = 14 is 56% higher than the XRD value of a virgin membrane. The mean

intensity values of used polyamide membranes at 2□ = 17 are 18,89% higher compared to the same intensity value of a virgin membrane. At the intensity of 2□ = 26 data obtained from XRD studies of used membranes are 49% higher than the data from virgin membranes. The intensity values of used polyamide membranes at 2□ = 32 are 44,44% higher compared to the values of virgin polyamide membranes.

After loading-unloading and reloading test had been applied to the used polyamide membranes, the mean intensity values of the four intensity peaks were increased by 226,2% compared with values of virgin membranes.

2.5 Differential Scanning Calorimetry Studies (DSC)

As the properties of polymers depend strongly on temperature, a thermal analysis technique is very suitable for the characterization of polymers [33, 34, 35, 36]. Like the other polymers, thermal stability of polysulfone and polyamide is very critical for the purpose of using these polymers [33, 34, 35, 36].

Virgin and used hollow fibers consisting of polyamide and polysulfone dialysis membranes were used as samples in DSC studies. Used membranes originated from eight end stage renal failure patients, who have no accompanying systemic illnesses, with dialysis ages less then two years. The studies were performed with Netzsch 404 C DSC analyzer shown in Figure 2.5.1.

Figure 2.5.1 Netzsch 404 C DSC analyzer.

2.5.1 Results Of The DSC Studies On Virgin Polysulfone Hollow Fibers

The results of the DSC experiments on virgin polysulfone hollow fibers are shown in Figure 2.5.2.

2.5.2 Results Of The DSC Studies On Used Polysulfone Hollow Fibers

DSC thermograms obtained from the used dialyzers with polysulfone membranes from four different patients are shown in Figures 2.5.3 – 2.5.6.

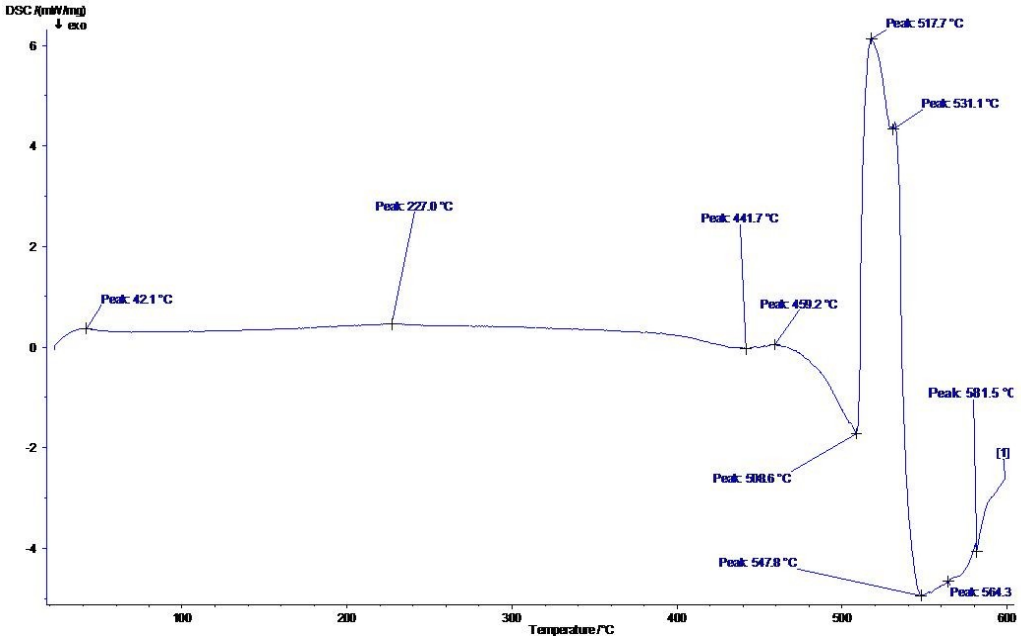

Figure 2.5.2 DSC Thermogram of a virgin polysulfone membrane.

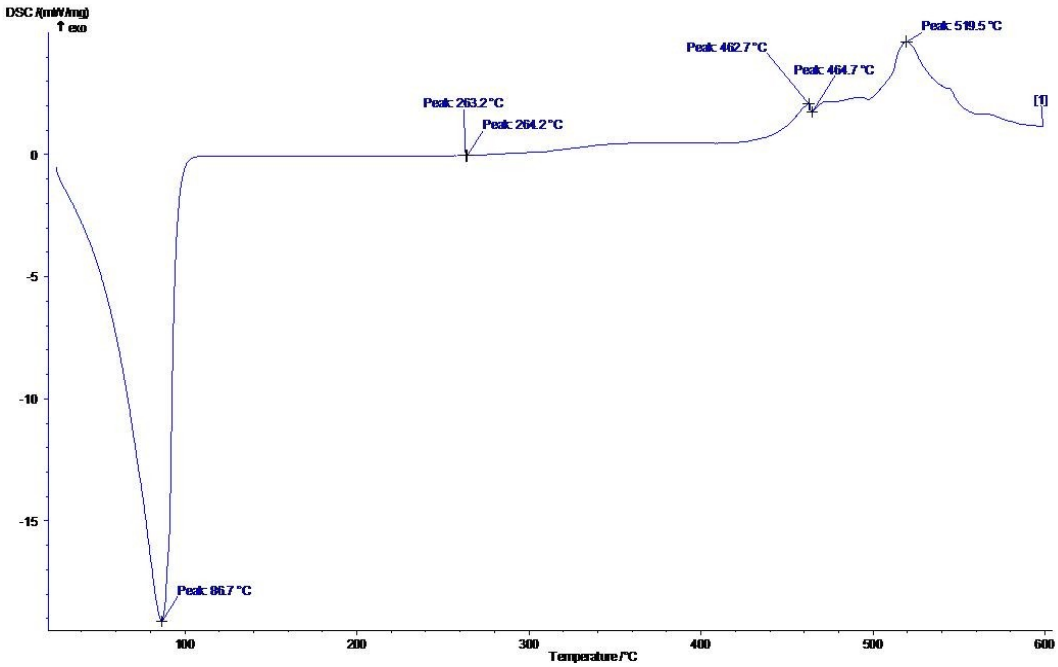

Figure 2.5.3 DSC Thermogram of a used polysulfone membrane (Patient M.K.).

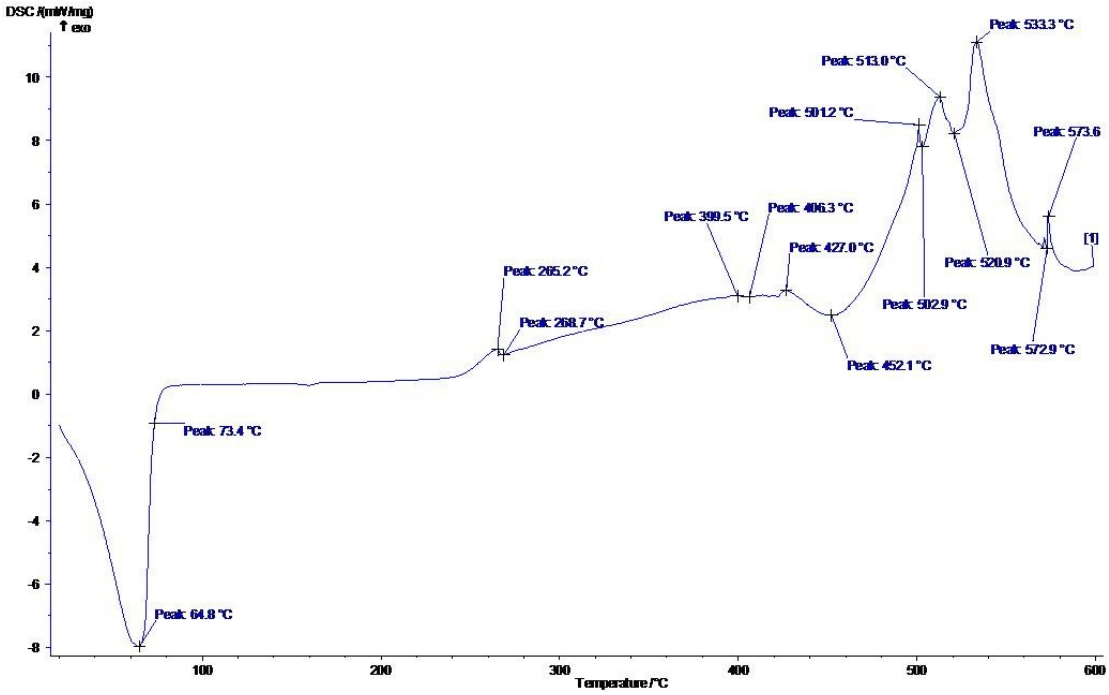

Figure 2.5.4 DSC Thermogram of a used polysulfone membrane (Patient M.D.).

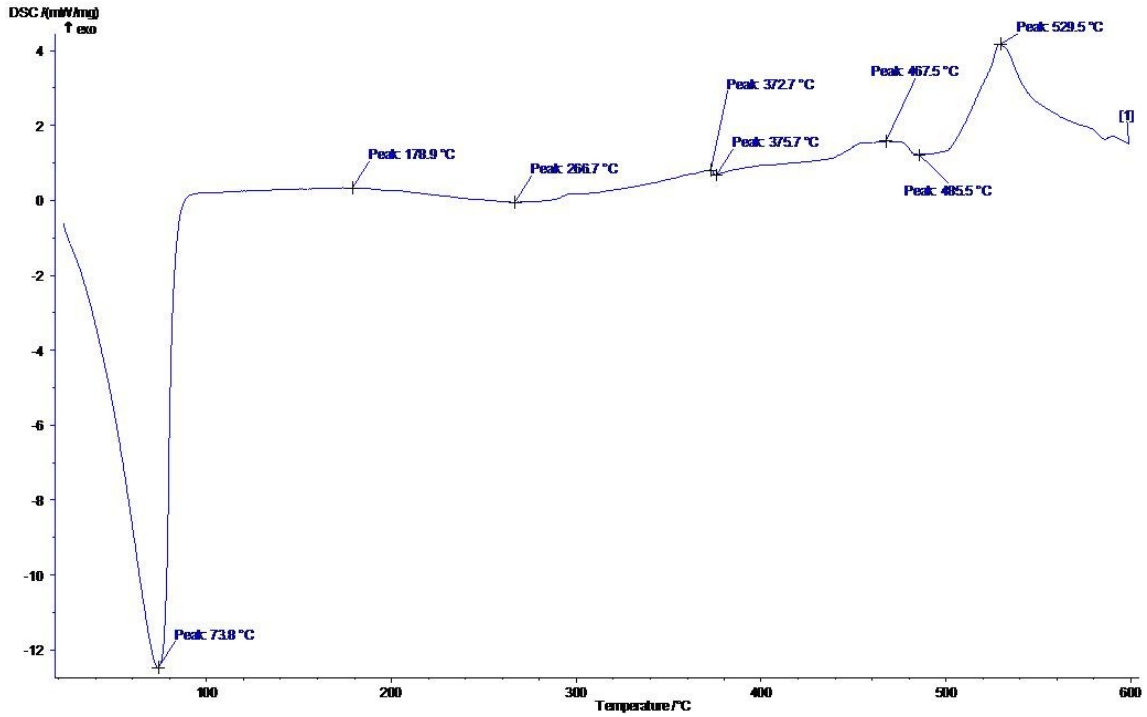

Figure 2.5.5 DSC Thermogram of a used polysulfone membrane (Patient A.F.K.).

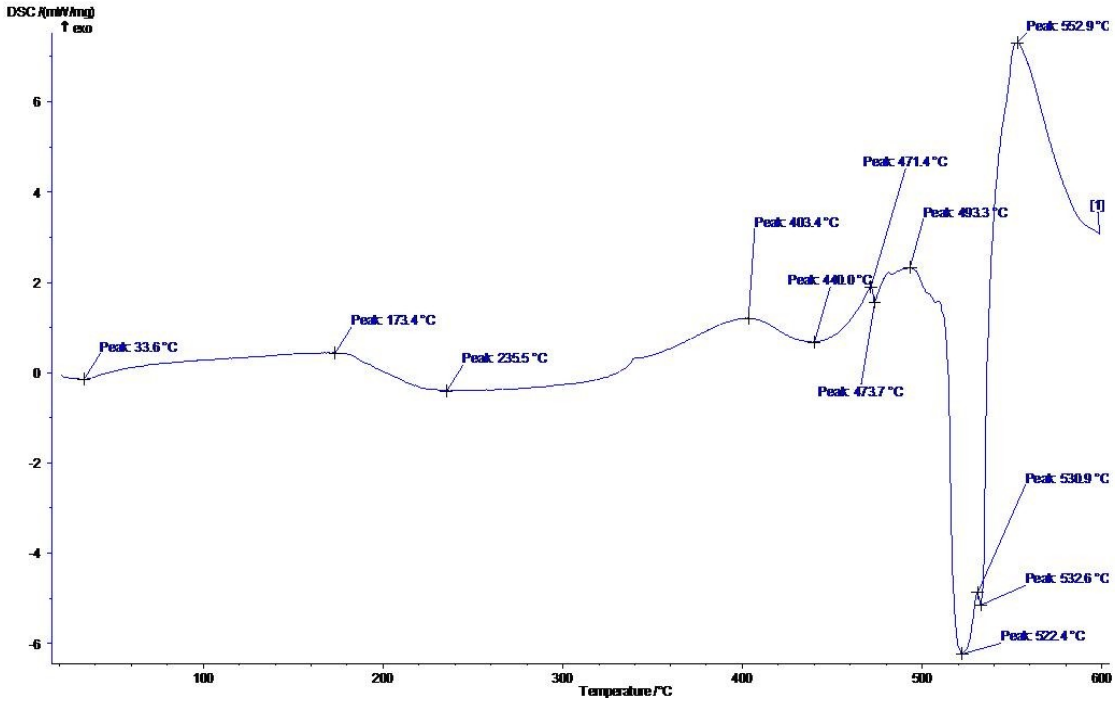

Figure 2.5.6 DSC Thermogram of a used polysulfone membrane (Patient I.C.).

2.5.3 Results Of The DSC Studies On Virgin Polyamide Hollow Fibers

The result DSC study on virgin polyamide membrane is shown in Figure 2.5.7.

2.5.4 Results Of The DSC Studies On Used Polyamide Hollow Fibers

Figures 2.5.8, 2.5.9, 2.5.10 and 2.5.11 show DSC thermograms acquired from four hollow fibers originating from used polyamide dialyzers from four different patients.

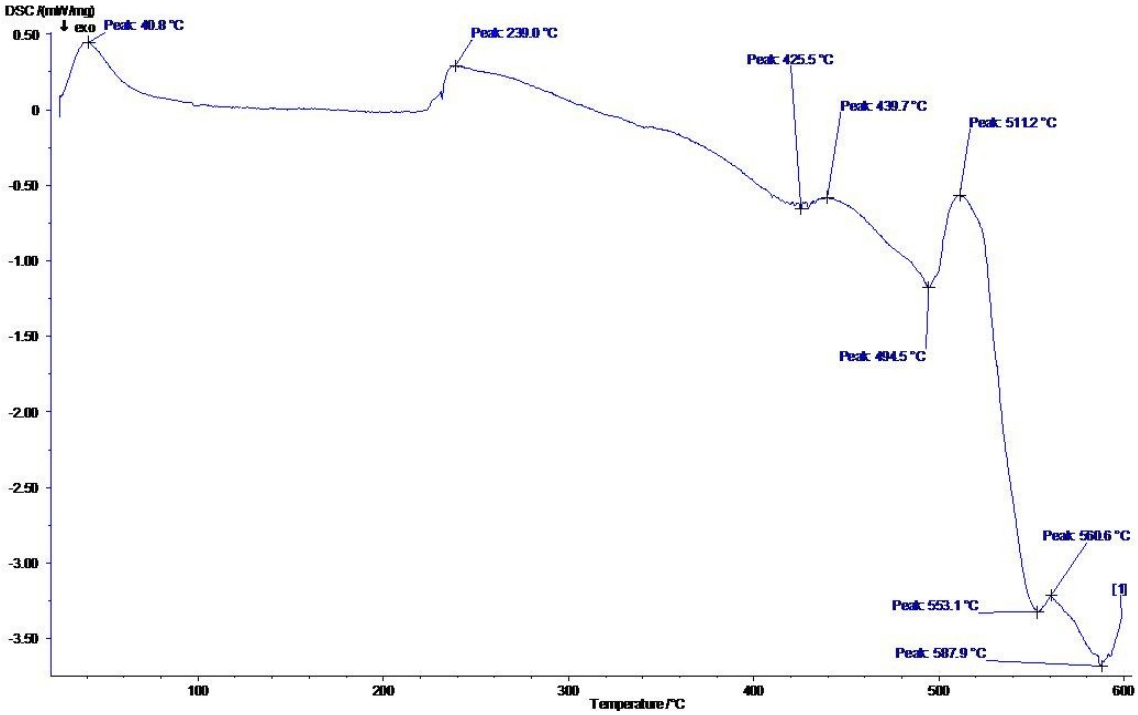

Figure 2.5.7 DSC Thermogram of a virgin polyamide membrane.

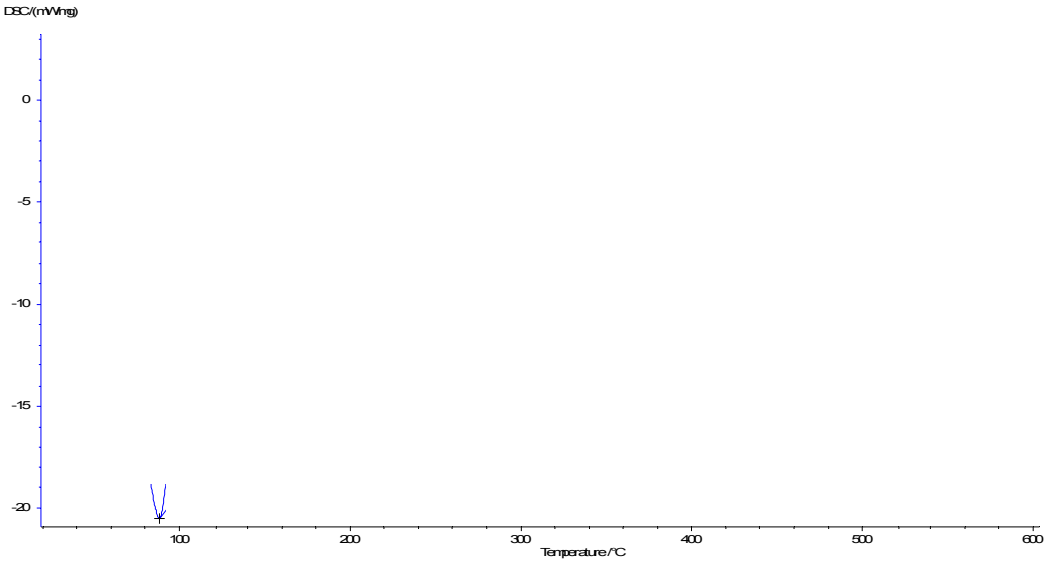

Figure 2.5.8 DSC Thermogram of a used polyamide membrane (Patient H.O.).

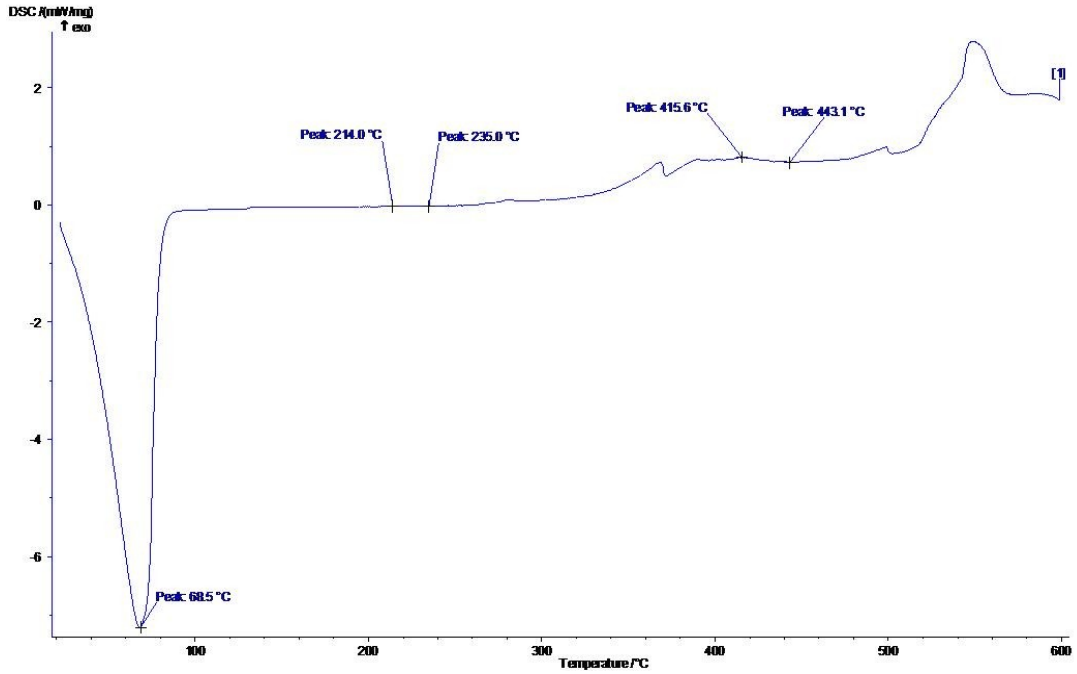

Figure 2.5.9 DSC Thermogram of a used polyamide membrane (Patient R.U.).

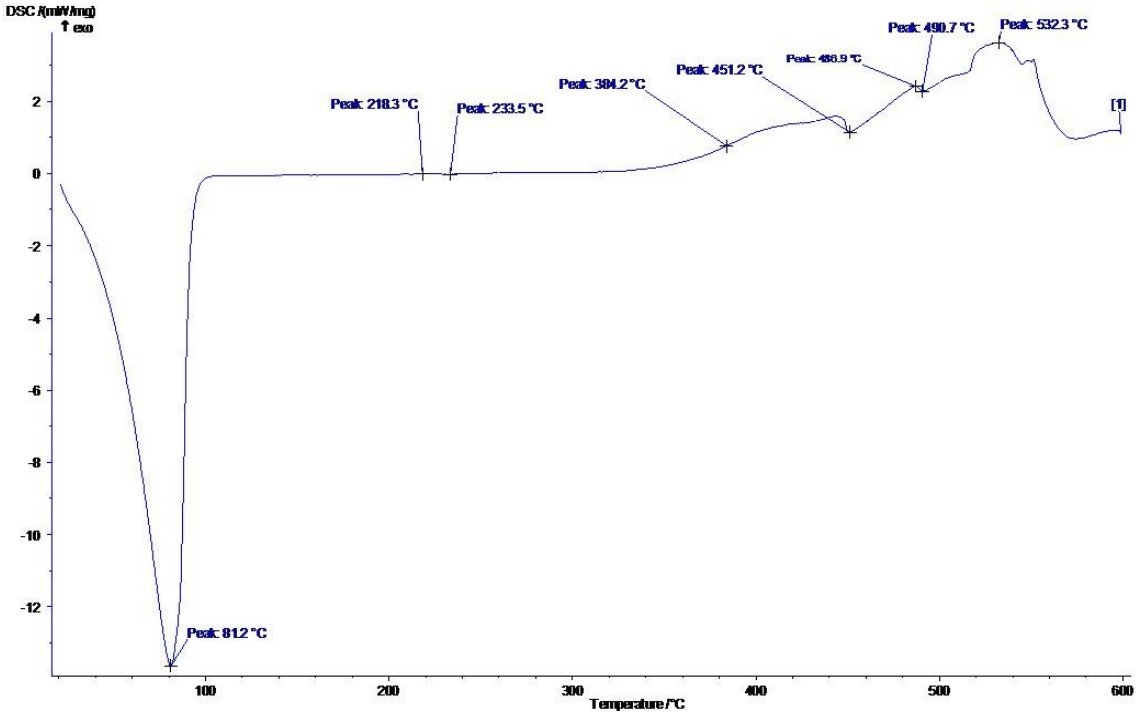

Figure 2.5.10 DSC Thermogram of a used polyamide membrane (Patient O.D.).

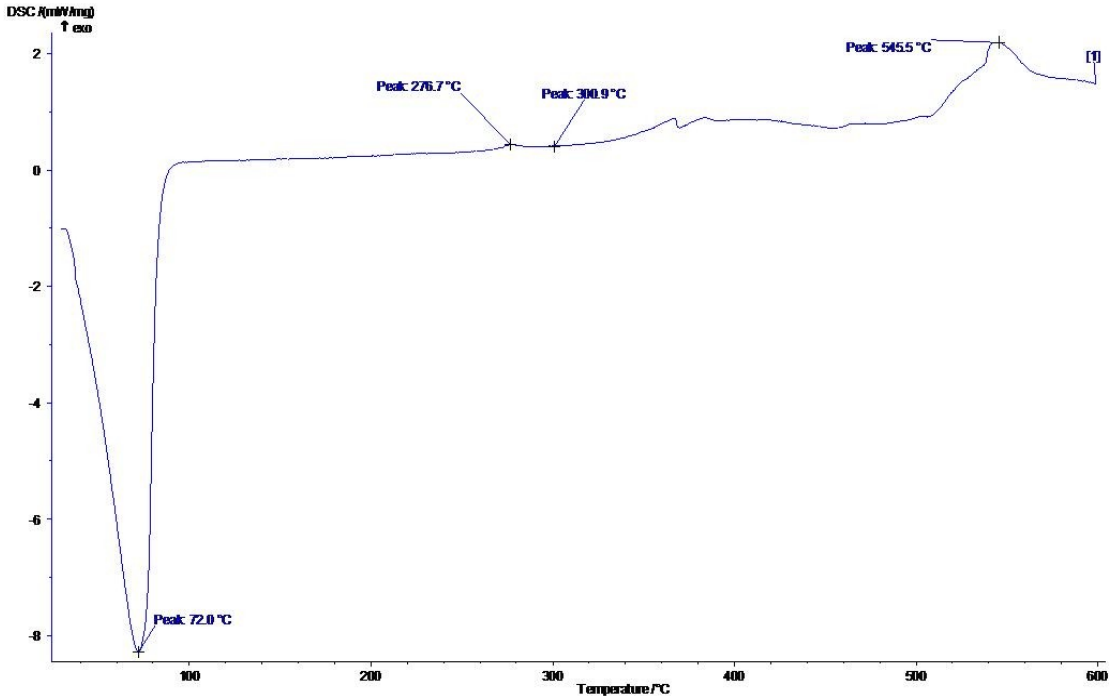

Figure 2.5.11 DSC Thermogram of a used polyamide membrane (Patient H.A).

After the evaluation of the DSC thermogram of a virgin polyamide membrane, there is an endogenous peak at 40.8ºC (with a magnitude of 0.50 mW/mg) as seen in Figure 2.5.7. Virgin polysulfone membranes have a similar peak at 42.1ºC (with a magnitude of 0.40 mW/mg) as seen in Figure 2.5.2.

Endogenous peaks of polysulfone membranes varied between 33.6ºC and 86.7 ºC (with magnitudes between 0.3 mW/mg and 15 mW/mg) as seen in Figures 2.5.3 – 2-5.6. DSC analysis of used polyamide membranes revealed endogenous peaks between 72ºC and 88.5 ºC (with magnitudes between 7.5 mW/mg and 20.5 mW/mg) as seen in Figures 2.5.8 – 2-5.11. These peaks in both membrane types may be caused by the rinsing solutions used after hemodialysis.

At higher temperatures energy absorbed differ from each other in both types of hollow fibers as seen in Figures 2.5.2 – 2.5.11.

2.6 Fourier Transform Infrared Spectroscopy (FTIR)

The aim of using the FTIR technique in our study was trying to show any change between virgin and used membranes in terms of chemical degradation [31, 32].

Like in our other experiments both virgin and used polysulfone and polyamide membranes were used for our FTIR studies. Used membranes originated from 8 different patients with dialysis ages less than two years and without any other accompanying systemic disease. FTIR experiments were performed with Mattson 1000 FTIR device was used for the experiments as seen in Figure 2.6.1.

Figure 2.6.1 Mattson 1000 FTIR spectrometer.

2.6.1 FTIR Experiments On Virgin Polysulfone Membranes

Data obtained from the experimental results of virgin polysulfone is shown on Figure 2.6.2.

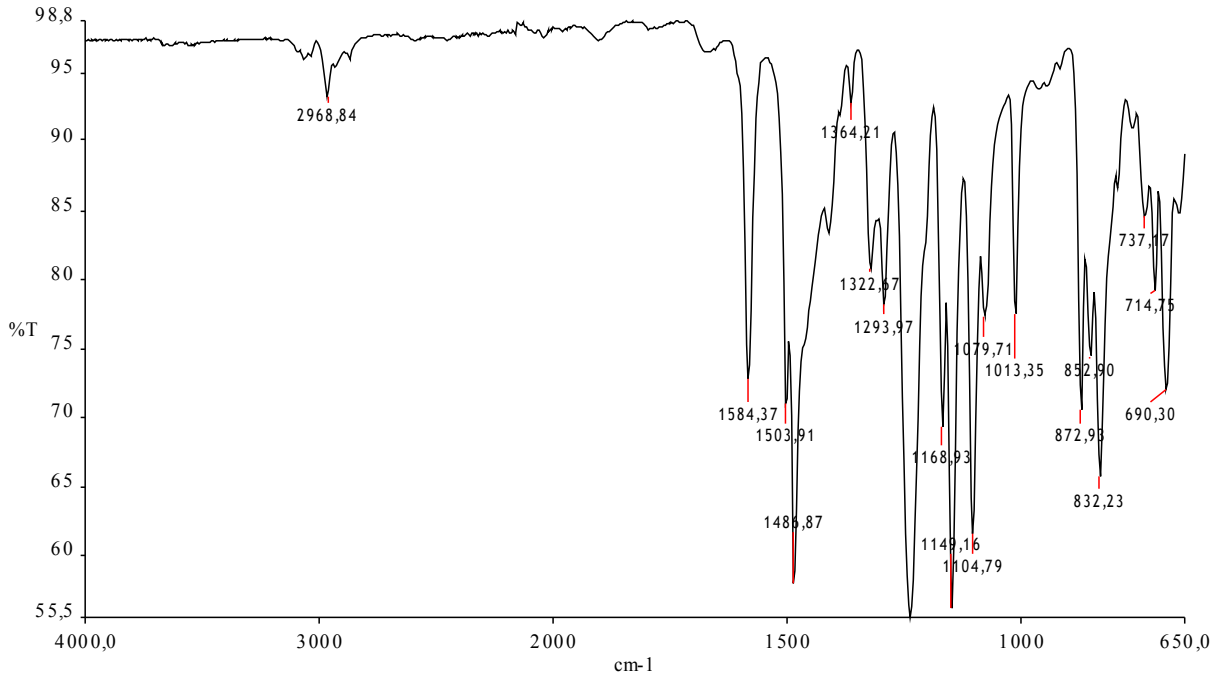

Figure 2.6.2 FTIR spectrum of a virgin polysulfone membrane.

2.6.2 FTIR Experiments On Used Polysulfone Membranes

Data obtained from the experimental results of used polysulfone membranes are shown in Figures 2.6.3 – 2.6.6.

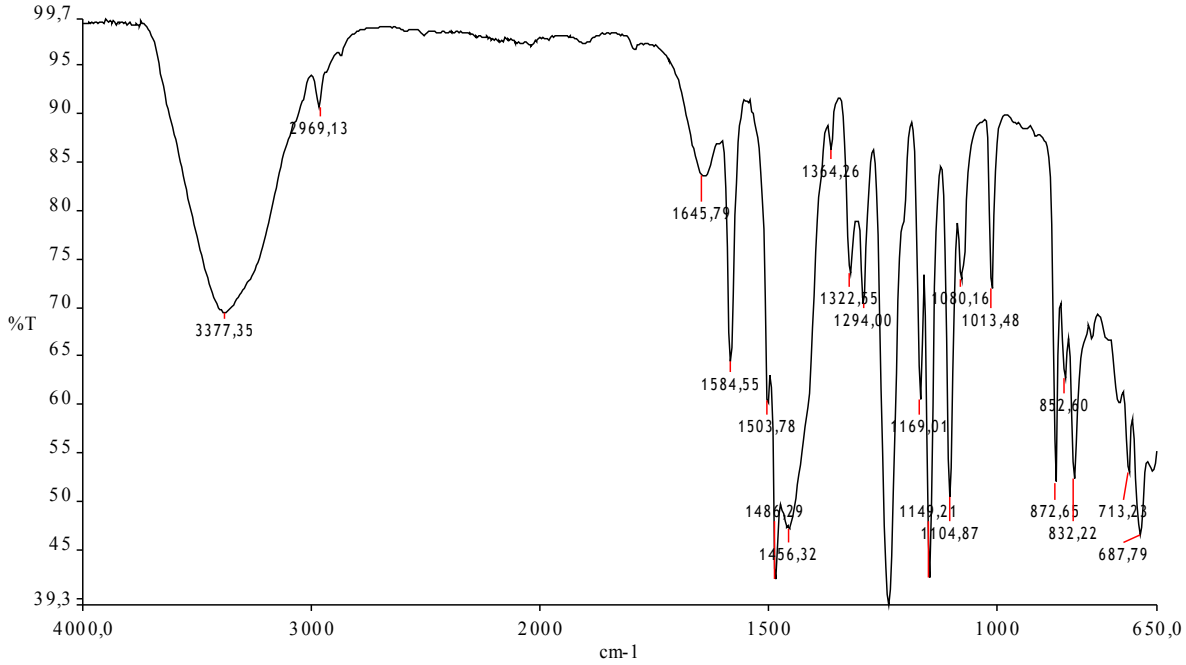

Figure 2.6.3 FTIR spectrum of a used polysulfone membrane (Patient A.F.K.).

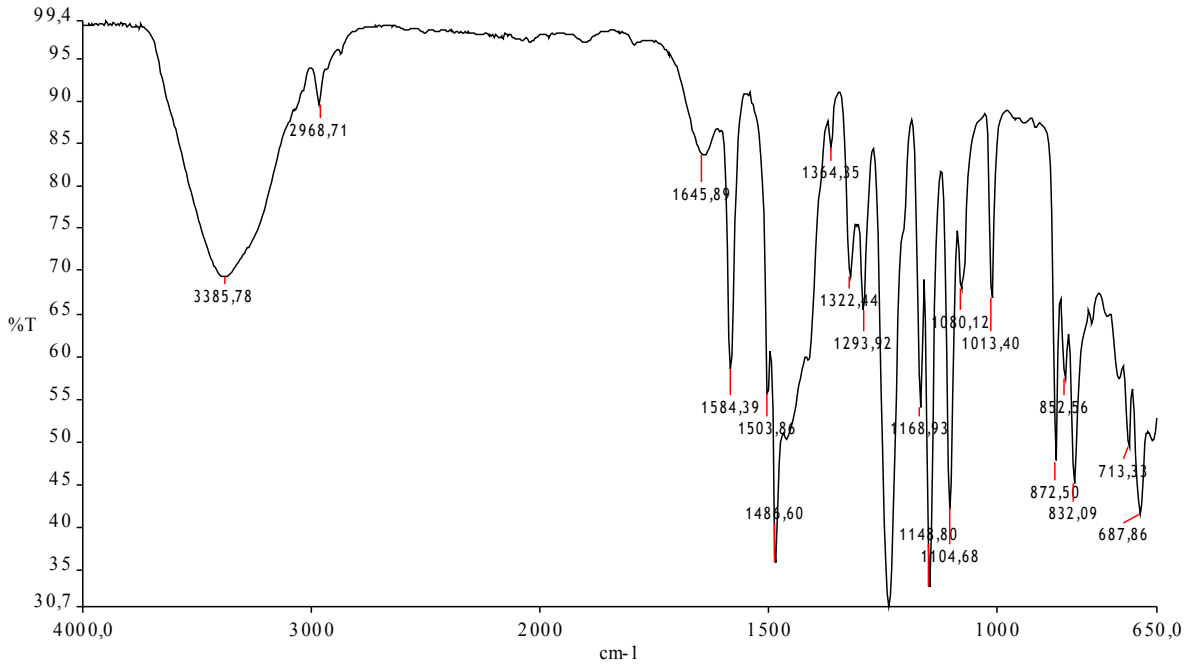

Figure 2.6.4 FTIR spectrum of a used polysulfone membrane (Patient M.D.).

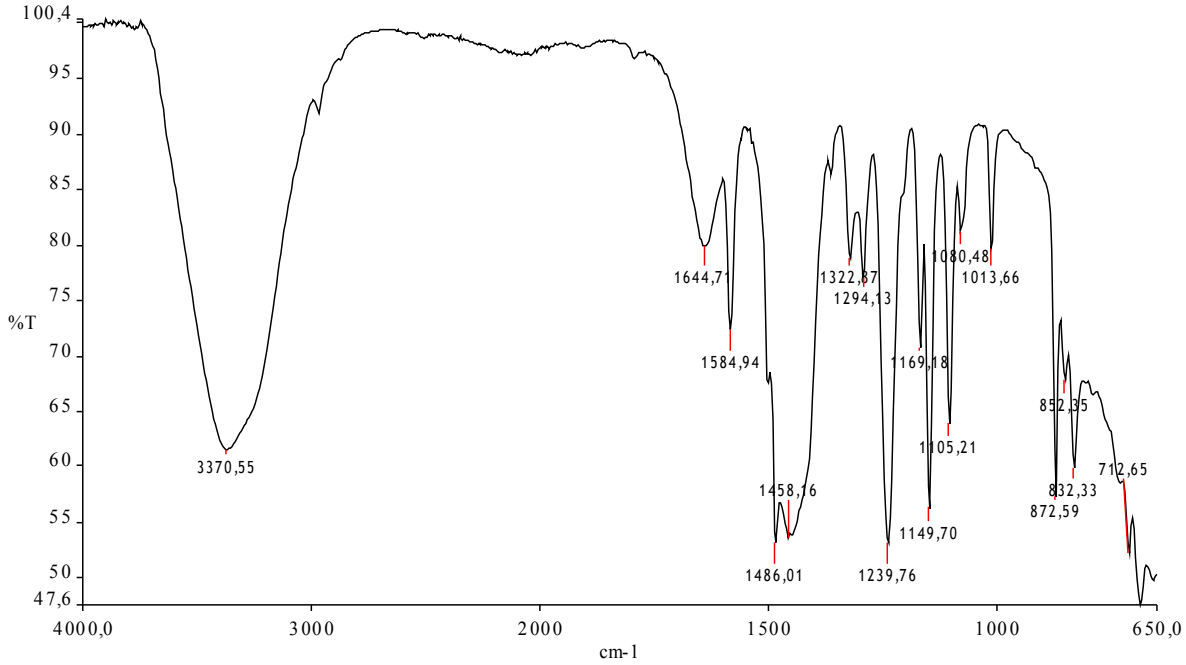

Figure 2.6.5 FTIR spectrum of a used polysulfone membrane (Patient I.C.).

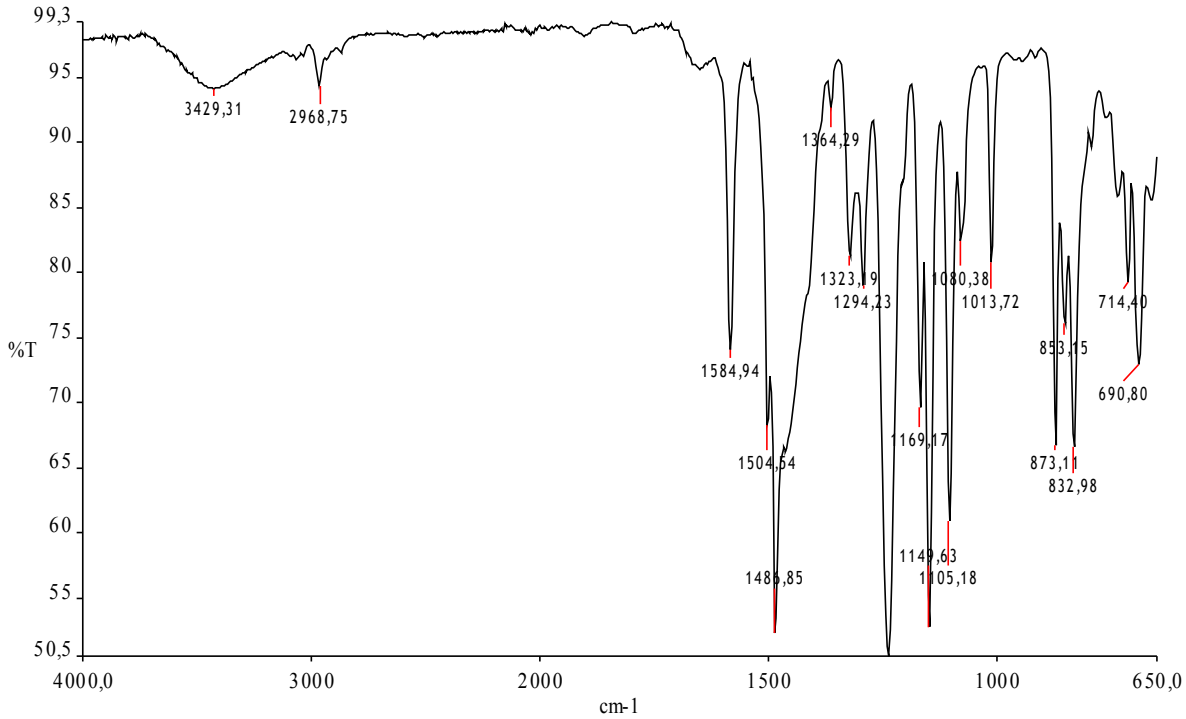

Figure 2.6.6 FTIR spectrum of a used polysulfone membrane (Patient M.K.).

.

2.6.3 FTIR Experiments On Virgin Polyamide Membranes

FTIR spectrum of a virgin polyamide membrane is shown on Figure 2.6.7.

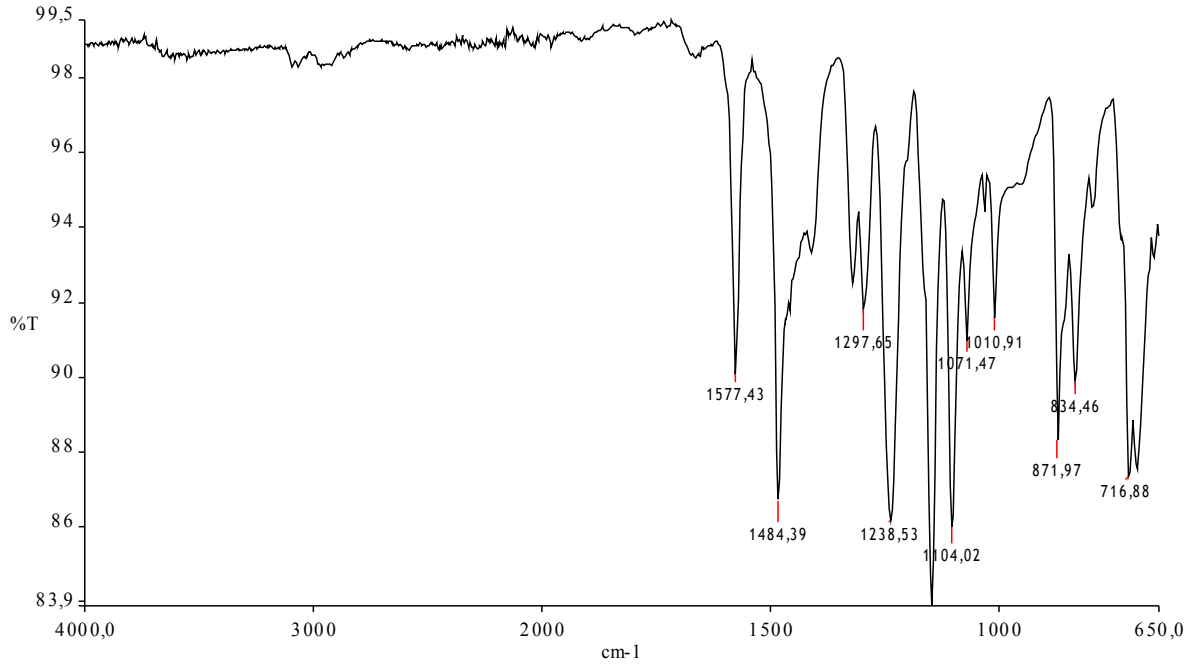

Figure 2.6.7 FTIR spectrum of a virgin polyamide membrane.

2.6.4 FTIR Experiments On Used Polyamide Membranes

Data obtained from the experimental results of used polyamide membranes are shown in Figures 2.6.8 – 2.6.11.

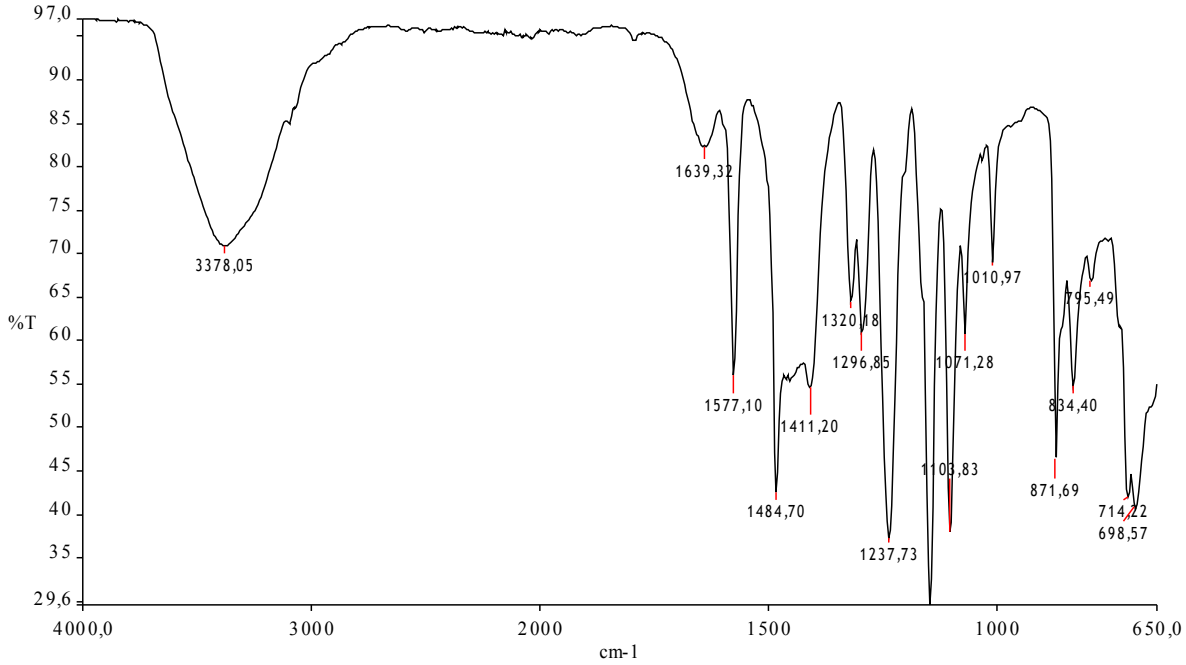

Figure 2.6.8 FTIR spectrum of a used polyamide membrane (Patient R.U).

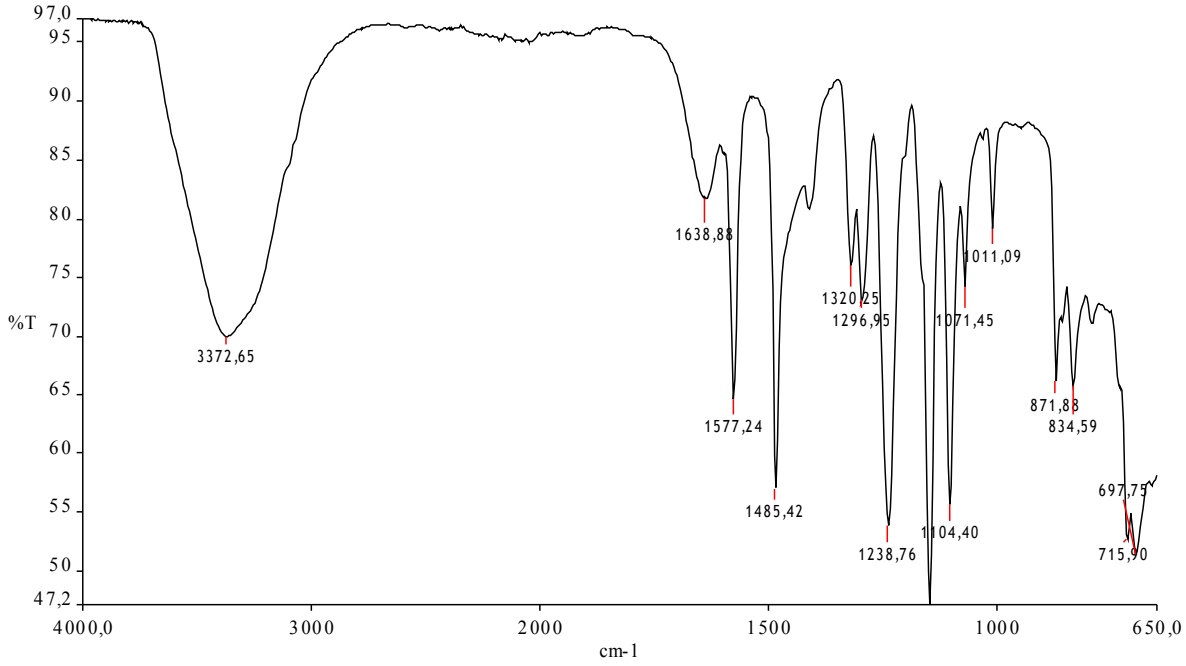

Figure 2.6.9 FTIR spectrum of a used polyamide membrane (Patient H.O.).

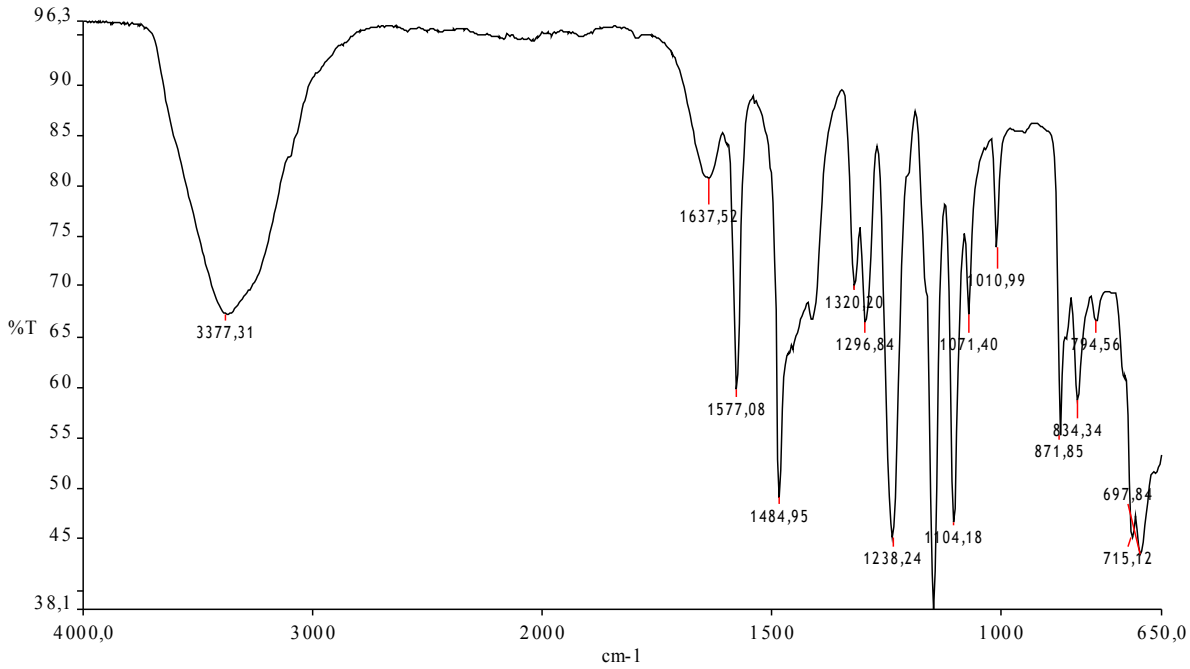

Figure 2.6.10 FTIR spectrum of a used polyamide membrane (Patient O.D.).

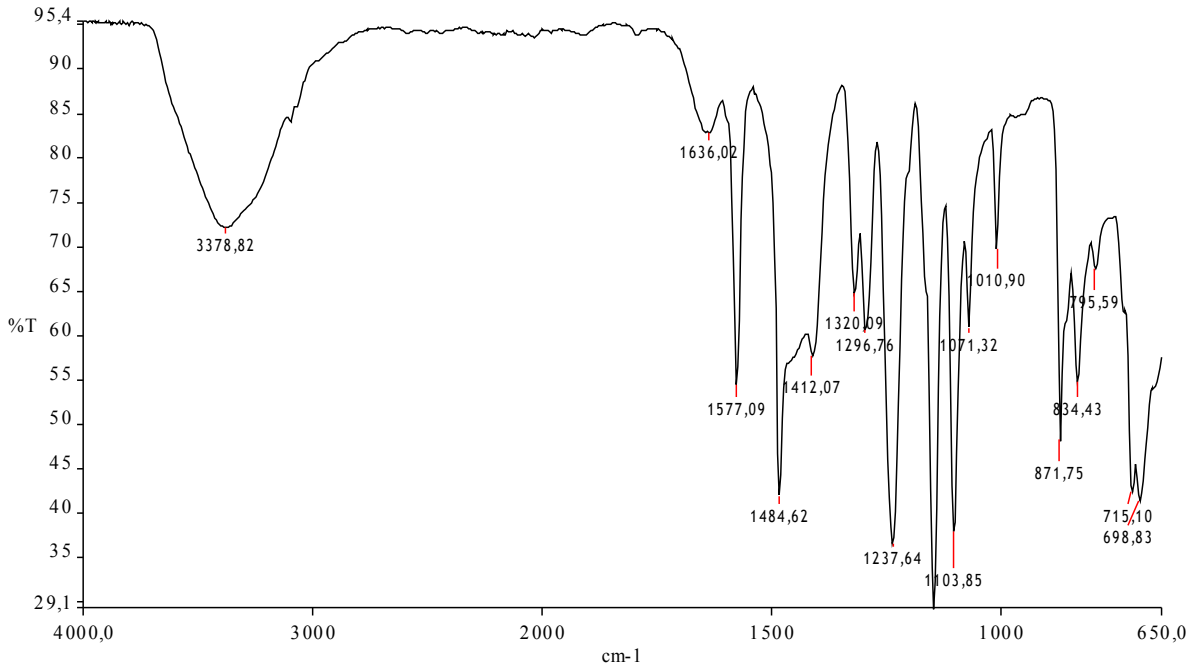

Figure 2.6.11 FTIR spectrum of a used polyamide membrane (Patient H.A.).

The FTIR spectra of the virgin polysulfone membrane and the data obtained from the used polysulfone membrane look mostly analogous to each other except the vibration seen between the wave number ranges 3329.31 cm-1 and 3385.78 cm-1.

The same comparison was also made for virgin and used polyamide membranes. The analogy between the virgin and used membranes was only interrupted between the wave number ranges 3372.85 cm-1 and 3378.82 cm-1. The wave number ranges 3329.31 cm-1 and 3385.78 cm-1 and 3372.85 cm-1 and 3378.82 cm-1 were compared with the values on the table for the interpretation of the FTIR spectra shown in Table 2.6.1.

The stretch type vibration between the wave number ranges “3350±150” belonged to the OH-group as seen in Table 2.6.1.

Table 2.6.1 Infrared functional groups for the interpretation of FTIR spectra [31].

Group	Vibration	Type	Range	
CH_3	*Stretch*	Antisymmetric	2962± 10	
		symmetric	2872± 10	
	Bend	Antisymmetric	1460± 10	
		symmetric	1375± 10	Umbrella
CH_2	*Stretch*	Antisymmetric	2926± 10	
		symmetric	2853± 10	
	Bend	Scissors	1455± 10	
	Rocking	Concerted	720± 10	Four or more
$=CH_2$	*Stretch*	Antisymmetric	3080	
		Symmetric	2997	
	Twist	Out-of-plane	993	Mono or Trans only
	Bend	Out-of-Plane	909	Terminal alkene
			1821	Overtone frequency
C=C	*Stretch*	Cis and Vinyl	1640+ 20	
		Trans, tri and tetra	1670+ 10	
≡CH	*Stretch*	Normal	3300± 20	Always very sharp
	Bend	Normal	630	
			1238	Overtone frequency
C≡C	*Stretch*	Normal	2220± 10	Terminal alkynes
			2225± 10	Internal alkynes
C@N	*Stretch*	Normal	2250± 10	10 to 20 lower when conjugated
CH_2	*Bend*	Scissoring	1426	Shifted with @
$C(sp^2)$-H (aromatic)	*Stretch*	Aromatic or unsaturated	3050± 50	Not assigned
Aromatic Ring	*Ring Stretch*	Symmetric	1590± 10	Non-symmetrical substitution
			1500± 10	Variable intensity
		Sideways	1450± 10	CH_3 bend overlap
	Bend	Hydrogen	730± 20	Out of Plane
		Out of Plane Ring	690± 20	Mono, meta or 1,3,5 substitution
OH	***Stretch***	***OH stretch***	***3350± 150***	***Broad***
	Bend	***Broad***	***1400± 100***	
	Wag	***Band***	***660***	***Not a good frequency***
C-O to C-C	*Stretch*	Anti-symmetrically coupled	1°: 1050± 25 2°: 1125± 25 3°: 1150± 50	
NH_2	*Stretch*	Antisymm	3300± 100	
		Symmetrical	3290	
	Bend	Scissoring	1615±15	1° only
	Wag	Band	797	1° and 2° only

3. DISCUSSION

Both optical stereo microscopical and scanning electron microscopical studies were performed to reveal both differences between two types of polymeric hollow fibers used in dialysis system and the effect of dialysis on the fiber in the range of the capacities of two microscopical methods. Stereo microscopical studies certainly give information with relatively low resolution with respect to what scanning electron microscopical studies give. However, as it is seen from Figures 2.1.10 and 2.1.11, the condition of dialysis damages dialyzer regardless of the patient. Increasing magnification in stereo microscope shows how fibers are distributed inside of dialyzer as shown in Figures 2.1.6. and 2.1.7 and also accumulation of blood and residues inside and surrounding fibers are visible in Figure 2.1.12. Thus dialysis leaves residues, which in turn may cause clinical complications, on polymeric material used for dialysis.

Blood residues are caused due to two main reasons, which are suboptimal anticoagulation of blood and improper rinsing of the dialyzer. Thus even in the level which can be accepted as macro level, the difference between virgin and used hollow fibers is remarkable. Any blood clotting in the dialyzer could reduce the optimal dialyzer performance; in such cases the clinician should adjust the dose of anticoagulant agents depending on the clinical situation of the patient so that complications may decrease.

SEM studies on the surface of virgin and used polysulfone hollow fibers were given in Figures 2.2.5 and 2.2.13. Comparing all the SEM micrographs in terms of revealing what dialysis session does, can easily be compared on the SEM Figures mentioned as well as stereo microscopical pictures. By the help of SEM studies damages on the surface and accumulation of the residues inside of the membranes were observed. In addition also continuation of the pores into inner parts of the membrane just below the surface between are different in virgin and used dialysis membranes shown in Figure 3.1.

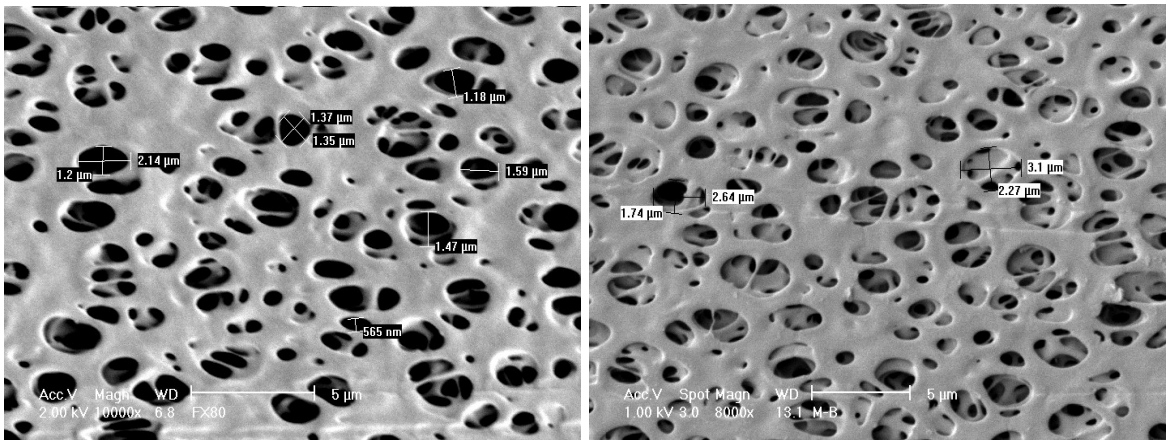

Figure 3.1 Comparison of pore sizes on the images belonging to virgin (on the left side) and used (on the right side) polysulfone membranes.

In that case it may be concluded that dialysis session has also effect on the cross sectional feature which may be one of the reasons for the difference in the mechanical behavior between virgin and used hollow fibers. Stressing via tensile test also has effect on the morphology of pores on polysulfone hollow fiber. Strain induced morphological changes is another mechanism affecting SEM micrographs showing surfaces of used polysulfone membranes exposed to tensile test.

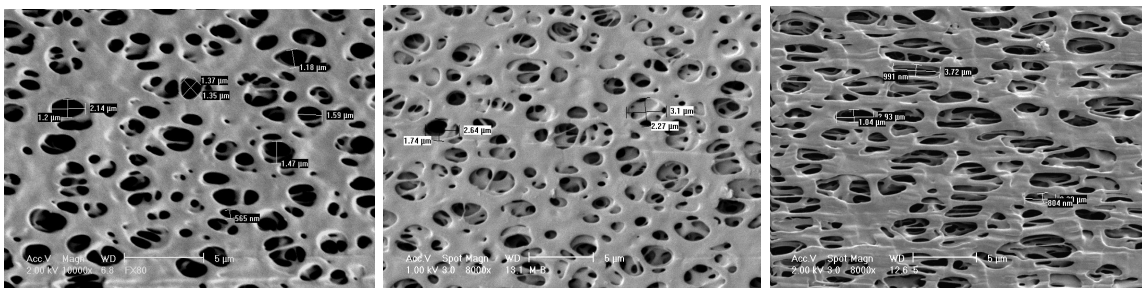

Figure 3.2 Comparison of pore sizes on the images belonging to virgin (on the left side), used (in the middle) and used polysulfone membranes after tensile test (on the left side).

Stressing causes changes in the geometry of the pores on the surface. As it is seen in Figure 3.2 pores are elongated due to tensile stressing. Pores are themselves mechanical defects purposely added during manufacturing. Elongation of the pores according to fracture mechanics point of view increases the number of locations of stress concentrations where crack initiations and then crack propagations become easier [28, 29, 30]. Dialysis contains fluctuating pressures. Therefore in dialysis session, in addition to having aggressive environmental, effect of defects during mechanical stressing should be considered.

Fracture surface studies of virgin and used polysulfone ruptured in liquid nitrogen are shown in Figures 2.2.7 and 2.2.14. Fracture surface of used hollow fiber has relatively big holes as if pores coalesce during dialysis session. This observation together with the observation obtained on the surface of used polysulfone hollow fiber confirm each other in terms of having changes in the cross section of hollow fiber due to dialysis. Certainly having more holes is a kind of degradation, which in turn should be resulted in fast propagation of cracks and/or rupturing as seen in Figure 2.2.15 [28, 29, 30, 33, 34, 35, 36]. Also tensile test causes creation of holes on the fracture surface.

Surface studies of polyamide type hollow fiber show that the outside diameter is larger than that of polysulfone fiber and the size of pores being visible on the surface is generally bigger than that of polysulfone fiber although there are relatively small pores together with big pores. This condition gives possibility to get rid of toxic material to the outside of the dialysis system faster. However the other factors affecting cleaning of the blood should not be ignored.

Surface studies of used polyamide clearly show an increase in pore size and morphological changes just below the membrane surface resulted by dialysis environment as seen on Figure 2.2.24. Figure 2.2.24 informs about changes in the surface morphology which are most probably due both aggressive environment and mechanical effects during dialysis. Tensile test of the used polyamide membrane causes shrinkage in outer diameter of the hollow fiber and the elongation of pores as seen in Figure 2.2.25. Merging of pores includes also rupturing of the ligaments between neighboring pores as seen in Figure 2.2.26.

It is necessary to reveal at least qualitatively what dialysis, where combined chemical, thermal and mechanical attacks on polymers exist, makes to the polymers being generally time and rate dependent materials. It is expected to get a high level of degradation, creep, fatigue and creep-fatigue interactions due to dialysis environment. In order to design new material for future applications it is necessary to have data related to what dialysis environment has. Clinical considerations have to be taken into account not only for the selection of the material also what combined mechanical and thermal

parameters for the initial usage and for the reuse application are requested.

The pore sizes of the dialysis membranes should be designed such a way that essential large proteins such as albumin are not allowed to pass through the pores of the membrane during hemodialysis and stability of the pores should also remain even in the case of combined thermal, mechanical and chemical attacks. High-flux hemodialysis allows the elimination of far larger uremic toxins than those removable by conventional low-flux dialysis. Enlarging the pore size of the membrane is limited, because essential large proteins such as albumin may get lost during hemodialysis resulting in a deficiency state [37, 38, 39].

Hypoalbuminaemia is associated with increased morbidity and mortality in end-stage renal disease patients. Because of that the amount of albumin lost through a dialyzer is a very critical parameter which may contribute to hypoalbuminaemia. The definition of the acceptable maximum pore size of dialyzer membrane depends on the size of essential large molecules like albumin [37, 38, 39]. Reuse of high-flux dialyzer membranes also appears to augment albumin losses during dialysis. This effect appears to be dialyzer membrane-dependent, being greater with high-flux membranes, and still greater with the reuse of such membranes.

Fracture surface obtained in liquid nitrogen rupturing shows big holes and internal cracks. Having holes together with pores or instead of pores and internal crackings on the fracture surface obtained in liquid nitrogen rupturing is due to nature of polymer and design of hollow fiber in macro, micro and submicron level in dialysis environment [19].

Mechanical stressing under tension, tensile test applied to the used polyamide membrane shows many different features in the same time. The number and the size of holes on the fracture surface representing high level of plastic deformation are increased as seen in Figure 2.2.25. Uniaxial loading causes coalescence of the pores that gives cylindrical or conical surfaces. Thus inclination from the uniaxiality and changing of the loading axis may give other type of conical surfaces on the fracture surface. In that case

there will be locally and distributed micro-stress risers. During dialysis session the mode of stress changes depending on the cross section. When fibers are designed in bundles inside of the dialyzer, case would be more drastic.

All mechanical tests show decrease in both yield and ultimate tensile strength after dialysis sessions. Generally in most cases toughness, which may be accepted in this case as total area under stress-strain curve, decreases after dialysis. The amount of the decrease in the mechanical parameters varies depending on the patient. Although the patients in our study did not have any other complications other than kidney failure, the quantitative differences in mechanical parameters may be due to changes in blood chemistry and unknown factors.

"Loading-unloading-reloading" experiments for used hollow fibers clearly show the decrease in all mechanical parameters. This condition implies at least initially during fatigue high amount of damage may be obtained. Figure 2.3.7 explains what may happen in the first cycle during fatigue. Increasing the number of cycles certainly will cause additional damages and damage accumulation in aggressive environment should be considered. Every cycle causes different constitutive equation for the material considered. Therefore in the dialysis session every incremental time would be bringing different condition with higher damage comparing to the previous increment.

Tensile tests were performed at room temperature, but it is well known that the mechanical characteristics of the polymers may change when temperature is increased above room temperature. In a study by L'Clerc et al. it was observed that either in single fiber tests by increasing the temperature of the surroundings or through internal heating of the fibers in a bundle or cord, the fatigue-fracture mode changes [35, 36].

Hypotension during hemodialysis is treated by placing the patient in the Trendelenburg position (a position in which the body is laid flat on the back with the feet higher than the head position), administering a 100 to 200 ml normal saline injection and reducing the ultrafiltration rate, at least temporarily [6].

During hemodialysis the pump speed or the transmembrane pressure is reduced to lower the ultrafiltration rate when patients have severe hypotension periods. When the clinical status of the patient stabilizes, the pump speed or transmembrane pressure is slowly elevated by the physicians. From the mechanical point of view this situation resembles the cyclic loading procedure performed during our experiments. Assuming that several hypotensive periods may happen during hemodialysis and that lowering the transmembrane pressure is imperative during severe hypotension causing damages on the dialysis membranes.

X-Ray diffraction studies give comparison between virgin and used membranes in terms of crystallinity. Hemodialysis caused an increase in the number of XRD peaks and in some cases an increase in the intensity of the available ones. Thus dialysis causes structural changes towards increasing crystallinity. Structural changes also mean having different constitutive equation. The difference results in different behavior such as what is obtained after mechanical tests, microscopical studies and the others.

After the FTIR studies, it has been concluded that the stretch type vibration between the wave number ranges “3350±150” belonged to the OH-group. The OH-group detected during these studies belong to the rinsing solution used after dialysis for giving the residual blood in the dialyzer back to the blood circulation of the patient. The FTIR studies of both virgin and used membranes did not give any major indication. The possible changes of the FTIR spectra after several dialysis sessions with reuse technique should be further investigated and combined with the other analytical techniques.

Reuse of dialyzers is an example of medical practice, where economic considerations are weighed against safety and effectiveness for patients and medical staff [40]. In open literature, the reuse issue is discussed in clinical case studies [41, 42]. Clinical case studies on dialysis do not include, what happens to the materials during dialysis session, so that clinical data do not have any information on the stability of membranes from materials science and engineering point of view. Thus the present work fills the gap between clinic and engineering in the field of hemodialysis.

1. CONCLUSION

The effect of hemodialysis on polysulfone and polyamide types of hollow fibers used is clearly observed in different degrees. Both types of polymeric hollow fibers show deterioration on surfaces and below the surface, decrease in mechanical parameters and structural unstability.

Qualitative and quantitative values of the degradation are not the same on both types of hollow fibers because of their constituents, pore geometries and dimensions.

It was observed that dialysis environment has a significant effect on the pore morphology as well as structural stability. Structurally, the degree of crystallinity after dialysis was changed. Pores are partially merged to each other. All of these factors made material constitutively different from the initial state.

Mechanically, dialysis environment decreased the strength and the toughness. Cyclic-like loading, loading-unloading-reloading until fracture, drastically reduced toughness.

All the observations indicate that reuse issue should critically be considered because of the membrane damage and the tendency to structural instability.

REFERENCES

1. Reuß, M., "Gesundheitsindustrie – ein Wachstumsmarkt am Beispiel Dialyse," Fresenius Medical Care, Schweinfurt, pp. 6-7, 2007.

2. Turkish Society of Nephrology, "The number of hemodialysis patients in Turkey between the years 1990 and 2006," Annual Registry , 2006 .

3. USRDS 2007, "Incidence of ESRD (per million population) in 2005," Annual Data Report, 2007.

4. Gitto, L., "Dialysis modality selection according to the medical care provided at dialysis units: An econometric analysis," Health Serv Outcomes Res Method, Vol. 5, pp. 227–241, 2004.

5. Hirth, R.A., "The organization and financing of kidney dialysis and transplant care in the United States of America," Int J Health Care Finance Econ, Vol.7, pp. 301–318, 2007.

6. Barry, M., and M.D. Brenner, *The Kidney*, Elsevier Inc. pp. 4-5, 2004.

7. Fankhauser, D.B., Urinary Tract Anatomy, University of Cincinnati Clermont College, 2005. Available : http:// biology.clc.uc.edu/Fankhauser/Labs/ Anatomy_&_Physiology/ A&P203/ Urinary_Tract_Histology/Anatomy/urinary_anatomy.html.

8. Malluche H.H. , B.P. Sawaya, R.M. Hakim and M.H. Sayegh, *Clinical Nephrology, Dialysis and Transplantation*, Boston, Dustri Verlag, Vol. 2, pp. 1-32, 1999.

9. Graham, T., "The Bakerian lecture: Osmotic force," Philos Trans R Soc, London, Vol. 144, pp. 117-128, 1854.

10. Dialysis Compact, The invention, development and success of the artificial kidney, Fresenius Medical Care, 2007. Available: www.fmc-ag.com.

11. Haas, G., "Versuche der Blutauswaschung am Lebenden mit Hilfe der Dialyse," *Klin Wochenschrift, Germany, Vol.* 4, pp. 13, 1925.

12. Woo, K. T., and Tan H K, "Development of Newer Therapies in Haemodialysis," Singapore Med J, Vol. 43, pp. 441, 2002.

13. Frost, T.H., *Technical aspects of renal dialysis,* England: Tunbridge Wells, Pitman Medical, 1978.

14. Eloot, S., Experimental and Numerical Modeling of Dialysis. PhD Thesis, Ghent University, Ghent, Belgium, 2004.

15. Schrier, R.W., *Atlas of Diseases of the Kidney,* Vol. 5, pp.1-3, 2008.

16. Hoenich, N.A., C. Woffindin, and C. Ronco, *Replacement of renal function by dialysis*, Dordrecht, Kluwer Academic Publisher, pp.188-230, 1996.

17. Tokars, J.I., M.J. Alter, and E. Miller, "National surveillance of dialysis associated disease in the United States 1994," ASAIO J, Vol. 43, pp.108–119, 1997.

18. Schiffl, H., M. Fischereder and T. Sitter, “Biokompatibilität der Nierenersatztherapie,” Internist, Springer-Verlag, Vol. 40, pp. 37–48, 1999.

19. Aksoy, M.E., “Biocompatability of dialysis membranes,” Master’s thesis, Bogazici University, Istanbul, Turkey, 1996.

20. Chauveau, D., ”Cumulative survival according to membrane characteristics,” Am J Kidney Dis, Vol. 45, pp.565-571, 2005.

21. Woods, H.F., and M. Nandakumar, “Improved outcome for haemodialysis patients treated with high flux membranes,” Nephrol Dial Transplant, Vol. 15 , pp. 36-42, 2000.

22. Wang, Y.X., J.L. Robertson, W.B. Spillman and R.O. Claus, Effects of the Chemical Structure and the Surface Properties of Polymeric Biomaterials on Their Biocompatibility, Pharmaceutical Research, Vol. 21, pp. 1362-1373, 2004.

23. Polyamide, “Werkstoffkenndaten,” 2008. Available:http://www.chemikus.com.

24. Ronco, C., S.K. Bowry, A. Brendolan, C. Crepaldi, G. Soffiati, A. Fortunato, V. Bordoni, A. Granziero, G. Torsello and G. La Greca, ”Hemodialyzer: from macro-design to membrane nanostructure; the case of the FX-class of hemodialyzers,” Kidney Int, Vol. 61, pp. 126-142, 2006.

25. Ronco, C., N. Levin, A. Brendolan, “Flow distribution analysis by helical scanning in polysulfone hemodialyzers: Effects of fiber structure and design on flow patterns and solute clearances,” Hemodialysis International, Vol. 10, pp. 380–388, 2006.

26. Fresenius Medical Care Deutschland GmbH, “FX Class,” Germany: pp. 7-8, 2004. Available: http//www.fmc-ag.com.

27. Gambro Renal Products, “Polyflux™ S Series Technical Datasheet,” Sweden: pp.1-2., 2002. Available: http//www.gambro.com.

28. Meyers, M. A., K. K. Chawla, *Mechanical Behaviour of Materials,* Prentice-Hall, 1999.

29. McMahon, C.J., *Structural Materials*, Merion Press, pp. 13-39, 2004.

30. McClintock, F. A., A. S. Argon, *Mechanical Behavior of Materials*, Addison Wesley, 1966.

31. Mohan, J., Organic Analytical Chemistry Theory and Practice, England: Alpha Science Ltd., pp. 195-244, 2003.

32. Rintoul, L, H. Panayiotou and S. Kokot, “Fourier transform infrared spectrometry: a versatile technique for real world samples” Analyst, , Vol. 123, pp. 571–577,1998.

33. Zhang Y., X. Wang, N. Pan and R. Postle, “Weibull analysis of the tensile behavior of fibers with geometrical irregularities,” J Mater Sci, Vol. 37, pp. 1401 – 1406, 2002.

34. Liu, Z.Y., S. Beniwal, C.H.M. Jenkins and R.M. Winter,”The Coupled Thermal and Mechanical Influence on a Glassy Thermoplastic Polyamide: Nylon 6, 6 Under Vibro-Creep,” Mechanics of Time-Dependent Materials, Vol. 8, pp. 235–253, 2004.

35. Le Clerc, C, B. Monasse and A.R. Bunsell, “Influence of temperature on fracture initiation in PET and PA66 fibres under cyclic loading,” J Mater Sci, Vol. 42, pp. 9276–9283, 2007.

36. Ramirez, J.M.H., A.R. Bunsell and P. Colomban,” Microstructural mechanisms governing the fatigue failure of polyamide 66 fibres,” J Mater Sci, Vol. 41, pp. 7261–7271, 2006.

37. Ofsthun, N.J.,”Limitations of Membrane Structure and Dialyzer Design on Large Solute Removal in Dialysis,” Blood Purif, Vol.18, pp. 264–266, 2000.

38. Detlef, H., K. Canaud and B Canaud, “High permeability of dialysis membranes: what is the limit of albumin loss?” Nephrol Dial Transplant, Vol. 18, pp. 651-654, 2003.

39. Kobaisi, M.A., M. Tate, C. Rix, T.S. Jakubov and D.E. Mainwaring,”The effect of molecular imprinting on the pore size distribution of polymers,” Adsorption, Vol.13, pp. 315–321, 2007.

40. Lameire, N., “ Management of the Hemodialysis Patient: A European Perspective,” Blood Purif, Vol.20, pp.93–102, 2002.

41. Twardowski, Z.J.,” Dialyzer Reuse—Part II: Advantages and Disadvantages,”Seminars in Dialysis, Vol.19, pp. 217–226, 2006.

42. Tanaka, N., T. Fujisawa, T. Daimon, K.Fujiwara and M. Yamamoto, “The use of electrolyzed solutions for the cleaning and disinfecting of the dialyzers,” Artificial Organs, Vol. 24, pp.921-928, 2000.

VITA

Mehmet Emin Aksoy was born in Istanbul on April 12th, 1964. After graduating from Sankt Georg Austrian College in 1984, he obtained the degree of "Medical Doctor" from Karadeniz University in 1990. He worked in Sinop Hospital in 1991. He worked in the Dialysis Department of Istanbul State Hospital between 1992-1993. As a medical doctor, he was specialized in the field of "Family Medicine". In 1993, he admitted to the M.S. degree program in Biomedical Engineering Institute at Boğaziçi University. After completing his M.S. thesis on "Biocompatibility of Dialysis Membranes" in 1996, he applied for the Ph.D. program at the same Institute. He worked as the deputy medical director in Taksim State Hospital. He completed his military service in Ankara Gülhane Askeri Tıp Akademisi as deputy medical director.

Since 2003, he has been working as the deputy manager of the Turkish Ministry of Health Istanbul City Health Management.

A list of publications is presented below:

1. Aksoy M. E., M. Usta and A. H. Ucisik, "The Effect of Dialysis Environment On High Flux Dialysis Membranes," *Proceedings of World Congress on Medical Physics and Biomedical Engineering*, Springer Verlag, pp. 3165-3167, 2007.

2. Aksoy E., A.H. Üçışık, "Reducing the Costs of Medical Devices Purchased for the State Hospitals in Turkey," *Proceedings of International Medical Informatics an Biomedical Engineering The First Jordanien Eoropean Symposium (IMIBE'06)*, pp.171-173, Yarmouk University, Amman, Jordan, 2006.

3. Aksoy M.E., A. H. Ucisik, "Postdialytic Changes of High Flux Dialysis Membranes in Terms of Mechanical Properties and Crystallinity," *Proceedings of ISBME*, Bangkok, Thailand, 2006.

4. Aksoy M.E., M. Usta and A.H. Ucisik, "The Effect of Dialysis Environment On The Mechanical and Structural Stability of High Flux Dialysis Membranes," *Proceedings of World Congress of Nephrology* , Rio de Janeiro, Brazil, 2007.

5. Aksoy M.E., M. Usta and A.H. Ucisik, "The Effect of Dialysis On The Mechanical and Structural Stability of High Flux Dialysis Membranes," *Proceedings of WACBE*, pp. 1-3 Bangkok, Thailand, 2007.